

Ionic, Water-Soluble Polyfluorene-Type Copolymers

Dissertation

zur Erlangung des akademischen Grades
Doktor der Naturwissenschaften
(Dr. rer. nat.)
in der Wissenschaftsdisziplin Makromolekulare Chemie

eingereicht im
Fachbereich Mathematik und Naturwissenschaften
der Bergischen Universität Wuppertal

Swapna Pradhan

geb. am 20.03.1974
in Pune, India

Wuppertal, im October 2004

Die vorliegende Arbeit wurde in der Zeit von September 2001 bis October 2004 an der Universität Potsdam und an der Bergischen Universität Wuppertal unter der Anleitung von Herrn Prof. Dr. U. Scherf angefertigt.

Ich bedanke mich bei Herrn Prof. Dr. U. Scherf für die Überlassung des interessanten Themas dieser Arbeit, für seine stete Diskussionsbereitschaft sowie für seine persönliche Unterstützung.

*For my parents
&
Jiten*

Swapna

**Great discoveries and improvements invariably
involve the cooperation of many
minds.**

.....Alexander Graham Bell

List of Symbols or Abbreviations

UV/VIS	Ultraviolet/Visible
PL	Photoluminescence
EL	Electroluminescence
LEDs	Light Emitting Diodes
PLEDS	Polymer Light Emitting Diodes
OLEDs	Organic Light Emitting Diodes
PF	Polyfluorene
CPEs	Conjugated Polyelectrolytes
PPP	Poly (paraphenylene)
PPV	Poly (phenylene vinylene)
PPE	Poly (phenylene ethynylene)
LBL	Layer-by-layer
ITO	Indium tin oxide
CP	Conjugated Polymer
ssDNA	Single Stranded DNA
ddDNA	Double Stranded DNA
PNA	Peptide Nucleic Acid
FRET	Förster energy transfer
GPC	Gel permeation chromatography
\overline{M}_n	Number average molecular weight
MWCO	Molecular weight cutoff
C ₁₂ E ₃	Triethyleneglycol monododecyl ether
C ₁₂ E ₅	<i>n</i> -dodecyl pentaoxyethylene glycol ether
SANS	Small angle neutron scattering
PEDOT	Poly(3, 4-ethylenedioxythiophene)

RC	Regenerated Cellulose
CE	Cellulose Ester
COD	Cyclo-octadiene
LC	Liquid Crystalline
DSC	Differential Scanning Calorimetry

INDEX

1	MOTIVATION & OBJECTIVE	1
1.1	Motivation	1
1.2	Objective	2
2	INTRODUCTION	3
2.1	Conjugated polymers	3
2.2	Electronic structure of a conjugated polymer	4
2.3	Fluorene-based conjugated polymers	6
2.4	Conjugated polyelectrolytes (Water soluble polymers)	9
2.5	Applications of conjugated polyelectrolytes as water soluble polymers	15
2.5.1	Polymer light-emitting diode	15
2.5.2	Conjugated polymers as platforms for biological sensors	17
3	RESULTS AND DISCUSSION	22
3.1	Synthesis of an anionic water-soluble fluorene-type copolymer with a 1,4-phenylene spacer	22
3.1.1	Absorption and photoluminescence properties	27
3.1.2	Optical properties of the water-soluble, anionic fluorene-type copolymer 11 in presence of nonionic surfactants	28
3.1.3	Influence of surfactant concentration	28
3.1.4	PL spectra of the anionic fluorene-type copolymer 17 after surfactant (C ₁₂ E ₃) addition	29
3.1.5	Poly[9,9-bis(4-sulfonylbutoxyphenyl)fluorene-co-1,4-phenylene] 17 in PLEDs	31
3.1.6	Optical characterization of polymer films and corresponding OLED devices	31
3.2	Synthesis of the anionic water-soluble fluorene-type copolymer with a 4,4'-biphenylene spacer	33
3.2.1	Absorption and photoluminescence properties	35
3.3	Synthesis of the anionic water soluble fluorene-type copolymer with a thienylene spacer group	35
3.3.1	Absorption and photoluminescence properties	38
3.4	Synthesis of the anionic water soluble fluorene-type copolymer with a bithiophene spacer group	39
3.4.1	Absorption and photoluminescence properties	40
3.5	Synthesis of anionic water-soluble, fluorene-type copolymers containing alternating phenylene and benzothiadiazole units	41
3.5.1	Absorption and photoluminescence properties	43

3.6 Synthesis of the cationic water-soluble fluorene-type copolymer with a phenylene spacer group	43
3.6.2 Absorption and photoluminescence properties	48
3.6.3 Optical properties of the water-soluble, cationic fluorene-type copolymer in the presence of a nonionic surfactant (C ₁₂ E ₅)	48
3.6.4 Photoluminescence spectra of poly {9,9-bis[6-(N,N-trimethylammonium) hexyl] fluorene-co-1,4-phenylene} 22/C ₁₂ E ₅ mixtures in solution and the solid state	50
3.6.5 Small-Angle Neutron Scattering (SANS)	51
3.7 Synthesis of cationic, water-soluble fluorene-type copolymer with a 2,5-thienylene spacer	54
3.7.1 Absorption and photoluminescence properties	55
3.7.2 Absorption and photoluminescence properties	56
3.8 Synthesis of a cationic, water-soluble fluorene-type copolymer with a bithiophene spacer	57
3.8.1 Absorption and photoluminescence properties	58
3.8.2 Absorption and photoluminescence properties	59
3.9 Synthesis of a polyfluorene with liquid-crystalline side chains	60
3.9.1 Absorption and photoluminescence properties	63
4 EXPERIMENTAL	66
4.1 Instrumental details	66
4.2 Monomers	68
4.2.1 2,7-Dibromofluorene-9-one 2	68
4.2.2 2,7-Dibromo-9,9-bis(4-hydroxyphenyl)fluorene 3	69
4.2.3 2,7-Dibromo-9,9-bis(4-sulfonylbutoxyphenyl)fluorene 4	70
4.2.4 4,4'-Biphenyl-bis(4,4,5,5-tetramethyl-1,3,2-dioxaborolane) 6	71
4.2.5 2,7-Dibromo-9,9-bis-(6-bromohexyl)fluorene 8	72
4.2.6 2,7-Dibromo-9,9-bis-[6-(N,N-dimethylamino)hexyl]fluorene 9	74
4.2.7 2,5-Bis(trimethylstannyl)thiophene 11	75
4.2.8 5,5'-Bis(trimethylstannyl)-2,2'-bithiophene 13	76
4.2.9 4,7-Dibromo-benzo[1,2,5]thiadiazole 15	77
4.2.10 2,7 Dibromo-9,9-bis(4-cyanobiphenyl-4'-oxyhexyl)fluorene 16	78
4.3 Polymers	79
4.3.1 Poly[9,9-bis(4-sulfonylbutoxyphenyl)fluorene-co-1,4-phenylene] 17	79
4.3.2 Poly[9,9-bis(4-sulfonylbutoxyphenyl)fluorene-co-4,4'-biphenyl] 18	80
4.3.3 Poly[9,9-bis(4-sulfonylbutoxyphenyl)fluorene-co-2,5-thienylene] 19	81
4.3.4 Poly[9,9-bis(4-sulfonylbutoxyphenyl)fluorene-co-2,2'-bithiophene] 20	82
4.3.5 Poly {9,9-bis[6-(N,N-dimethylamino)hexyl]fluorene-co-1,4-phenylene} 21	83
4.3.6 Poly {9,9-bis[6-(N,N-trimethylammonium)hexyl]fluorene-co-1,4-phenylene} 22	84
4.3.7 Poly {9,9-bis[6-(N,N-dimethylamino)hexyl]fluorene-co-2,5-thienylene} 23	85
4.3.8 Poly {9,9-bis[6-(N,N-trimethylammonium)hexyl]fluorene-co-2,5-thienylene} 24	86
4.3.9 Poly {9,9-bis[6-(N,N-dimethylamino)hexyl]fluorene-co-2,2' bithiophene} 25	87
4.3.10 Poly {9,9-bis[6-(N,N-trimethylammonium)hexyl]fluorene-co-2,5-thienylene} 26	88
4.3.11 Poly[9,9-bis(4-sulfonylbutoxyphenyl)fluorene-1,4-phenylene]-co-([1,2,5]benzo-thiadiazole-4,7-diyl-1,4-phenylene) 27	89
4.3.12 Poly[9,9-bis(4-cyano-biphenyl-4'-oxyhexyl)fluorene] 28	90

4.3.13 Poly[9,9-bis(6-bromohexyl)fluorene]	29	92
4.3.14 Poly[9,9-bis(6-bromohexyl)fluorene-co-1,4-phenylene]	30	93
4.3.15 Poly[9,9-bis(6-carboxyhexyl)fluorene]	31	94
4.4 Fabrication of PLEDs using	17	95
4.5 Purification of water-soluble polymers		96
5 SUMMARY		99
6 FUTURE RESEARCH		102
7 REFERENCES		104
8 LIST OF PUBLICATIONS		113
9 CURRICULUM VITAE		114
10 ACKNOWLEDGEMENT		115

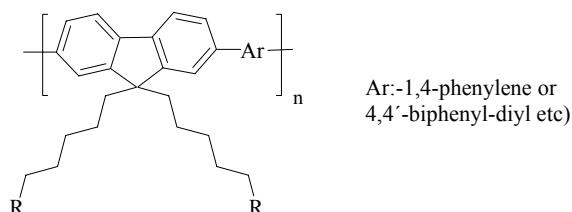
1 Motivation & Objective

1.1 Motivation

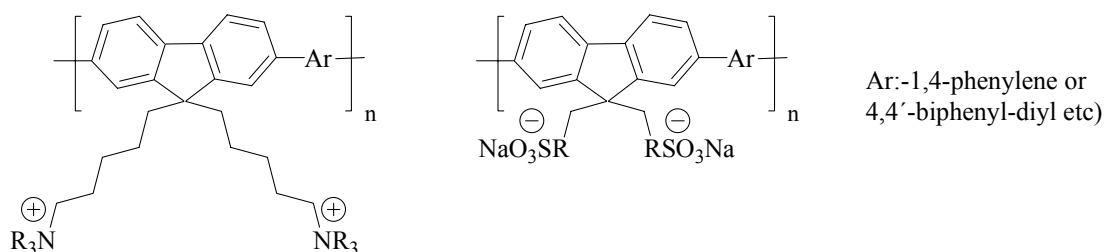
Fluorene-based polymers and copolymers are often targeted due to their strong blue fluorescence as well as chemical and photochemical stability and good synthetic accessibility. Nowadays there is a gaining importance for fluorene based water soluble polymers and copolymers as they might have some additional applications due to their water solubility.

Water soluble conjugated polymers are known to be attractive materials in OLEDs which are built in layer by layer self assembly approach. [89, 90] They can be also used as biological and chemical sensors as solubility in water is a prerequisite for interaction with biological substrates. [47, 62, 63, 64]

Efforts have to be done to synthesize new derivatives of water soluble polymers and copolymers which have improved optical, electronic and opto-electronic properties. Conjugated polymer/surfactant systems can be used to vary the aggregation behaviour and to increase the fluorescence quantum yield of the water soluble polymers in aqueous media. [19, 93, 94, 95]



Structure of a fluorene-type blue luminescent copolymer



Structures of Cationic & Anionic fluorene-type copolymers

1.2 Objective

The aim behind this work was to synthesize water soluble cationic and anionic semiconducting copolymers.

In our work we tried to synthesize some already known and a series of novel ionic, fluorene-type copolymers which can be interesting components in chemical and biological sensors. Solubility in water is essential for interacting with biological substrates such as proteins and DNA, and this property can be achieved by attaching charged, ionic functionalities as pendant groups of the conjugated backbone.

Some of the materials will be tested in polymer based light-emitting diodes (LEDs). A LED is a semiconductor device that emits visible light when an electric current passes through it. Several conjugated, water-soluble fluorene-type polymers and copolymers with phenylene, biphenyl, thienylene and bithiophene building blocks will be synthesized to vary the absorption and emission energies of the macromolecules.

The effect of ionic and non-ionic surfactants on the aqueous polymer solutions will be also studied. Different surfactants will be used to gain a deeper insight of the aggregation behaviour and the resulting optical properties, e.g. the fluorescence quantum yield after addition of surfactants.

These novel water-soluble materials will be tested for potential applications in optical, electronic and optoelectronic devices.

2 Introduction

2.1 Conjugated polymers

Due to their specific properties such as mechanical strength and good processability, polymer materials take a universal place in our daily life. A real current challenge for physicists and chemists is the design of novel functional polymers matching the (electronic) properties of semi-conductors for modern electronic applications.

In this context, π -conjugated polymers which are often intrinsic semi-conductors due to their delocalized π -electrons, have attracted much research effort in the last fifteen years. Most of the conjugated polymers studied today (Fig. 1) have a regular alternation of single and double bonds in the main chain as in the first known polymer of this type; polyacetylene. Such one-dimensional π -systems are often conceived, as having a two-band structure using the one-electron model approximation ^[98]. The highest occupied molecular orbitals (HOMO) form the occupied π -band (valence band) of the polymer and the lowest unoccupied molecular orbitals (LUMO) form the π^* -band (conduction band) of the polymer. As a consequence of the bond alternation, the band gap of neutral polymers lies in the range of ca. 1.5 (near IR) to 4 eV (UV), resulting in semiconductor properties.

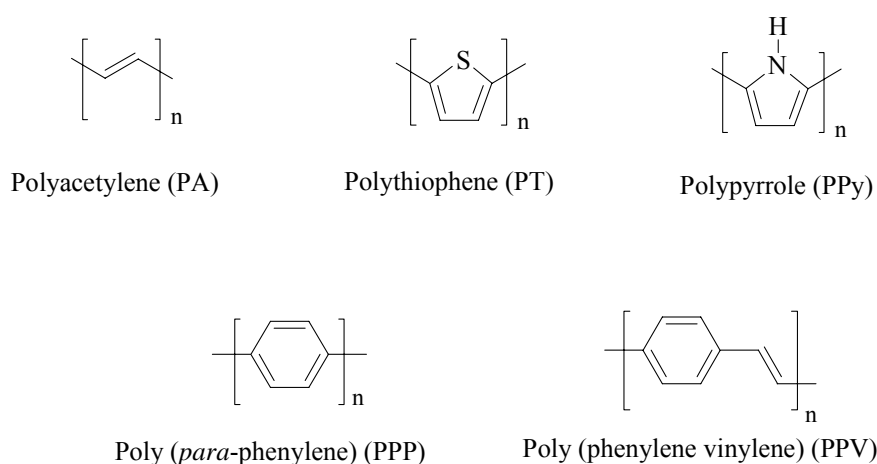


Fig. 1: Selection of conjugated polymers

A first major breakthrough in the field of conjugated polymers was achieved in 1977 when high electrical conductivities were observed by ‘doping’ neutral polyacetylene with strong oxidizing or reducing agents.^[1] Electrons are injected or removed (reduction or oxidation) during the interaction with so-called dopants. The polymer chains become oxidized or reduced; polaron or charged soliton states are formed which create midgap energy states. The materials show a dramatically increased electrical conductivity. For this reason interest in conjugated polymers was initially focused mainly on a high electrical conductivity of the materials.

Dopants are also used in inorganic semiconductors for altering their electronic properties in a controllable way. Semiconductors with excess electrons are called n-type semiconductors while semiconductor with a lack of electrons are called p-type semiconductor. Most common dopants for inorganic semiconductors (e.g. silicon) are phosphorus (P), arsenic (As), or antimony (Sb), for n-type doping; and boron (B) for p-type doping.

Recent interest in conjugated polymers is not focused to conductivity properties of doped conjugated materials. Now, the electronic and optical properties of neutral conjugated polymers have been also extensively studied and applied. Many new applications in photonic devices have been developed, including their use in organic light emitting diodes (OLEDs), organic field effect transistors (OFETs), organic solar cells etc. Conjugated polymers represent materials with both electronic and optical properties partially comparable to the properties of inorganic semiconductors, but have in addition the benefit of attractive mechanical and processing properties. Many of the original, unsubstituted conjugated polymers have been derivatized in order to control the processing. Of primary interest in this respect is the processability of the polymers from solution, in the form of soluble derivatives or via soluble precursor polymers which can be processed and subsequently converted to the insoluble conjugated form.

2.2 Electronic structure of a conjugated polymer ^[2]

The common feature of most polymeric organic semiconductors is that they consist of alternating single and double carbon–carbon bonds. Such materials

are said to be “conjugated” if it is possible to swap the positions of the single and double bonds and to end up with a structure that still satisfies the chemical-bonding requirements for carbon. Carbon–carbon double bonds are formed when two of the three 2p orbitals on each carbon atom combine with the 2s orbital to form three sp^2 “hybrid” orbitals. These orbitals lie in a plane, directed at 120° to one another, and form three σ “molecular” orbitals with neighbouring atoms, including two or more with carbons. The third p orbital on the carbon atom, p_z , points perpendicular to the other hybrid orbitals. It overlaps with the p_z orbital on neighbouring carbon atoms to form pairs of so-called π orbitals that are spread out or “delocalized” over the polymer chain. The low energy π (or bonding) occupied orbitals, form the valence band, while the higher energy π^* (or antibonding) orbitals forms the unoccupied conduction band. The occurrence of the “band gap” between valence and conduction band gives the polymer its semiconducting behaviour.

But a polymer must also satisfy two other conditions for it to work as a semiconductor. One is that the σ bonds should be much stronger than the π bonds so that they can hold the molecule intact even when there are excited states such as electrons and holes in the π bonds. (The excitation of the molecule weakens the π bonds and the molecule would split apart without strong σ bonds.) The other requirement is that π orbitals of neighbouring polymer molecules in the solid state should overlap with each other so that electrons and holes can move in three dimensions between molecules. Fortunately many polymers satisfy these three requirements.

Most conjugated polymers have semiconductor bandgaps of 1.5–4 eV, which means that they are ideal for optoelectronic devices that emit visible light. They can also be chemically modified in a variety of ways, and a lot of effort has been put into finding materials that can be processed easily from solution either as directly soluble polymers, or as “precursor” polymers that are first processed in solution and then converted *in situ* to form the semiconducting structure.

2.3 Fluorene-based conjugated polymers

Fluorene-based conjugated polymers have received considerable attention in the past few years for the high efficiencies both in PL^[3, 4] and in electroluminescence (EL).^[5, 76, 69, 82] Due to their pure blue and efficient electroluminescence coupled with a high charge-carrier mobility and good processability they have been discussed for display applications.^[6, 7, 8] Many new applications in photonic devices, other than as polymer LEDs, have been conceived for these materials. Polyfluorenes also possess excellent thermal stability^[9] and high stability against oxidants.^[10]

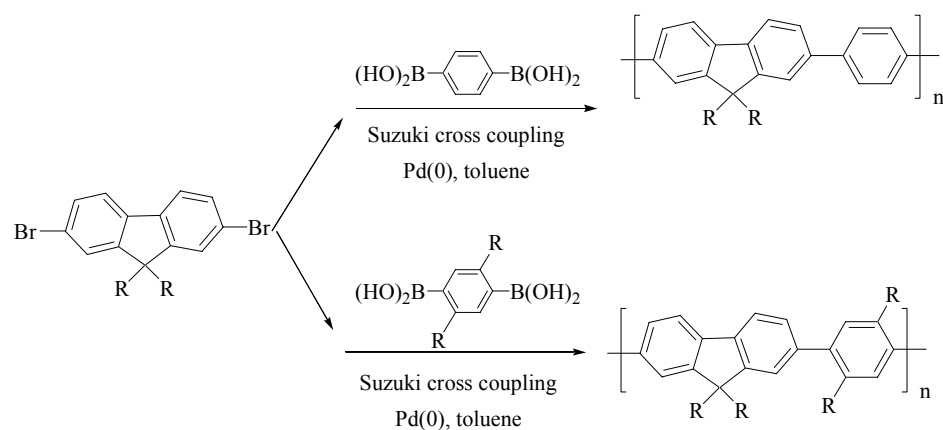


Fig. 2: a) Polyfluorene homopolymer b) Fluorene-type copolymer

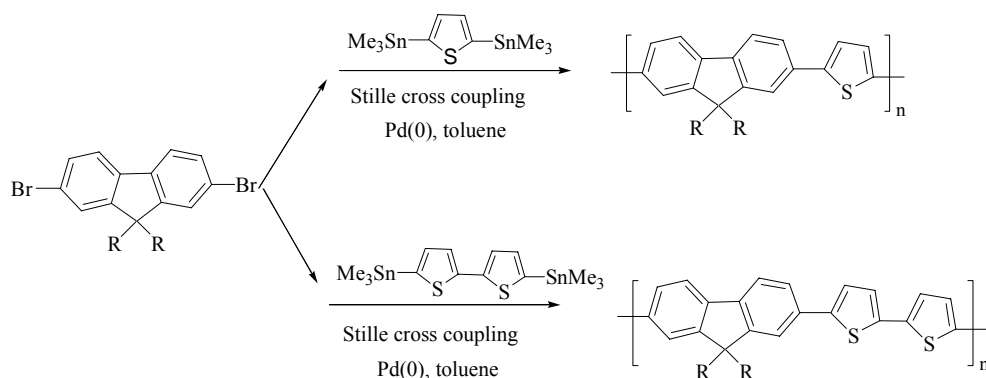
Conjugated copolymers based on alternating fluorene and phenylene building blocks (Fig. 2b, Ar:-1,4-phenylene) are also promising efficient and stable blue luminescent materials.^[11]

Polyfluorenes with alkyl side chains containing more than 6 carbons (Fig. 2a) are soluble in various organic solvents. They do not precipitate during the coupling reaction towards the polymers. For Polyfluorene synthesis both Suzuki and Yamamoto type coupling reactions have been successfully applied. The length of alkyl substituents does not alter the optical and electronic properties of polyfluorenes in dilute solutions. Additional chemically, chromophorically, or electronically active functional groups (endcaps) can be introduced into the terminal positions of the PF backbones.

Applying the cross-coupling methods according to *Suzuki* (Scheme 1) or *Stille* (Scheme 2) a bundle of alternating fluorene-type copolymers can be synthesized.



Scheme 1: Synthesis of alternating fluorene-type copolymers using the Suzuki-type cross coupling reaction.



Scheme 2: Synthesis of alternating fluorene-type copolymers using the Stille-type cross coupling reaction.

Polymers with large energy gaps that emit blue light efficiently are of special interest; these materials are desired for full color display applications and also serve as energy transfer donors in the presence of lower energy fluorophores. [101-104] Different copolymers based on fluorene building blocks have been found to emit light over the full range of colours (Fig. 4). The “colour triangle” of Fig. 4 shows some of the colours obtained using different -Ar-blocks of the copolymers. Pure red, green and blue light are at the apices of the triangle, with white near the centre. “Target” red–green–blue colours specified for the PAL colour co-ordinate system are also shown. Fig. 3 shows structures of different fluorene-based copolymers and their emission colour.

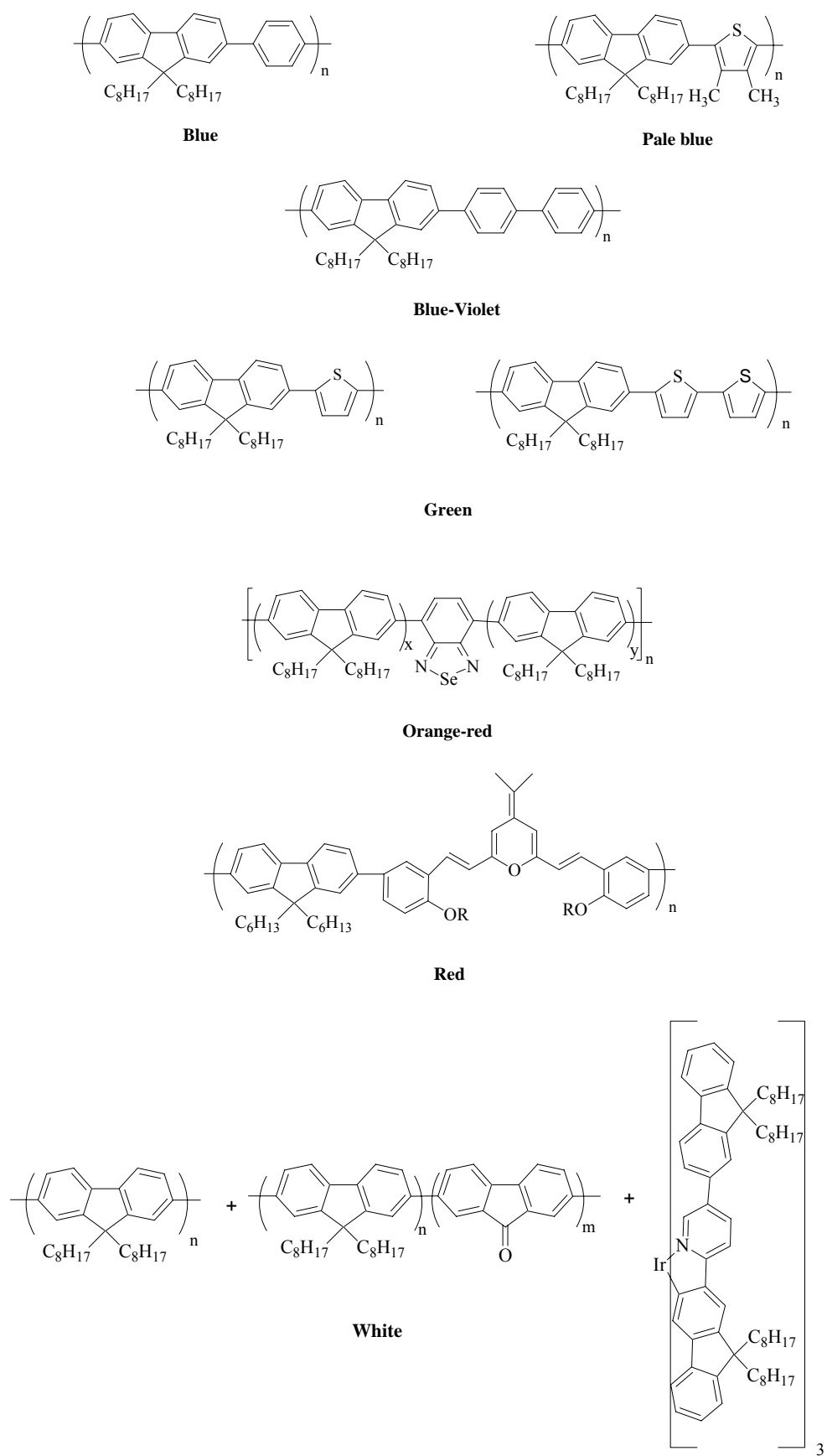


Fig. 3: Structures of fluorene-based copolymers used in OLED devices

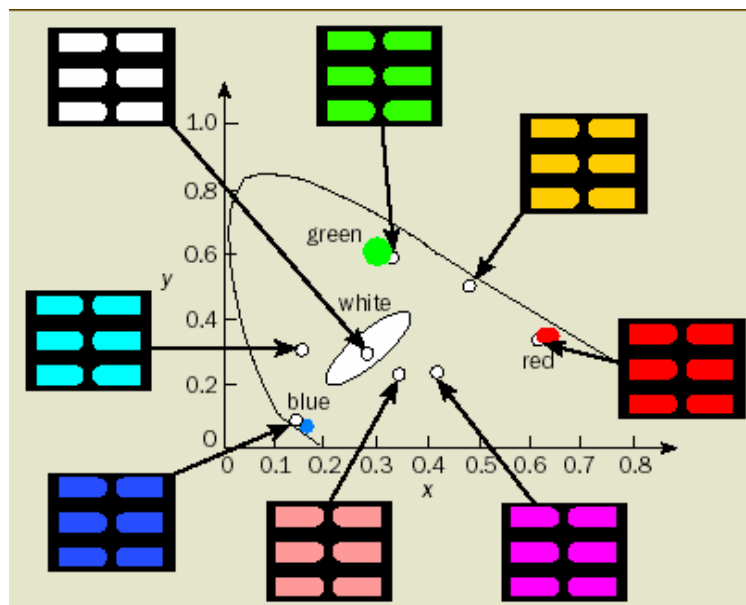


Fig. 4: Emission colours of different fluorene-based copolymers

2.4 Conjugated polyelectrolytes (Water soluble polymers)

Conjugated polyelectrolytes (CPEs) have recently received considerable interest due to their unique properties and promise that they may be technologically useful. ^[12-21] CPEs possess an intrinsic tendency to organize into supramolecular architectures in solution and in the solid state owing to electrostatic and hydrophobic interactions. ^[15, 16] In addition, the materials feature distinctive optical and electronic properties such as strong absorption in the visible region, ^[12, 14, 22] strong fluorescence and electrical conductivity in the doped state. ^[23, 24]

The unique combination of optical, electronic and materials properties exhibited by CPEs makes them versatile materials for a new generation of optical, electronic and optoelectronic devices. Potential applications of water soluble conjugated polymers include the construction of active layers in organic light-emitting diodes through a layer-by-layer self-assembly approach, ^[25] as buffer layer or emissive layer materials in inkjet printing fabricated organic LEDs, ^[26] and as highly sensitive fluorescent sensory materials. ^[27]

Pendant group functionalization of conjugated polymers has proven to be a useful method for improving the processability of the typically insoluble and infusible materials. The water-solubility in such polymers is achieved by

functionalizing the solubilizing side chains with ionic carboxylate, sulfonate, phosphonate and ammonium groups. These polymers are, therefore, anionic or cationic polyelectrolytes. For example, water soluble poly(phenylene vinylene) (PPV),^[22] poly(phenylene) (PP)^[28], poly(phenyleneethynylene) (PPE)^[29] and polythiophene (PT)^[30] have been obtained recently with either cationic or anionic functions.

Some of the examples will be now discussed in more detail: The various palladium-catalysed coupling methods (i.e. *Suzuki*, *Stille*, *Heck*, *Sonogashira*) have gained considerable popularity due to mild reaction conditions, wide functional group tolerance, and versatility of the solvent used for polymerisation. These reactions are especially useful for the preparation of mid and wide bandgap CPEs. The report of the synthesis of a water soluble PPV by *Shi and Wudl*^[22] and water soluble PPP by *Wallow and Novak*^[31] were the most important initial contributions to this area. In the decade since these early reports appeared, several synthetic methods have been developed, leading to many new CPE structures. Most of the CPEs that have been prepared contain PPP, PPV or PPE backbones decorated with ionic functional groups such as sulphonate (SO_3^-), carboxylate (CO_2^-), phosphonate (PO_3^{2-}) and ammonium (NR_3^+). Most of these CPEs are strongly fluorescent in solution and in the solid state. Materials properties like film formation, absorption and fluorescence behaviour have been important in development of CPEs as active materials for electronic devices.

The first synthesis of a PPP-type CPE, **A** was reported by *Wallow and Novak*^[31] using the Suzuki cross coupling reaction (Scheme 3). A noteworthy feature of PPPs is their relatively high thermal and chemical stability.^[33] *Rau and Rehahn*^[32] developed a precursor approach to synthesize a water soluble PPP, **B** (Scheme 4). Synthesis of the first sulphonated PPP **C** was reported by *Wegner and co-workers* (Scheme 5).^[34]

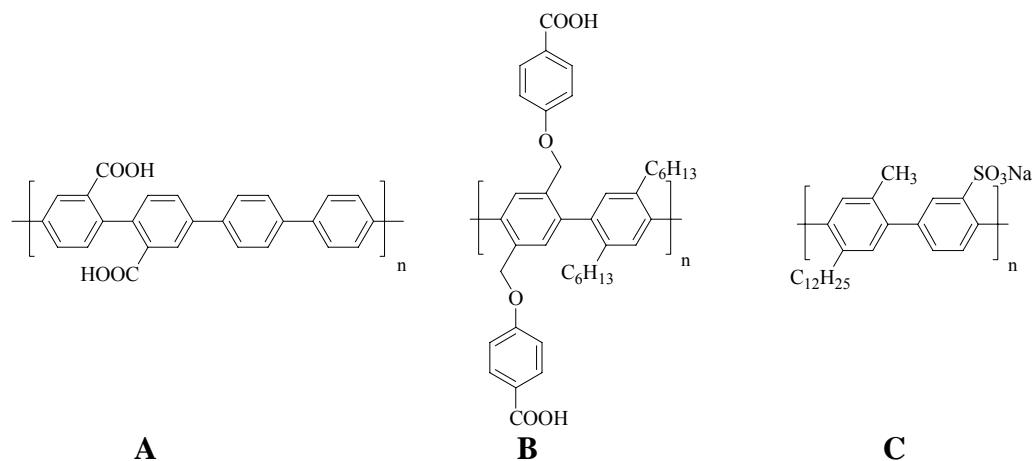
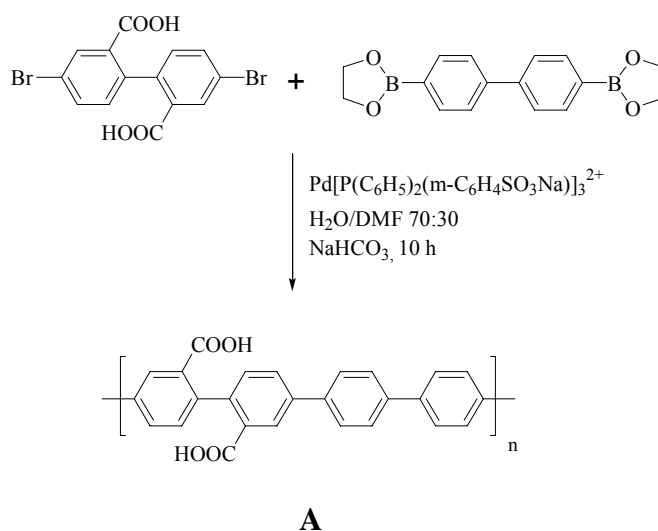
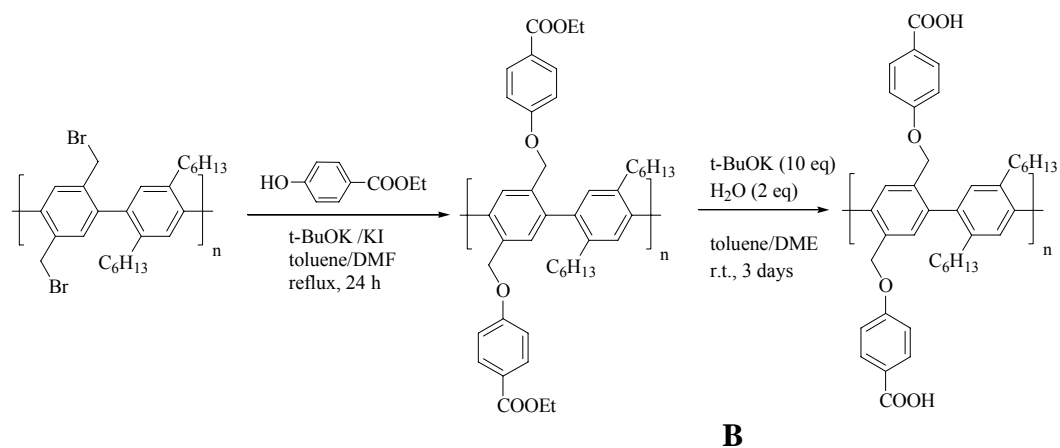


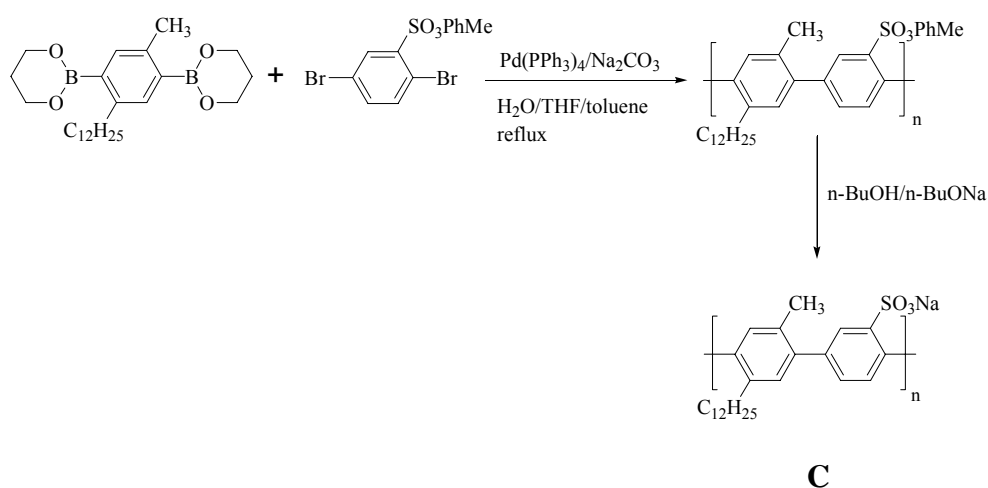
Fig. 5: Anionic poly(*para*-phenylene) (PPP)-type CPEs



Scheme 3: Synthesis of first PPP-type CPE **A** by Wallow and Novak

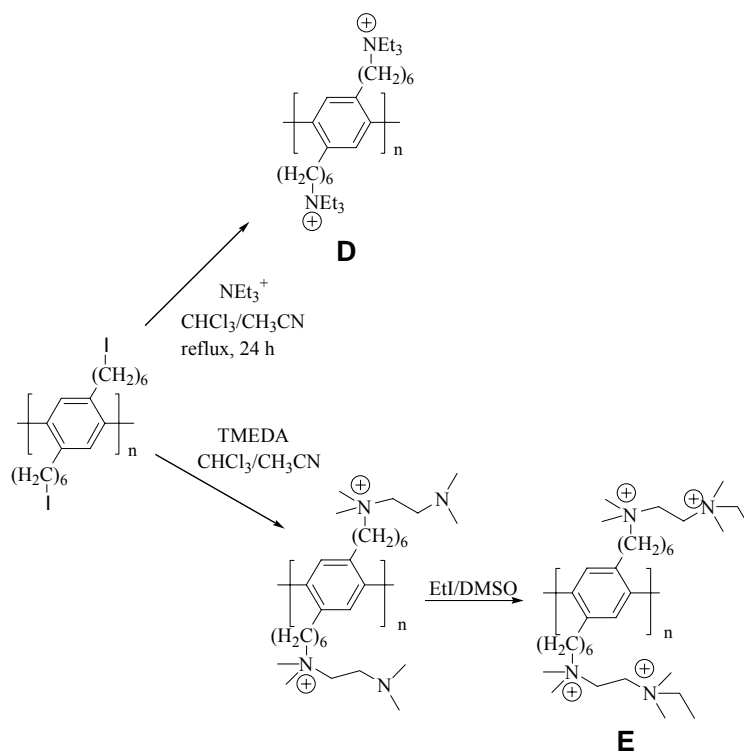


Scheme 4: Synthesis of a PPP-type CPE **B** by Rau and Rehahn



Scheme 5: Synthesis of PPP-type CPE **C** by Wegner and co-workers

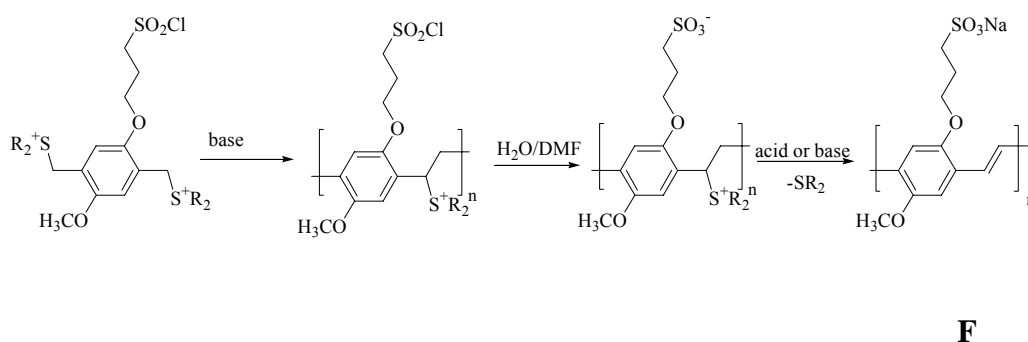
The first synthesis of a cationic PPP-based CPE was reported by *Ballauff and Rehahn*,^[31] **D**. Two years later, *Wittmann and Rehahn*^[36] reported the synthesis of a highly charged cationic PPP, **E**. (Scheme 6)



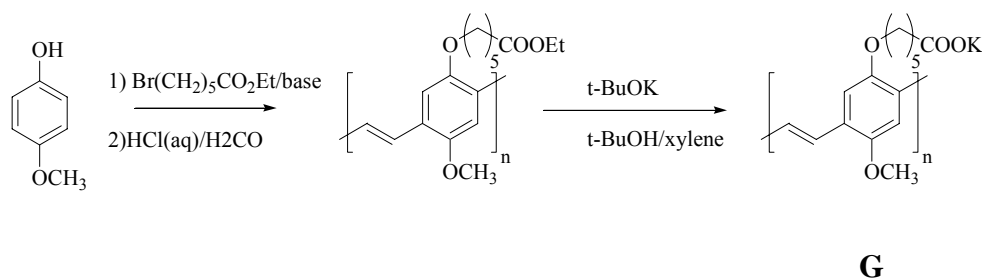
Scheme 6: Cationic Poly(*para*-phenylene) (PPP)-type CPEs

Shi and Wudl [22] reported the synthesis of a PPV-type polyelectrolyte **F** (Scheme 7), *Peng and coworkers* [37] designed a PPV-type CPE bearing cross-conjugated side chains with carboxylate groups. This polymer was designed with the objective of producing a nanoporous polymer network with controllable uniform pore sizes by means of layer-by-layer self assembly. The carboxylate groups provided the polymer with water solubility and interchain hydrogen bonds in the solid state, acting as 'anchors' during deposition.

Another water soluble PPV-type CPE, **G** was synthesized by *Fujii and coworkers* [38, 39] by using a straightforward synthetic approach. **G** was obtained by direct polymerization of the corresponding monomer by means of the so-called *Gilch* route (Scheme 8).

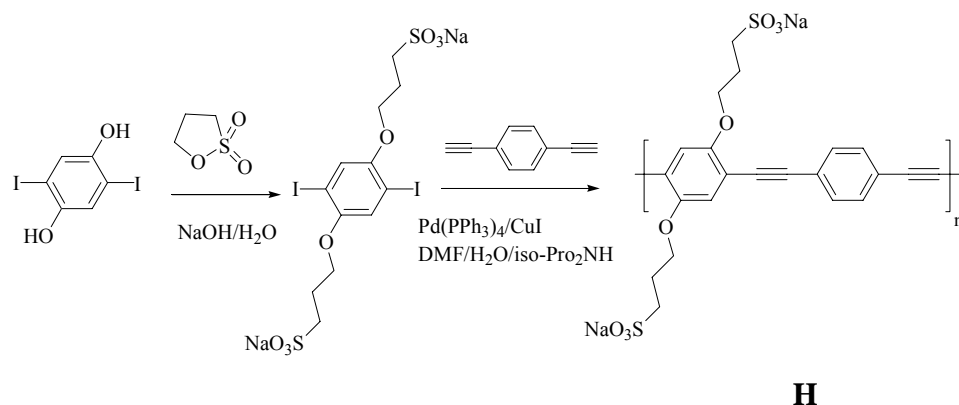


Scheme 7: Synthesis of a PPV-type polyelectrolyte **F** by *Shi and Wudl*



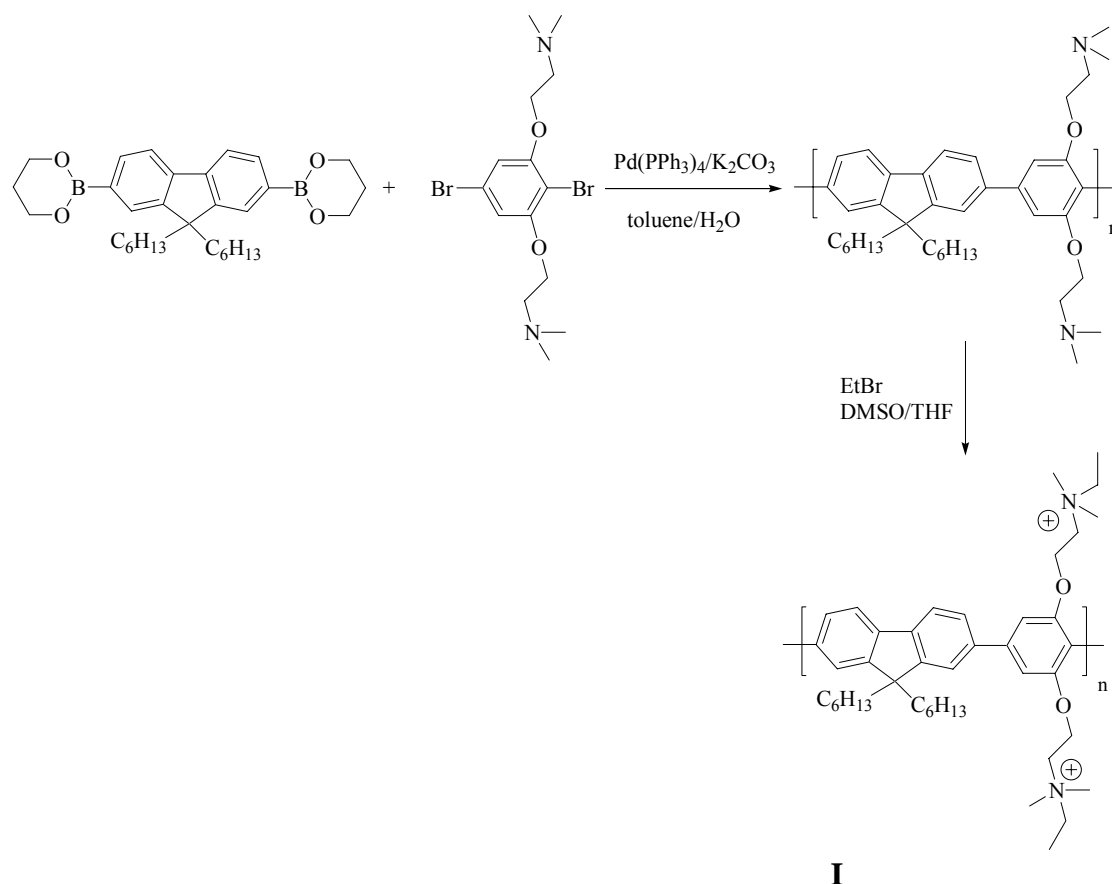
Scheme 8: Synthesis of a PPV-type polyelectrolyte **G** by *Fujii and co-workers*

The first PPE-type CPE was reported by *Li and co-workers*. [40, 41] *Pinto and Schanze* [42] described a PPE-type CPE, **H** (Scheme 9), which contains sulphonate groups attached to the polymer backbone, which was obtained by a *Sonogashira*-type coupling reaction.



Scheme 9: Synthesis of a PPE-type CPE by Pinto and Schanze

Nowadays cationic and anionic water-soluble fluorene-based alternating copolymers are gaining importance. ^[43] *Lai, Huang and co-workers* reported the synthesis of a fluorene-based cationic CPE, **I** by applying the neutral polymer precursor approach developed by *Reynolds and co-workers* (Scheme 10).



Scheme 10: Synthesis of a PF-type CPE by Lai, Huang and co-workers

2.5 Applications of conjugated polyelectrolytes as water soluble polymers

One of the most active areas in conjugated polymer chemistry and physics is the development of polymer light emitting diodes (PLEDs). A large number of groups have explored the application of CPEs to fabricate PLEDs. In one of the first applications in this area, *Rubner and Reynolds* ^[44] reported the fabrication of PLEDs.

Another area of widespread interest that involves the application of conjugated polymers is the construction of conjugated polymer-based photovoltaic (PV) devices. Work in this area was stimulated by the report by *Heeger, Wudl and co-workers* ^[45] that relatively efficient PV devices could be fabricated by blending a conjugated polymer with an electron acceptor (e.g. a fullerene derivative).

Another area which has received much attention for the application of CPEs is the development of highly sensitive fluorescence-based sensors for chemical and biological targets. ^[46]

Most applications of conjugated polymers in electronic, optoelectronic, ^[47-52] electrochemical or sensing devices require the materials to be fabricated in a thin film format. The most common method used is spincoating for neutral CPs. Langmuir-Blodgett method can be used for multilayer films. A method which involves layer-by-layer (LBL) deposition of oppositely charged polyelectrolytes, has received considerable attention since its discovery by *Decher and co-workers* in early 1990's. ^[53-54]

2.5.1 Polymer light-emitting diode

The first Polymer Light-Emitting Diode (PLED) was reported in 1990 and the development has since been very fast. Since the discovery of PLEDs ^[56] considerable progress has been made in the development of new conjugated polymers and in the performance of related PLEDs. ^[97-100] In the most simple configuration, a PLED consists of an undoped conjugated polymer, sandwiched between two proper electrodes at a short distance (50-100 nm). Simple PLEDs are usually constructed as shown in Fig. 6.

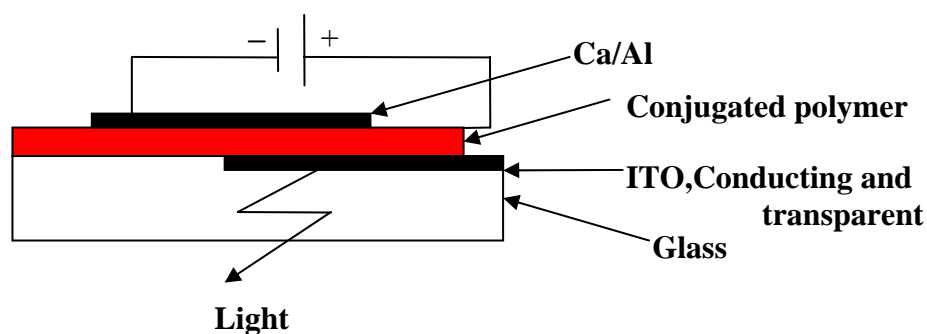


Fig. 6: Schematic design of a polymer light-emitting diode (PLED).

The advantage of PLEDs over semiconductor based-light emitting diodes is that large area diodes can be prepared by spincoating, commonly used for lithographic processes in semiconducting industry. The diodes are driven with low dc voltage of 2-10V. The state-of-the-art PLEDs today have an external quantum efficiency of up to 5 %.

Conjugated polymers derive their semiconducting properties ^[55] from having delocalized p-electron bonding along the polymer chain. The π bonding and π^* antibonding orbitals form delocalized valence and conduction wavefunctions, which support mobile charge carriers.

Electroluminescence from conjugated polymers was first reported ^[56] using poly(phenylene vinylene) (PPV), as the single semiconductor layer between two electrodes. In this structure, an indium-tin oxide (ITO) layer functions as a transparent electrode (anode) and allows the light generated within the diode to leave the device. The top electrode (cathode) is conveniently formed by thermal evaporation of a low work function metal (Ca, Al, Mg, Ag, etc). LED operation is achieved when the diode is biased sufficiently to achieve injection of positive and negative charge carriers from opposite electrodes. Capture of oppositely charged carriers within the region of the polymer layer result in the formation of excitons and subsequent photon emission. Diodes of this type can be readily fabricated by solution-processing the semiconducting polymer onto the ITO-coated glass, even though the film thickness is typically <100 nm. Spincoating from solution has been demonstrated to be capable of producing highly uniform layer thickness, with no more than a few Å thickness spread over several cm^2 . Electrodes are chosen to facilitate charge injection; ITO has a relatively high work function and is therefore suitable for use as a hole-

injecting electrode, and low work-function metals such as Al, Mg, or Ca are suitable for injection of electrons.

2.5.2 Conjugated polymers as platforms for biological sensors ^[57-60]

Conjugated polymers have unique optical, electrical, electrochemical and optoelectronic properties, which can be modified by environmental stimuli such as temperature, solvent, electrolyte, etc. Hence, conjugated polymers can detect, transduce, and amplify physical or chemical stimuli into an electrical, optical or electrochemical signal. In addition to the tremendous research and industrial progress in using conjugated polymers in organic light emitting diodes (OLED), photovoltaic cells, lasers, etc. Conjugated polymers have been found to be interesting and promising as sensory materials to detect chemical (chemosensors) or bioactive species (biosensors). ^[61-63]

Intrachain and interchain energy transfer processes ^[64, 65] allow excitations to sample multiple environments. ^[66] If one of these sites is in close proximity to a fluorescence quencher molecule, the result is an enhancement (amplification) of the quenching event. Especially if the removal of a quencher molecule from the vicinity of the conjugated polymer can be coupled to the presence of a target analyte, one obtains the platform for optical fluorescence sensing. In this case, all the advantages of fluorescence sensing can be used (high sensitivity).

Solubility in water is essential for interacting with biological substrates such as proteins and DNA, and this property can be achieved in conjugated polymers by attaching charged functionalities as pendant groups on the conjugated backbone ^[67] (formation of conjugated polyelectrolytes:CPEs).

2.5.3 Water soluble conjugated polymers for biosensors ^[68-72]

As a new class of highly sensitive chemo- and biosensors, water soluble conjugated polymers show great potential. ^[73-76] However, water solubility of the CPs is required. The resulting properties of aqueous solutions are typical of amphiphilic polyelectrolytes, for which interactions with DNA have been intensively studied. ^[77] Indeed, the strength of the interactions between cationic

polyelectrolytes and DNA has recently been used to recognize the tertiary structure of plasmid DNA. [78-81]

In one type of biosensors, a photoinduced electron transfer process from the excited water soluble conjugated polymer to quencher molecule is utilized to quench the fluorescence of the polymer. Due to the opposite charges of conjugated polymer and quencher molecule, a complex formation is observed. If this quencher is removed from the close proximity of the conjugated polymer, the electron transfer process is stopped and the polymer fluorescence can occur. Fluorene based ionic oligomers and polymers have been thereby favored due to their strong blue fluorescence as well as chemical and photochemical stability and good synthetic accessibility.

It is also known that there is a substantial specificity in the interaction between polyelectrolytes and the secondary and tertiary structure of DNA. [78] In case of conjugated polyelectrolytes, it is likely that aggregation of the fluorophores within the vicinity of DNA influences their optical properties by mechanisms such as relaxation or contraction of the polymer secondary structure, self-quenching, and photoinduced charge transfer to the DNA bases [2] Additionally, single stranded DNA (ssDNA) and double stranded DNA (dsDNA) have different hydrophilic surfaces, which influence the mode of interaction between the hydrophobic and charged regions of polyelectrolytes. Understanding how these phenomena come together in complex biological mixtures is an important for a rational design of quantitative conjugated polymer-based DNA assays.

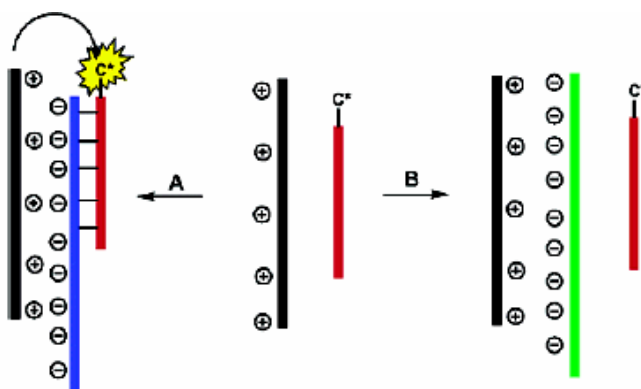


Fig. 7: Schematic design of the interaction of a water-soluble CPE/ Single-stranded DNA complex with a complementary, neutral C*-labelled PNA

Bazan et. al. developed sensors that detect single-stranded deoxyribonucleic acid (ssDNA) with a specific base sequence.^[79] The ssDNA sequence sensor comprises an aqueous solution containing a cationic water soluble conjugated polymer and a single stranded, neutral peptide nucleic acid (ssPNA) labeled with a dye (e.g. fluorescein). After complexation between the cationic conjugated polyelectrolyte and the negatively charged ssDNA analyte only the complementary neutral, dye-labelled PNA can bind to the complex. The emission of light with the wavelength characteristic of the dye label (C*) indicates the presence of ssDNA with a specific base sequence complementary to that of the probe ssPNA- C*:fluorescein-dyed. Maximum energy transfer from the cationic water soluble conjugated polymer to the signaling chromophore (C*:fluorescein) occurs when the ratio of polyelectrolyte chains to ssDNA strands is approximately 1:1. Fluorescence energy transfer (FRET) from the cationic water-soluble conjugated polymer to the dye C* results in a emission that is more intense than that observed by direct excitation of the chromophore. Furthermore, the decrease in energy transfer upon addition of salts indicates that electrostatic forces dominate the interactions between cationic water-soluble conjugated polymer and DNA.

The principle of the DNA sensor assay relying on light harvesting and electrostatic properties of cationic conjugated polymers (CPs) is shown in Fig. 7.^[82, 83] The assay contains a solution of cationic CP and a peptide nucleic acid (PNA) strand^[84] labelled with a chromophore dye (C*). The optical properties of the CP and C* are optimized so that Förster energy transfer (FRET) from CP (donor) to C* (acceptor) is favored. Because PNA is neutral, there are no electrostatic interactions between PNA-C* and the CP. Situation A of Fig. 7 corresponds to the addition of a complementary ssDNA, which hybridizes with the target PNA. Hybridization endows with a double-stranded C*-bearing macromolecular complex with multiple negative charges. Electrostatic attraction then causes the formation of a complex between CP and the DNA/PNA-C* hybrid, allowing for FRET from the CP to the dye C*. When a ssDNA is added that does not match the PNA sequence, (situation B), hybridization does not take place. Electrostatic complexation occurs only between the CP and DNA. The average distance between CP and PNA-C* is too large for an efficient FRET.

A modification of the scheme was based on the idea that the electrostatic interaction between a dsDNA and a cationic CP would be stronger than that of a ssDNA and the CP. Fig. 8 shows the two situations resulting from the interaction between ssDNA-C* (shown in red) and a complementary strand (in blue, situation A) or a noncomplementary strand (in green, situation B) in the presence of a cationic CP (in black). The higher local charge density of the double strand should result in a stronger dsDNA-C*/CP electrostatic attraction relative to ssDNA-C*/CP.^[85] Additionally, in the case of a noncomplementary sequence, the nonhybridized strand will interfere with the ssDNA-C*/CP interactions. Based exclusively on these considerations, one would expect closer proximity when the “target” strand is present and therefore more efficient FRET from the CP to C* in situation A. This principle was realised in sensors by *Bazan et. al.*

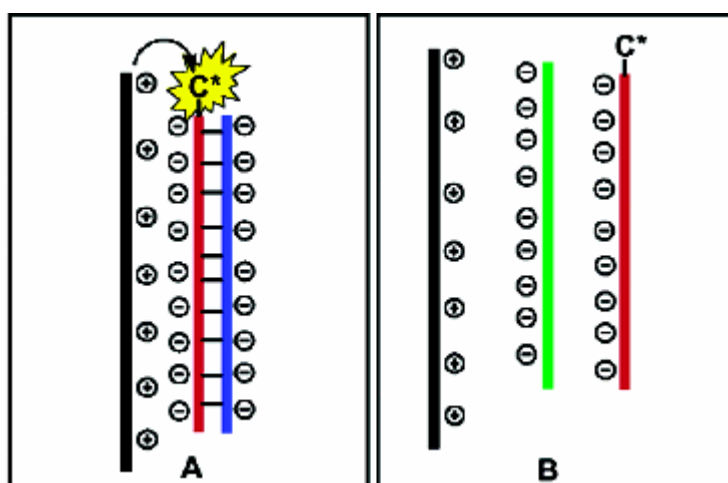


Fig. 8: Schematic design of the interaction of a water-soluble CPE/ss DNA-C* complex with a complementary (A), with a non-complementary strand (B)

2.5.4 Layer-by-Layer self-assembly method

Most applications of conjugated polymers in electronic, optoelectronic, electrochemical or sensing devices require the materials to be fabricated in a thin film format. The most common technique for fabricating thin films of neutral CPs is by spincoating; however some groups have successfully fabricated organized multi-molecular layer films also by the so-called Langmuir-Blodgett method.^[86, 87] Another alternative method is available for

fabricating, multilayer thin films of CPEs. This method, which involves layer-by-layer (LBL) deposition of oppositely charged polyelectrolytes, has received considerable attention since its discovery in the early 1990's. ^[88, 89]

Interestingly, it is possible to control the thickness and morphology of LBL films by varying the deposition conditions as concentration, temperature, solvent etc. ^[90] Specifically, polyelectrolyte deposition from low ionic strength solutions produces relatively thin and flat films, in which the polymer chains are tightly packed. ^[91] Conversely, deposition from high ionic strength solutions produces relatively thicker films with a rough surface topology, presumably due to polymer chain entanglement and interpenetration between layers. ^[91]

3 Results and Discussion

Water-solubility of conjugated polymers may offer many new application opportunities. Potential applications of water-soluble conjugated polymers include the construction of active layers in organic light-emitting diodes through a layer-by-layer (LBL) self-assembly approach, and as highly sensitive fluorescent sensory materials in sensor assays. Such applications generally favor materials with high photoluminescence (PL) efficiencies. The LBL self-assembly approach requires anionic as well as cationic conjugated polymer electrolytes (CPEs).

Fluorene-based conjugated polymers have received considerable attention in the past few years for their high efficiencies both in PL and in electroluminescence (EL).^[5] The water-solubility in such polymers can be achieved by functionalizing the solubilizing side chains with terminal sulfonate or ammonium groups. The resulting polymers and co-polymers are, therefore, anionic or cationic polyelectrolytes.

In this work, anionic and cationic conjugated polyelectrolytes (CPEs) of the fluorine-type with phenylene, biphenylene, thiophene and bithiophene moieties (“spacers”) have been synthesized and characterized.

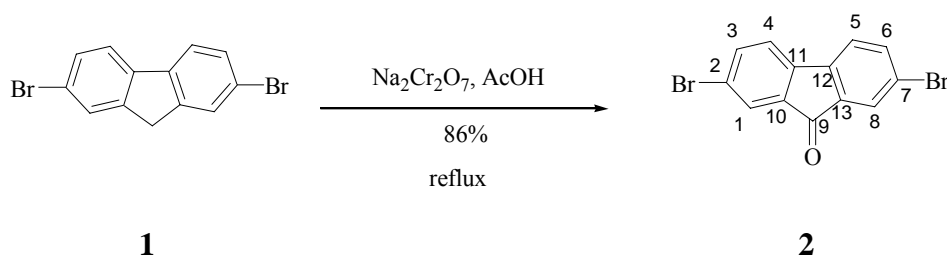
3.1 Synthesis of an anionic water-soluble fluorene-type copolymer with a 1,4-phenylene spacer

The copolymerisation approach has been widely used in the preparation of conjugated polymers to achieve specific electronic & physical properties. It is demonstrated that copolymerisation of the fluorene unit with various other aryl moieties allows for a tunability of the electronic properties and an enhanced stability.^[134, 135]

By copolymerisation of ionic fluorene monomers with different aryl comonomers, the electronic properties of the resulting copolymers can be tuned in a wide range, absorption and emission as well as their redox potentials.

First, fluorene-based alternating copolymers with additional phenylene spacer units will be discussed.

Synthesis of poly[9,9-bis(4-sulfonylbutoxyphenyl)fluorene-co-1,4-phenylene] **17** started from the commercially available 2,7-dibromofluorene **1**. 2,7-dibromofluorene **1** was oxidized to 2,7-dibromofluoren-9-one **2** with sodium dichromate and acetic acid in 86 % yield (Scheme 11).

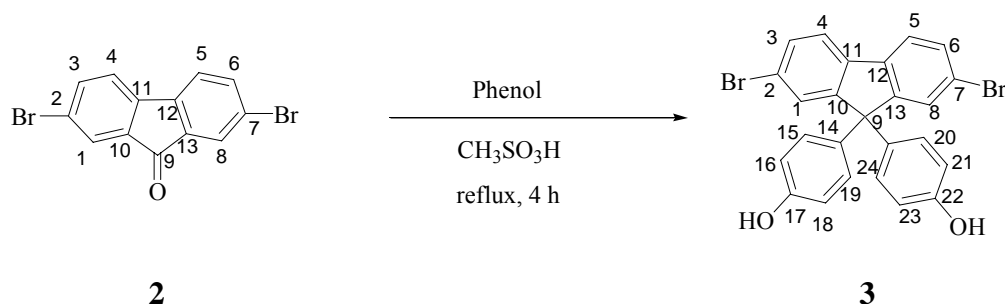


Scheme 11: Synthesis of 2,7-dibromofluoren-9-one **2**

2,7-dibromofluoren-9-one **2** was characterized by $^1\text{H-NMR}$ and $^{13}\text{C-NMR}$ spectroscopy, as well as mass spectrometry. From $^1\text{H-NMR}$ spectroscopy, we could see three aromatic signals at 7.93 ppm (H1, H8), 7.68 ppm (H3, H6) and 7.4 ppm (H4, H5) indicating quantitative oxidation of 2,7-dibromofluorene **1**. Signal at 7.93 ppm is deshielded because of the adjacent carbonyl carbon and bromine functionalities. There is ortho coupling between protons H3 & H4, H5 & H6 ($J=8.1$ Hz).

Oxidation of 2,7-dibromofluorene **1** was confirmed by $^{13}\text{C-NMR}$ spectroscopy. $^{13}\text{C-NMR}$ spectroscopy shows 6 signals of non-equivalent aromatic carbons (δ : 138.9, 137.2, 136.0, 133.9, 129.3, 121.7 ppm). The signal at 185.5 ppm indicates the presence of carbonyl carbon at C9 position, which is present in the starting compound **1**. In mass spectrum, the base peak is observed at 338 (M^+) and a typical fragmentation pattern is also seen.

The next step was conversion of 2,7-dibromofluoren-9-one **2** to 2,7-dibromo-9,9-bis(4-hydroxyphenyl)fluorene **3**, by reacting **2** with phenol and methanesulfonic acid in about 60 % yield (Scheme 12).

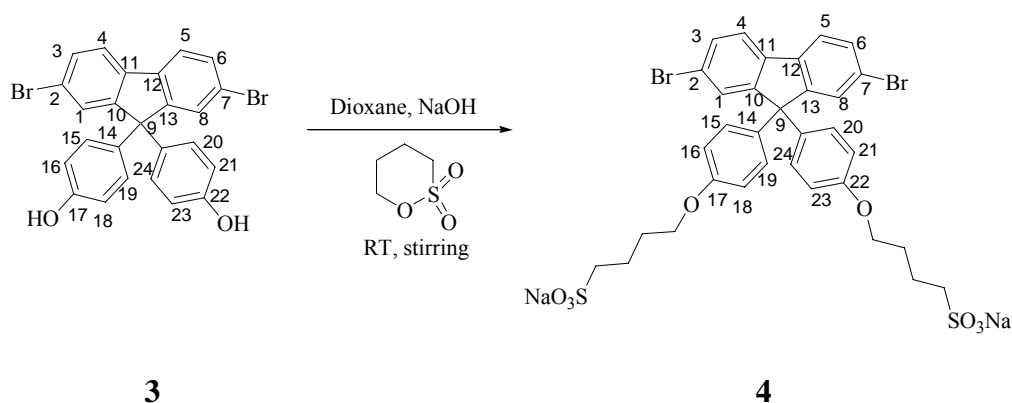


Scheme 12: Synthesis of 2,7-dibromo-9,9-bis(4-hydroxyphenyl)fluorene **3**

$^1\text{H-NMR}$ spectroscopy of **3** shows 5 doublet signals for aromatic protons at 7.82 ppm (H1, H8), 7.62 ppm (H3, H6), 7.50 ppm (H4, H5), 6.85 ppm (H15, H19, H20, H24) and 6.65 ppm (H16, H18, H21, H23) respectively. Aromatic protons H1 and H8 are more deshielded than the other aromatic protons as they are adjacent to the electron withdrawing bromine group and phenyl groups.

The $^{13}\text{C-NMR}$ spectrum of 2,7-dibromo-9,9-bis(4-hydroxyphenyl)fluorene **3** shows 11 signals, 10 of non-equivalent aromatic carbons (δ :115.2, 118.7, 122.8, 128.5, 129.2, 130.5, 134.3, 137.4, 153.8, 156.3 ppm) and one signal at 63.9 ppm for the aliphatic carbon. Signal at 156.3 ppm represents C22 and C17 which are attached to the $-\text{OH}$ group. Mass spectrum shows a base peak at 508 (M^+).

Our first aim was to synthesize an anionic water soluble copolymer so the OH-group of 2,7-dibromo-9,9-bis(4-hydroxyphenyl)fluorene **3** has to be converted to an ionic group. This was achieved by reacting **3** with 1,4-butane-sultone in dioxane and NaOH (Scheme 13).^[133, 134]



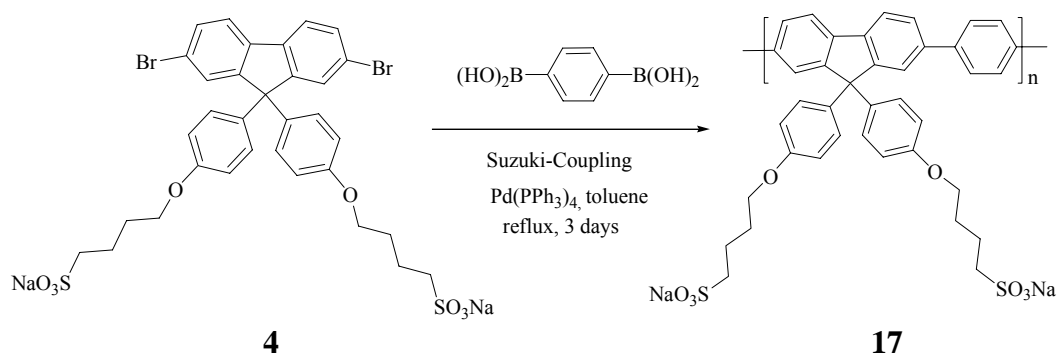
Scheme 13: Synthesis of 2,7-dibromo-9,9-bis(4-sulfonylbutoxyphenyl)fluorene **4**

2,7-dibromo-9,9-bis(4-sulfonylbutoxyphenyl)fluorene **4** was characterized by $^1\text{H-NMR}$, $^{13}\text{C-NMR}$, and IR-spectroscopy, as well as mass spectrometry. $^1\text{H-NMR}$ spectrum showed 9 signals, 4 additional signals for the alkyl ($-\text{CH}_2$) groups were detected which are not present in the starter. Five signals for aromatic protons at 7.82 ppm (H1, H8) 7.62 ppm (H3, H6), 7.50 ppm (H4, H5), 6.85 ppm (H15, H19, H21, H25), 6.65 ppm (H16, H18, H22, H24), and four signals for alkyl ($-\text{CH}_2$) groups at 3.9 ppm ($\alpha\text{-CH}_2$), 3.3 ppm ($\delta\text{-CH}_2$), 2.3 ppm ($\gamma\text{-CH}_2$), 1.7 ppm ($\beta\text{-CH}_2$) have been observed. Signal at 3.9 ppm is for the CH_2 protons which are close to the oxygen which is directly attached to the aromatic functionality. Signal at 3.3 ppm is for the CH_2 protons which are close to the sulphonate group.

$^{13}\text{C-NMR}$ spectroscopy of 2,7-dibromo-9,9-bis(4-sulfonylbutoxyphenyl)fluorene **4** showed 15 signals, 10 signals for non-equivalent aromatic carbons (δ : 114.9, 118.7, 122.8, 128.5, 129.2, 130.5, 134.3, 137.4, 153.8, 157.7 ppm), 4 signals (δ : 21.7, 27.9, 51.3, 67.2 ppm) for the methylene ($-\text{CH}_2$) groups, and one signal at 63.9 ppm for C9.

The mass spectrum shows a base peak at 824 (M^+) for **4** and IR-spectra shows peaks at 3070, 2942, 2872, 1607, 1569, 1508, 1452, 1178, 1048, 807, 604 cm^{-1} . Peak at 3070 cm^{-1} is for aromatic C-H stretching, peaks at 2942 and 2872 cm^{-1} are for C-H stretching due to the butyl group. Aromatic C=C stretching is observed at 1600 cm^{-1} . Asymmetric and symmetric stretching of S=O is observed at 1178 and 1048 cm^{-1} .

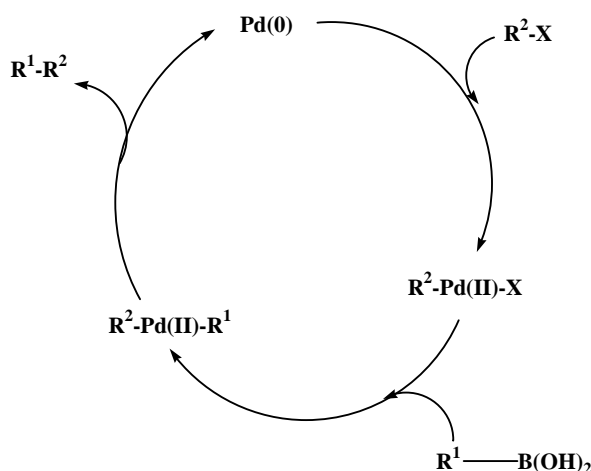
Finally this monomer was subjected to a Suzuki-type cross coupling reaction of 2,7-dibromo-9,9-bis(4-sulfonylbutoxyphenyl)fluorene **4** and 1,4-phenylene di-boronic acid in 1:1 molar ratio. Pd(0) is used in catalytic amount (5 mol %). Reaction was carried out in refluxing toluene/aqueous sodium carbonate solution for 4 days (Scheme **14**). The copolymer obtained was a water soluble solid. Purification of **17** was done by dialysis with water using a dialysis membrane cutoff of $\overline{M}_n = 3,500 \text{ gmol}^{-1}$ (details in section **4.5**).



Scheme 14: Synthesis of poly[9,9-bis(4-sulfonylbutoxyphenyl)fluorene-co-1,4-phenylene] **17**

A general catalytic cycle for the *Suzuki-type* ^[96, 116, 117] cross-coupling reaction involves oxidative addition, transmetalation and subsequent elimination (Scheme 15).

Oxidative addition is often the rate determining step in the catalytic cycle. An electron withdrawing group on the aryl halide increases the reactivity towards palladium catalysts. Normally the transmetalation between organopalladium (II) halide and organoboron compounds does not occur readily due to the moderate nucleophilicity of organic group on boron atom.



Scheme 15: A general catalytic cycle for the cross-coupling reaction after Suzuki

However, the reaction is carried out under basic condition so that the nucleophilicity of boron atom can be enhanced by forming a so-called “ate” complex with negatively charged base. Such “ate” complexes undergo a clean transmetalation reaction with the aryl halide.

$^1\text{H-NMR}$ data of the copolymer **17** is given in the experimental section (measured in D_2O). The GPC analysis (PS calibration) for this copolymer was done using NMP/LiBr as eluent, providing a number average molecular weight (\overline{M}_n) of 6500 gmol^{-1} . The degree of polymerisation is ca 9. The determination of molecular weights of such water soluble copolymer was difficult. The reason for the relatively low molecular weights detected by GPC analysis might be the formation of aggregates.

3.1.1 Absorption and photoluminescence properties of **17**

Absorption and emission spectra for poly[9,9-bis(4-sulfonylbutoxyphenyl)-fluorene-*co*-1,4-phenylene] **17** were measured in water at room temperature (Fig. 9). Poly[9,9-bis(4-sulfonylbutoxyphenyl)fluorene-*co*-1,4-phenylene] **17** shows an absorption band at $\lambda_{\text{max}} = 368 \text{ nm}$. There is some blue shift of 6 nm as compared to the homopolymer polyfluorene ($\lambda_{\text{max}} = 374 \text{ nm}$), caused by a somewhat higher distortion of the aromatic subunits in the polymer chain.

Optical excitation at $\lambda_{\text{max}} = 368 \text{ nm}$ gives a strong blue fluorescence in the range of 400-500 nm with a maximum $\lambda_{\text{max}} = 425 \text{ nm}$ (shoulder at 455 nm).

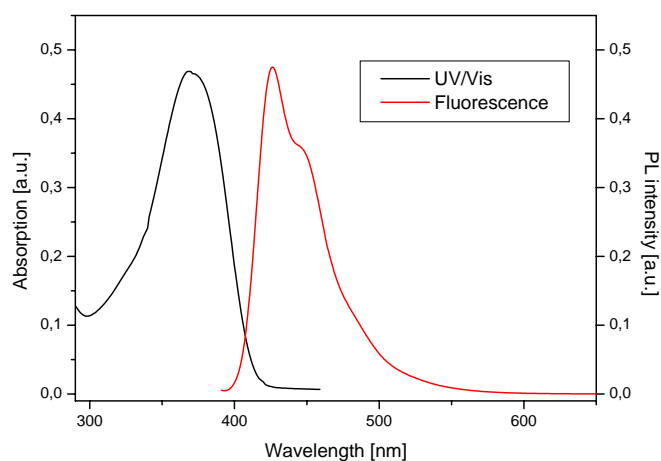


Fig. 9: UV/VIS & fluorescence spectra of **17** in water at room temperature

3.1.2 Optical properties of the water-soluble, anionic fluorene-type co-polymer **11** in presence of nonionic surfactants

Studies of the anionic fluorene-type co-polymer, poly[9,9-bis(4-sulfonyl-butoxyphenyl) fluorene-*co*-1,4-phenylene] **17** in the presence of nonionic surfactants were carried out in collaboration with the group of *Prof. H. Burrows and co-workers*, Univ. Coimbra, Portugal.

The high fluorescence quantum yields and blue light emission of polymers and copolymers involving 2,7-linked fluorene units make them one of the most attractive classes of conjugated polymers for electronic devices.^[5, 79, 105] Marked changes in the fluorescence of the water soluble polyelectrolytes can occur on adding surfactants.^[18, 72] Both surfactant complexation and break-up of polymer aggregates^[72] have been proposed to explain this effect.

Solutions in water of poly[9,9-bis(4-sulfonylbutoxyphenyl) fluorene-*co*-1,4-phenylene] **17** were turbid and show a low PL efficiency of ca. 23 %. Addition of the non-ionic surfactant C₁₂E₃ (triethyleneglycol monododecyl ether) leads to a clear solution with a high PL efficiency near unity.

3.1.3 Influence of surfactant concentration

The behaviour of the **17**-surfactant (C₁₂E₃) system for two different polymer concentrations (1.4 and 7*10⁻⁴ M per repeat unit) when varying the concentration of the surfactant (between 4*10⁻⁴ and 5*10⁻² M) was analysed (Fig. **10**).

The solubility of **17** is determined by the absolute concentration of the surfactant. At >10⁻³ M, clear solutions were obtained. The upper limit of polymer solubility was not detected but it was at least 20 times higher than without surfactant, as derived from the absorption spectra. However, increasing the surfactant concentration does not effect the UV/VIS-spectrum of the water-soluble CPE **17** (Fig. **10**).

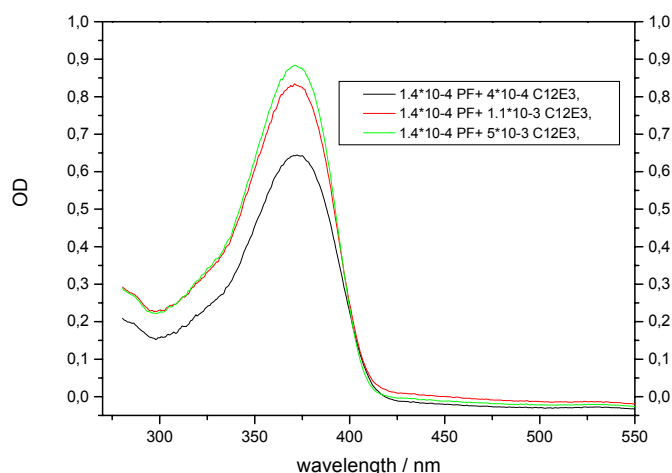


Fig. 10: Variation in the concentration of surfactant (between $4 \cdot 10^{-4}$ and $5 \cdot 10^{-2} M$)

3.1.4 PL spectra of the anionic fluorene-type copolymer **17** after surfactant ($C_{12}E_3$) addition

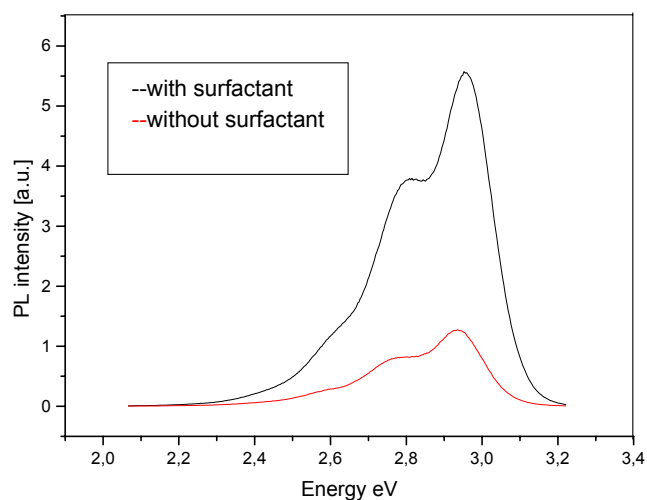


Fig. 11: Emission intensity of **17** before and after surfactant ($C_{12}E_3$) addition

Fluorescence (PL) spectra of **17** before and after surfactant addition ($C_{12}E_3$) have been measured. Without surfactant the PL quantum yield was found to be 23 % (relative to dye standards). After addition of the surfactant the PL quantum yield increased to around 100 %. The effect of the addition of the non-ionic surfactant *n*-dodecyl pentaoxy-ethylene glycol ether ($C_{12}E_5$) on the PL spectra of the water soluble poly[9,9-bis(4-sulfonylbutoxyphenyl)fluorene-*co*-1,4-phenylene] **17** was also studied. Upon addition of $C_{12}E_5$ (3.3×10^{-8} to

5.34×10^{-4} M) to poly[9,9-bis(4-sulfonyl-butoxyphenyl)fluorene-*co*-1,4-phenylene] **17** (6 mg/L, 9.2×10^{-7} M)⁷, a 10 nm blue shift of the PL emission maximum is observed (normalized PL spectra see Fig. 12).

To explain the observed PL blue shift and the increase in PL intensity, two hypotheses can be considered. Either it is due to changes in environment resulting from surfactant complexation, or surfactant induces break-up of polymer aggregates.^[72] Fluorescence quantum yields in aqueous solutions may be up to an order of magnitude lower than in non-polar solvents,^[106] and changing polarity is a possible explanation for these differences.

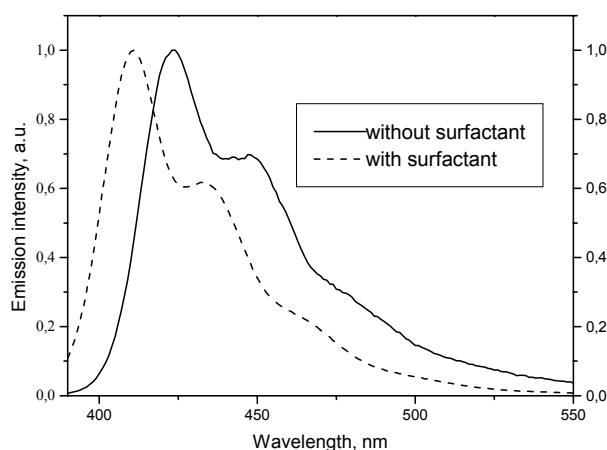


Fig. 12: Fluorescence spectra of **17** with and without surfactant ($C_{12}E_5$)

However, this may not be the case. For fluorene and many other aromatic compounds, the lowest electronic energy transition is relatively insensitive to solvent polarity,^[107] which contrasts with the pronounced blue shifts upon micellisation. In contrast, breaking up of aggregates explains both these observations. With aggregates, similar inter-chain interactions are present in the fluorene *co*-polymer films. Breaking up these aggregates by incorporation into micelles is equivalent to going from thin films to isolated polymer chains. The differences in the spectra and fluorescence quantum yields of poly[9,9-bis(4-sulfonylbutoxy-phenyl)fluorene-*co*-1,4-phenylene] **17** in water and $C_{12}E_5$ micelles are very similar to those with fluorene copolymers in thin films and cyclohexane solutions,^[108] supporting the above model. With a water soluble

poly(*p*-phenylene-vinylene), aggregation and its break-up with an oppositely charged surfactant has been indicated by small angle neutron scattering (SANS).^[93]

3.1.5 Poly[9,9-bis(4-sulfonylbutoxyphenyl)fluorene-co-1,4-phenylene] **17** in PLEDs

Poly[9,9-bis(4-sulfonylbutoxyphenyl)fluorene-co-1,4-phenylene] **17** was used as active layer in PLEDs. Experiments were carried out in the group of *Prof. Emil J. W. List* at the Institute of Solid State Physics, Graz University of Technology, Austria. Details of fabrication of PLEDs are included in the experimental part.

The best devices performances were observed in the simple device configuration ITO/CPE/Al without a PEDOT intermediate layer. Polymer concentrations of 8 mg/ml and ca.1 % surfactant (C₁₂E₃) have been the optimum parameters for spincoating the CPE films from aqueous solution.

3.1.6 Optical characterization of polymer films and corresponding OLED devices

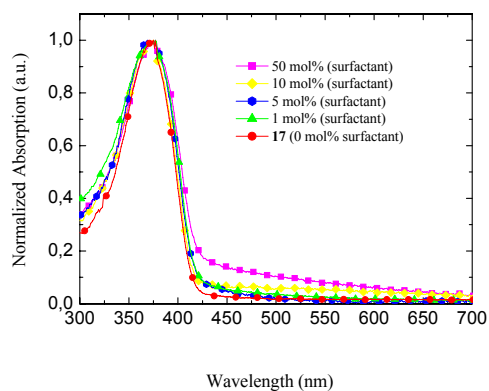


Fig. 13: Absorption spectra of poly[9,9-bis(4-sulfonylbutoxyphenyl)fluorene-co-1,4-phenylene] (**17**) films for different surfactant concentrations

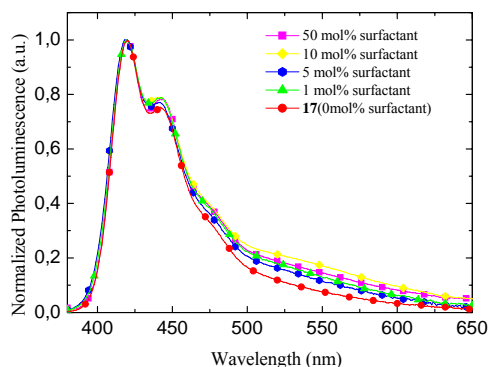


Fig. 14: Photoluminescence spectra of poly[9,9-bis(4-sulfonylbutoxyphenyl)fluorene-co-1,4-phenylene] (**17**) in films for different surfactant concentrations

Fig. 13 and Fig. 14 show absorption and PL emission spectra of **17** in thin films for different surfactant concentrations ($C_{12}E_3$) prior to spincoating. The optical spectra of **17** in the solid state are not affected by the presence of the non-ionic surfactant.

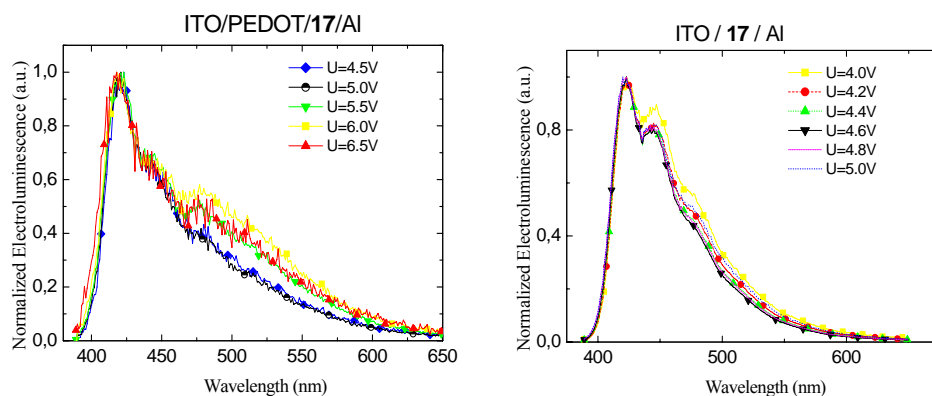


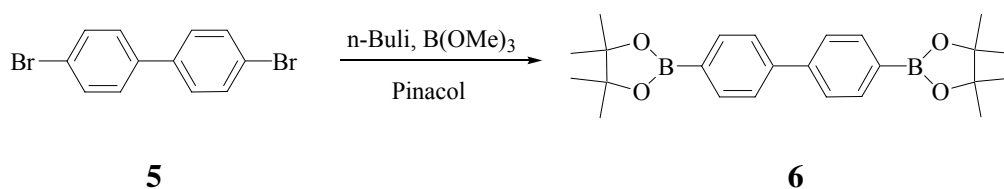
Fig. 15: Electroluminescence spectra of OLEDs with **17** as the active layer for different voltages without and with a PEDOT injection layer.

The OLED devices with **17** as the active layer were built without and with a PEDOT injection layer. Without PEDOT relatively well working devices could be achieved, showing luminescence values up to 144 cd/m^2 at bias voltages as low as 4.5 V. The interesting fact is that all devices with or without PEDOT have luminescence onset voltages around 3V. For voltages higher than 5V the devices were damaged. These low onset voltages are indicative for a doping of the Al/polymer **17** interface. This effect is currently under investigation.

3.2 Synthesis of the anionic water-soluble fluorene-type co-polymer 18 with a 4,4'-biphenylene spacer

First have studied a fluorene-phenylene alternating copolymer. Here we study the similar co-polymer with a 4,4'-biphenylene spacer unit. Changes of their absorption and photoluminescence properties will be discussed.

Synthesis started from the commercially available 4,4'-dibromobiphenyl **5**. 4,4'-dibromobiphenyl **5** was first converted to the subsequent diboronic acid with n-BuLi and trimethyl borate. The product in turn was reacted with pinacol and toluene to yield 20% of biphenyl-4,4'-bis[4,4,5,5-tetramethyl-1,3,2-dioxaborolane] **6** (Scheme 16).



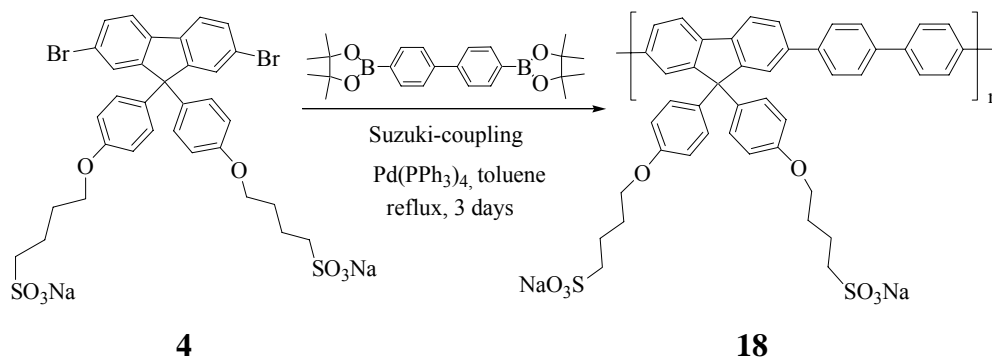
Scheme 16: Synthesis of biphenyl-4,4'-bis[4,4,5,5-tetramethyl-1,3,2-dioxaborolane] **6**

The yield was less because a mixture of mono and diboronic acids was obtained. Separation of the mono from diboronic acid was difficult. The crude product was purified by column chromatography using hexane:ethylacetate (90:10) as eluent. So only 20 % of pure product (diboronic acid) was obtained.

Biphenyl-4,4'-bis[4,4,5,5-tetramethyl-1,3,2-dioxaborolane] **6** was characterized by ¹H-NMR and ¹³C-NMR spectroscopy as well as mass spectrometry. The ¹H-NMR spectrum showed 3 signals, 2 signals for aromatic protons at 7.9 and 7.6 ppm, with the signal near the boronic ester group more shielded than the other aromatic proton. The methyl protons appear at 1.26 ppm.

From ¹³C-NMR spectroscopy, 6 signals were observed, four of non-equivalent aromatic carbons (δ : 126.4, 128.7, 135.3, 143.6 ppm) and two of alkyl carbons (δ : 24.8, 83.8 ppm). Signal at 143.6 ppm is for the bridge carbon adjacent to the other phenyl ring. The methyl carbons appear at 24.8 ppm and signal at 83.8 ppm is for the carbon of the dioxaborolane ring. In the mass spectrum, the base peak was observed at 406 (M^+).

The diboronic acid **6** was used as co-monomer in the synthesis of poly[9,9-bis(4-sulfonylbutoxyphenyl)fluorene-co-4,4'-biphenyl] **18**. Biphenyl-4,4'-bis-[4,4,5,5-tetramethyl-1,3,2-dioxaborolane] **6** and 2,7-dibromo-9,9'-bis(4-sulfonyl-butoxyphenyl)fluorene **4** in a 1:1 molar ratio were subjected to a Suzuki-type coupling reaction with a palladium(0)catalyst and toluene/aqueous sodium carbonate solution as reaction medium. The reaction time was 3 days (Scheme 17).



Scheme 17: Synthesis of poly[9,9-bis(4-sulfonylbutoxyphenyl)fluorene-co-4,4'-biphenyl] **18**

The raw copolymer was purified by dialysis using a membrane with a molecular weight cutoff of 3,500 g mol^{-1} . Poly[9,9-bis(4-sulfonylbutoxyphenyl)fluorene-co-4,4'-biphenyl] **18** was characterized by $^1\text{H-NMR}$ spectroscopy. The $^1\text{H-NMR}$ spectrum in D_2O showed 3 broad signals, one for aromatic protons (5.5-7.9 ppm) and other two for the outer and inner methylene ($-\text{CH}_2$) protons (2.5-3.5 ppm and 1.1-2.2 ppm).

The gel permeation chromatography (GPC) analysis of this copolymer was done using NMP/LiBr as solvent (PS calibration) providing a number average molecular weight (\overline{M}_n) of 8,400 g mol^{-1} . The degree of polymerisation was found to be around 11. The determination of molecular weights was also difficult for this water soluble copolymer. The reason for difficulty in characterisation was again aggregation formation, which can lead to an underestimation of the \overline{M}_n values.

3.2.1 Absorption and photoluminescence properties of **18**

Absorption and emission spectra for poly[9,9-bis(4-sulfonylbutoxyphenyl)-fluorene-*co*-4,4'-biphenyl] **18** were measured in water at room temperature. Fig. **16** shows the UV/VIS and fluorescence spectra for this copolymer.

Poly[9,9-bis(4-sulfonylbutoxyphenyl)fluorene-*co*-4,4'-biphenyl] **18** shows an absorption band peaking at $\lambda_{\text{max}} = 362$ nm. The spectrum is blue shifted by ca. 6 nm, if compared to the previously described copolymer **17** because of higher distortion of the polyphenylene backbone. Optical excitation at $\lambda_{\text{max}} = 362$ nm gives a strong blue fluorescence in the range of 400-550 nm with maximum at $\lambda_{\text{max}} = 425$ nm. The PL spectra of the related fluorene/phenylene copolymer **17** shows an emission at almost similar wavelength indicating a nearly identical excited state geometry.

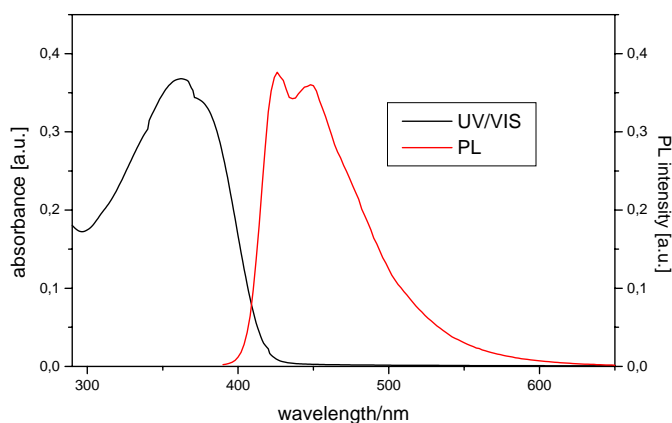


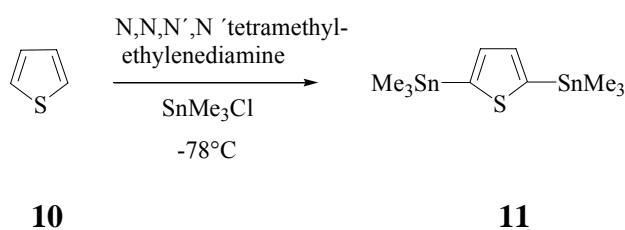
Fig. 16: UV/VIS & Fluorescence spectra of **18** in water at room temperature

3.3 Synthesis of the anionic water soluble fluorene-type copolymer **19** with a thienylene spacer group.

9,9-dialkyl fluorene-type homopolymers exhibit high bandgap energies of ca. 3.1 eV, which makes electron injection difficult using conventional cathode materials and limits their use in polymer LEDs. It has been found that incorporation of heteroarylene moieties in fluorene-based copolymers allows for a tuning of the electronic potentials. The incorporation of thienylene

building blocks in the CPE backbone opens a possibility to tune the electronic properties of the alternating copolymers. (lowering the bandgap energy).

Synthesis of 2,5-bis(trimethylstannyl)thiophene **11** started from commercially available thiophene. N,N,N',N'-tetramethylethylenediamine, TMEDA, n-BuLi and trimethyltinchloride were added subsequently to thiophene to get 2,5-bis(trimethylstannyl)thiophene **11** in about 70 % yield (Scheme 18).^[132]



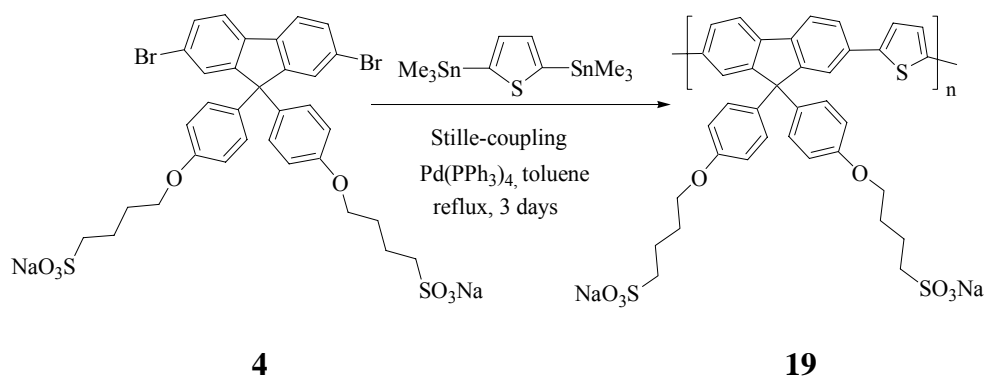
Scheme 18: Synthesis of 2,5-bis(trimethylstannyl)thiophene **11**

¹H-NMR spectroscopy of 2,5-bis(trimethylstannyl)thiophene **11** shows 2 signals, one signal as a singlet for aromatic protons at 7.37 ppm and other singlet for the methyl groups at 0.37 ppm.

The ¹³C-NMR spectrum of 2,5-bis(trimethylstannyl)thiophene shows 3 signals, 2 signals from non-equivalent aromatic carbons (δ : 143.4, 136.2 ppm) and one from the CH₃ protons (7.68 ppm). The signal at 136.2 ppm stands for the carbon which is flanked by Sn(CH₃)₃ group, the signal at 143.4 ppm for the (=CH-) carbon of the thiophene ring. In mass spectrum, M⁺ peak was observed at 409.

The distannylated monomer was used as comonomer for the synthesis of poly[9,9-bis(4-sulfonylbutoxyphenyl)fluorene-*co*-2,5-thienylene] **19**. Therefore, monomers **11** and **4** in the ratio 1:1 were subjected to a Stille-type cross-coupling reaction using a palladium(0) catalyst and toluene/aqueous sodium carbonate solution as solvent (Scheme 19).

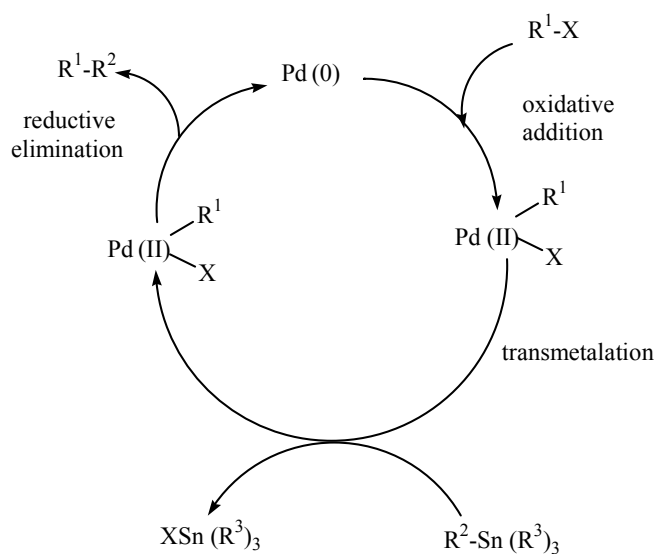
The co-polymer was further purified by dialysis using a membrane with a molecular weight cutoff of 3,500 gmol⁻¹. Poly[9,9-bis(4-sulfonylbutoxyphenyl)fluorene-*co*-2,5-thienylene] **19** was obtained as yellow solid in about 42 % yield. Copolymer **19** was water-soluble.



Scheme 19: Synthesis of poly[9,9-bis(4-sulfonylbutoxyphenyl)fluorene-co-2,5-thienylene] **19**

The mechanism for the Stille-type coupling is given below.

A general catalytic cycle for the *Stille-type* ^[114, 115] cross coupling reaction involves oxidative addition, transmetalation, and subsequent reductive elimination (Scheme 20).



Scheme 20: A general catalytic cycle for Stille type cross coupling reaction

The palladium catalyst can be used either as Pd(II) or Pd(0). In the case of Pd(II), the organotin compound initially reduces the palladium(II) complex precursor to the palladium(0) species. First an organopalladium intermediate is formed by oxidative addition of the catalyst to the aryl halide. Transmetalation is proposed rate determining step in the catalytic cycle. Which takes place to form diarylated palladium moiety. Finally, a reductive elimination gives the biaryl product and the palladium(0) species to complete the catalytic cycle. An

electron withdrawing group on the aryl halide increases the reactivity towards palladium catalysts. Relative order of ligand transfer from Sn is alkynyl > alkenyl > aryl > allyl > benzyl > alkyl. The details of the mechanism are still being elucidated, and mechanism may change with different reaction conditions.

The $^1\text{H-NMR}$ data of **19** are given in the experimental section. The GPC analysis for this copolymer was done using NMP/LiBr as solvent, providing a number average molecular weight (\overline{M}_n) of ca. $3,500 \text{ gmol}^{-1}$, corresponding to a degree of polymerisation of around 5.

As mentioned before, it is difficult to perform the GPC analysis.

3.3.1 Absorption and photoluminescence properties of **19**

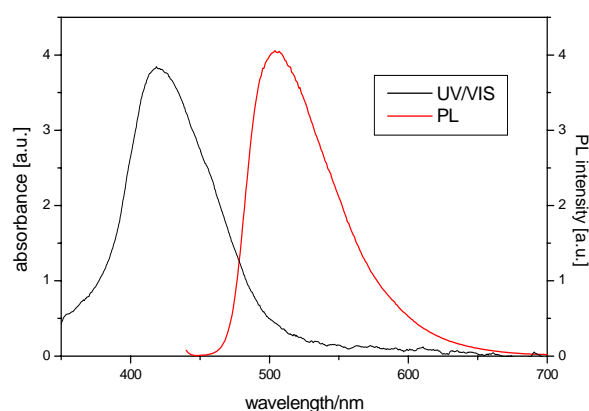


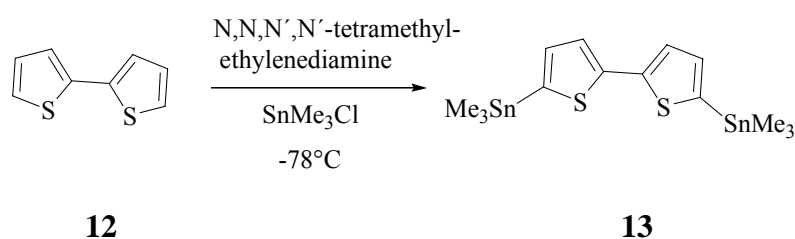
Fig. 17: UV/VIS & fluorescence spectra of **19** in water at room temperature

UV/VIS and fluorescence spectra of poly[9,9-bis(4-sulfonylbutoxyphenyl)fluorene-co-2,5-thienylene] **19** were recorded in water. **19** shows a structured absorption band peaking at $\lambda_{\text{max}} = 418 \text{ nm}$. The spectrum is red shifted by 50 and 56 nm, respectively, compared to the previously described phenylene and biphenylene containing copolymers **17** and **18**, resp. This shift is caused by the incorporation of the thiophene spacer group. Optical excitation at $\lambda_{\text{max}}=418 \text{ nm}$ gives an emission band peaking at $\lambda_{\text{max}} = 504 \text{ nm}$, Fig. **19** shows the UV/VIS and fluorescence spectra of **19**. There is also a red shift observed in the emission spectrum of **19** as compared to the previous copolymers **17** and **18** (19 nm each).

3.4 Synthesis of the anionic water soluble fluorene-type copolymer **20** with a bithiophene spacer group.

Following a related CPE, co-polymer with bithiophene spacer units will be described.

For co-monomer synthesis, bithiophene **12** was converted to 5,5'-bis(trimethylstannyl)-2,2'-bithiophene **13** in 72 % yield, in a procedure similar to the synthesis of **11** (Scheme **21**).^[132]

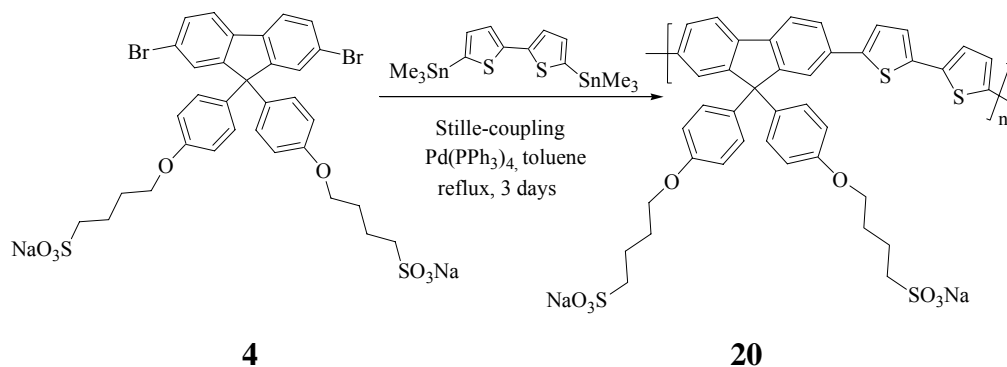


Scheme 21: Synthesis of 5,5'-bis(trimethylstannyl)-2,2'-bithiophene **13**

¹H-NMR spectroscopy of 5,5'-bis(trimethylstannyl)-2,2'-bithiophene **13** shows 3 signals, 2 signals for non-equivalent aromatic protons at 7.20 and 7.02 ppm, both showing a doublet signal, and one signal for the methyl protons.

The ¹³C-NMR spectrum shows 5 signals, 4 for non-equivalent aromatic carbons (δ : 143.1, 137.6, 136.3, 125.1 ppm) and one for the methyl carbons (δ : 7.73 ppm). The signal at 143.1 ppm stands for the carbons of the thienyl-thienyl bridge, the signal at 125.1 ppm belongs to the carbon which is directly attached to the Sn(CH₃)₃ group. Peak at 491.8 (M⁺) was observed in mass spectrum, which was the base peak.

The monomers **13** and **4** in a 1:1 molar ratio were reacted using a palladium(0) catalyst in a Stille-type cross-coupling reaction for 3 days. Poly[9,9-bis(4-sulfonylbutoxyphenyl)fluorene-*co*-2,2'-bithiophene] **20** was obtained as a reddish brown solid (Scheme **22**). It was purified by dialysis using a membrane cutoff of 3,500 gmol⁻¹. The copolymer **20** was water-soluble and obtained in around 64 % yield. Poly[9,9-bis(4-sulfonylbutoxyphenyl)fluorene-*co*-2,2'-bithiophene] **20** was characterized by ¹H-NMR spectroscopy.



Scheme 22: Synthesis of poly[9,9-bis(4-sulfonylbutoxyphenyl)fluorene-co-2,2'-bithiophene] **20**

3 broad signals were observed, one signal for the aromatic protons (6.55-7.9 ppm) and other 2 signals for the outer and inner side chain methylene (-CH₂-) groups at 3.1-4.45 ppm and 0.9-2.0 ppm, respectively.

The GPC analysis for this co-polymer was done using DMF (PS calibration), providing a number average molecular weight (\overline{M}_n) of 3,300 g/mol⁻¹, corresponding to a low degree of polymerisation of only 4. However, the molecular weight values may be underestimated due to an aggregation of polymer chains.

3.4.1 Absorption and photoluminescence properties of **20**

UV/VIS and fluorescence spectra of poly[9,9-bis(4-sulfonylbutoxyphenyl)fluorene-co-2,2'-bithiophene] **20** were recorded in water. **20** shows a structured absorption band peaking at $\lambda_{\text{max}} = 405$ nm (with two shoulders at 530 and 575

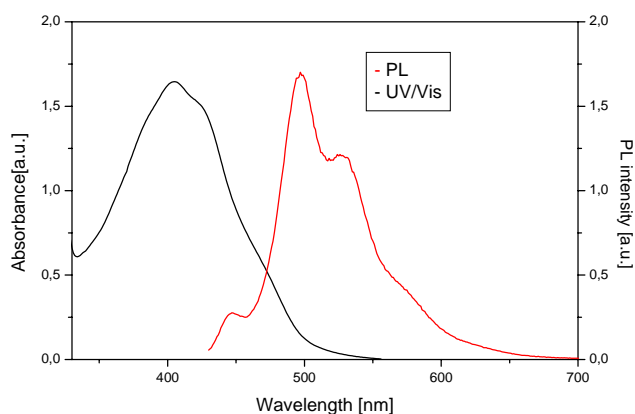


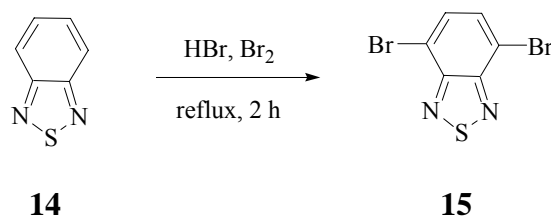
Fig. 18: UV/VIS & fluorescence spectra of **20** in water at room temperature

nm). The spectrum is red shifted by 37 and 43 nm, respectively, compared to the previously described phenylene and biphenylene containing copolymers **17** and **18**, resp. This low energy shift is caused by the incorporation of the bi-thiophene spacer group. Optical excitation at $\lambda_{\text{max}} = 405$ nm gives an emission band peaking at $\lambda_{\text{max}} = 502$ and 530 nm, red-shifted by ca 17 nm each with respect to the co-polymers **17** and **18**, resp. Fig. **18** shows the UV/VIS and fluorescence spectra of **20**.

3.5 Synthesis of anionic water-soluble, fluorene-type copolymers **27** containing alternating phenylene and benzothiadiazole units

Efforts have been made to tune the conjugated polyelectrolyte emission to match different probe chromophores.^[124] Recent experimental and theoretical studies indicate that intra- or intermolecular “through-space” energy transfer between segments in conjugated polymers may be substantially more important than along the backbone.^[130, 131] External perturbations that decrease backbone elongation, or that bring segments closer together can be used to substantially modify the emissive properties of a polymer in solution. With this considerations a CPE-type, copolymer with fluorene, phenylene, and a small number of 2,1,3-benzothiadiazole units was synthesized and characterized.

Synthesis of anionic poly[9,9-bis(4-sulfonylbutoxyphenyl)fluorene-1,4-phenylene]-*co*-([1,2,5]benzothiadiazole-4,7-diyl-1,4-phenylene) **27** started from the commercially available 1,2,5-benzothiadiazole **14**, which was brominated with aq. HBr and Br₂. Recrystallisation from methanol gave 4,7-dibromobenzo-[1,2,5]-thiadiazole **15** in about 59 % yield (Scheme **23**).

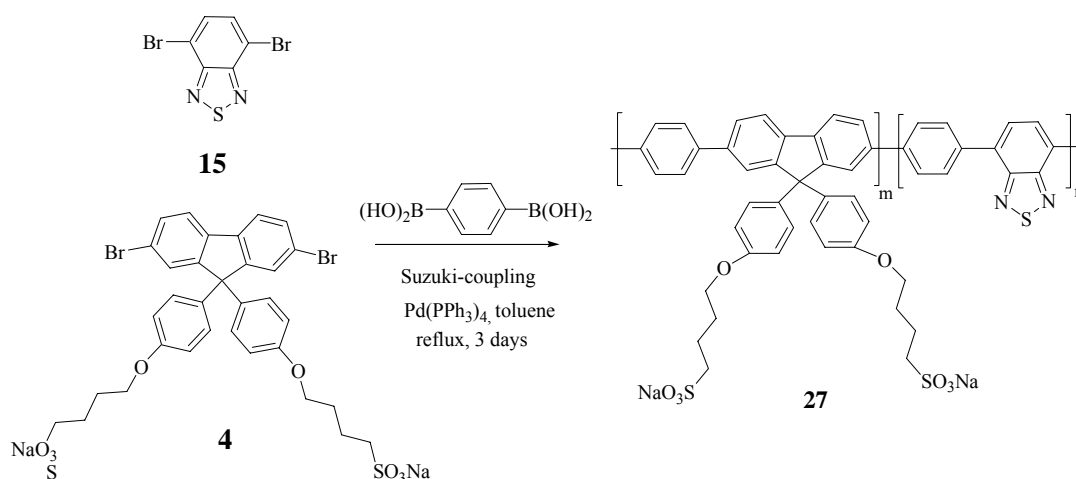


Scheme 23: Synthesis of 4,7-dibromobenzo-[1,2,5]-thiadiazole **15**

The $^1\text{H-NMR}$ spectrum of **15** showed a singlet at 7.78 ppm for the two aromatic protons.

In the $^{13}\text{C-NMR}$ spectrum, 3 signals were observed for 3 non-equivalent aromatic carbons (δ : 152.9, 132.24, 113.83 ppm). The deshielded signal at 152.9 ppm stands for the carbon adjacent to the nitrogen group. In the mass spectrum, the M^+ peak was observed at 293.

Anionic poly[9,9-bis(4-sulfonylbutoxyphenyl)fluorene-1,4-phenylene]-*co*-([1,2,5]-benzo-thiadiazole-4,7-diyl-1,4-phenylene) **27** was synthesized with 3 different mole ratios (0.90:0.10; 0.75:0.25; 0.50:0.50) of 2,7-dibromo-9,9-bis(4-sulfonylbutoxyphenyl)fluorene **4** to 4,7-dibromobenzo-[1,2,5]-thiadiazole **15** and 1,4-phenylenediboric acid. The Suzuki-type cross-coupling reaction gave water-soluble copolymers (Scheme 24). Purification was done by dialysis (details in section 4.5). There was a solubility problem so it was not possible to do the G.P.C measurement.



Scheme 24: Synthesis of anionic poly[9,9-bis(4-sulfonylbutoxyphenyl)-fluorene-1,4-phenylene]-*co*-([1,2,5]benzo-thiadiazole-4,7-diyl-1,4-phenylene) **27**

3.5.1 Absorption and photoluminescence properties of **27**

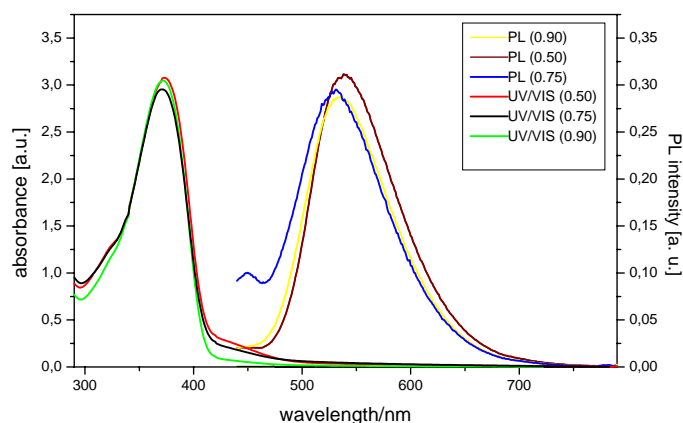


Fig. 19: UV/Vis & fluorescence spectra of **27** in water at room temperature

UV/VIS and fluorescence spectra of the copolymers **27** are shown in Fig. **19**. Absorption and emission spectra of **27** in different mole ratios have been measured in water. Surfactant $C_{12}E_3$ was added to deaggregate the polymer chains. The absorption bands peak at ca. 372+1-2 nm for all copolymer compositions. The main absorption bands originate from the fluorene/phenylene units, the weaker contributions around 420-480 nm from the benzothiadiazole units (they increase with increasing amount of the heteroaromatic building blocks). The emission spectra peak at 531-538 nm with a moderate bathochromic shift with increasing amount of benzothiadiazole units. The PL spectra are dominated by the benzothiadiazole emission.

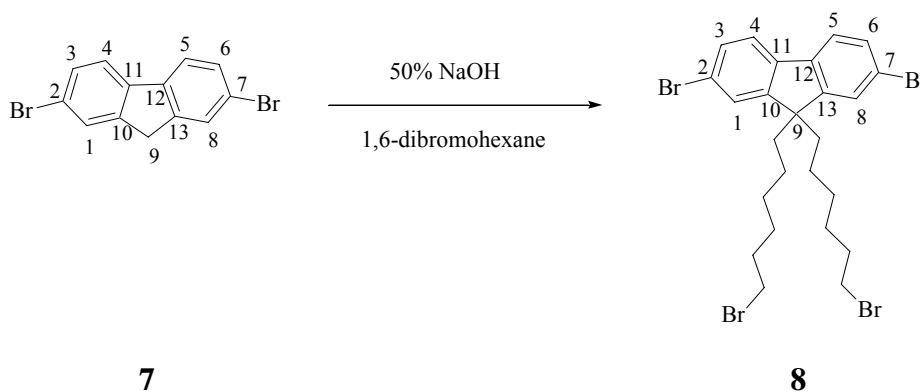
3.6 Synthesis of the cationic water-soluble fluorene-type copolymer with a phenylene spacer group.

Cationic, conjugated polyelectrolytes can be used as the optical platform in fluorescent chemical and biological sensors. ^[46, 75] Solubility in water is essential for interacting with biological substrates such as DNA and can be achieved by attaching ammonium functionalities to the side chains of the conjugated backbone. *Bazan and coworkers* have synthesized cationic oligo- and polyelectrolytes for DNA sensing. Electrostatic interactions between

cationic oligomers/polymers and negatively charged DNA can be applied to design sequence-specific DNA assays.

We have used the route developed by *Bazan and coworkers* for the synthesis of known and related cationic, water-soluble fluorene-type polymers. First, we have synthesized the known fluorene-type copolymer with phenylene spacer groups in a Suzuki-type cross-coupling reaction.

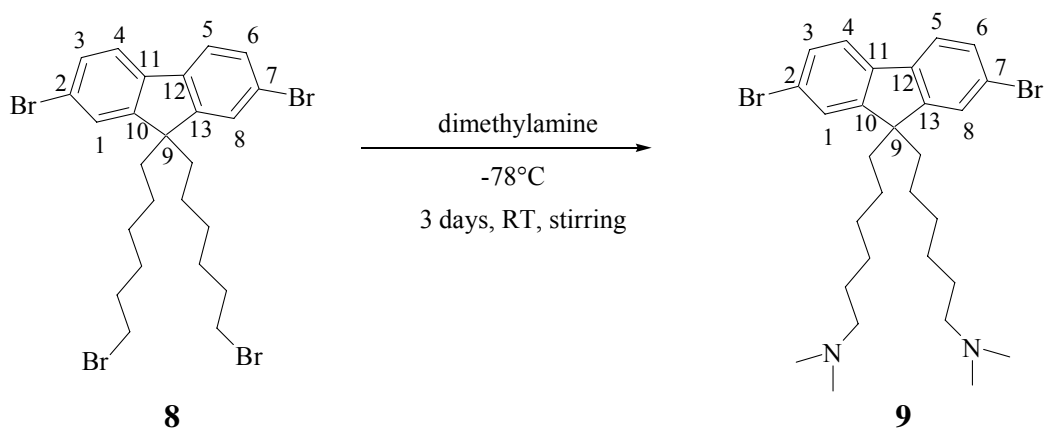
Synthesis of 2,7-dibromo-9,9-bis(6-bromohexyl)fluorene **8** monomer started from the commercially available 2,7-dibromofluorene **7** which was alkylated with 1,6-dibromohexane/NaOH. The work-up gave 2,7-dibromo-9,9-bis-(6-bromohex-yl)fluorene **8** as a viscous oil in about 65 % yield (Scheme 25).



Scheme 25: Synthesis of 2,7-dibromo-9,9-bis-(6-bromohexyl)fluorene **8**

8 was characterised by $^1\text{H-NMR}$ and $^{13}\text{C-NMR}$ spectroscopy. $^1\text{H-NMR}$ spectrum showed 8 signals, 3 signals at 7.35, 7.3 and 7.2 ppm respectively for 6 aromatic protons, and 5 signals (3.34, 1.85, 1.65, 1.15, 0.55 ppm) for the alkyl protons. Signal at 3.34 ppm appears as a triplet for 4 protons near bromine group, which are more deshielded as compared to other alkyl protons. Signals at 1.85 ppm, 1.65 ppm, 1.15 ppm and 0.55 ppm were seen for other alkyl protons.

In the $^{13}\text{C-NMR}$ spectrum, 13 signals were observed, 6 of non-equivalent aromatic carbons (δ : 121.4, 121.7, 126.2, 130.2, 139.2, 152.3 ppm) and 7 signals for the alkyl chain carbons (δ : 23.6, 27.9, 29.08, 32.7, 34.1, 40.1, 55.6 ppm). Signal at 152.3 ppm is for C10 and C13. Signal at 55.6 ppm is for the C9 carbon. In the mass spectrum, the M^+ peak was observed at 650.



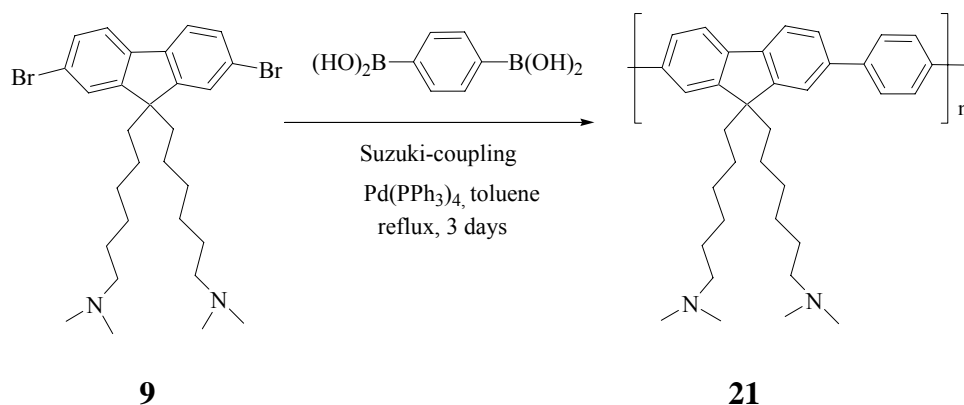
Scheme 26: Synthesis of 2,7-dibromo-9,9-bis-[6-(N,N-dimethylamino)hexyl]fluorene **9**

2,7-dibromo-9,9-bis(6-bromohexyl)fluorene **8** was converted to 2,7-dibromo-9,9-bis[6-(N, N-dimethylamino)hexyl]fluorene **9** in 50 % yield with dimethylamine in THF at -78° C (Scheme **26**).

In the $^1\text{H-NMR}$ spectrum of **9**, 7 signals were observed, 3 signals for aromatic protons at 7.55, 7.5, 7.42 ppm, and 4 signals at 2.1-2.2 ppm, 1.3 ppm, 1.1 ppm, 0.6 ppm were for alkyl protons. Signal at 2.1-2.2 ppm is for the methylene (-CH₂-) protons close to the N(Me)₂ group.

$^{13}\text{C-NMR}$ spectroscopy shows 14 signals, 6 signals (δ : 121.1, 121.4, 126.1, 130.2, 139.0, 152.4 ppm) for non-equivalent aromatic carbons and 8 signals (δ : 23.6, 27.0, 27.53, 29.7, 40.1, 45.4, 55.6, 59.7 ppm) for aliphatic carbons. Signal at 59.7 ppm is for the -CH₂ carbon near the N(Me)₂ group, the signal at 55.6 ppm for the C9 carbon. In the mass spectrum, the M^{+} peak was observed at 584 (M^{+}).

2,7-dibromo-9,9-bis[6-(N,N-dimethylamino)hexyl]fluorene **9** was subjected to a Suzuki-type cross-coupling reaction with 1,4-phenylene-diboronic acid using a palladium(0) catalyst (5 mol %) in THF as solvent. Reaction time was 3 days. Extraction and precipitation yielded a yellowish solid in about 50 % yield (Scheme **27**).



Scheme 27: Synthesis of poly{9,9-bis[6-(*N,N*-dimethylamino)hexyl]fluorene-*co*-1,4-phenylene} **21**

$^1\text{H-NMR}$ spectroscopy of **21** showed 5 broad signals, one broad signal at 7.6-7.8 ppm for the aromatic protons and 4 signals at 2.0-2.3 ppm, 1.2-1.3 ppm, 1.1 ppm and 0.7-0.8 ppm for alkyl protons. Signal at 2.0-2.3 ppm is for the methylene ($-\text{CH}_2-$) group close to the $\text{N}(\text{Me})_2$ group.

The characterization of molecular weight is often a problem for water-soluble conjugated polymers. However, the post-polymerization approach involving the synthesis of an organo-soluble precursor polymer allows us to characterize the molecular weight at the stage of the “neutral” precursor **21**. Polymer **21** can be readily dissolved in CHCl_3 , THF and toluene, but is insoluble in DMSO, methanol and water. Another advantage of the post-polymerization approach is that the quaternization degree can be controlled and thus the “water-solubility” of the resulting polyelectrolyte is tunable. A tunable solubility is useful for the application of such materials as buffer layers in inkjet fabrication of LEDs. ^[26] The GPC analysis of **21** in THF (PS calibration) showed an average molecular weight (\overline{M}_n) of $3,500 \text{ gmol}^{-1}$, corresponding to a degree of polymerisation of ca. 7. *Bazan and coworkers* have obtained an average molecular weight of (\overline{M}_n) $\sim 8,000 \text{ gmol}^{-1}$, for the fluorene-type copolymer with phenylene spacer.

3.6.1 Absorption and photoluminescence properties of **21**

The UV/VIS and fluorescence spectra of poly{9,9-bis[6-(*N,N*-dimethylamino)hexyl]fluorene-*co*-1,4-phenylene} **21** show an absorption maximum at $\lambda_{\text{max}} = 360 \text{ nm}$ and an emission maximum at $\lambda_{\text{max}} = 425 \text{ nm}$ by excitation at $\lambda = 360 \text{ nm}$. The spectra were recorded in chloroform solution (Fig. **20**).

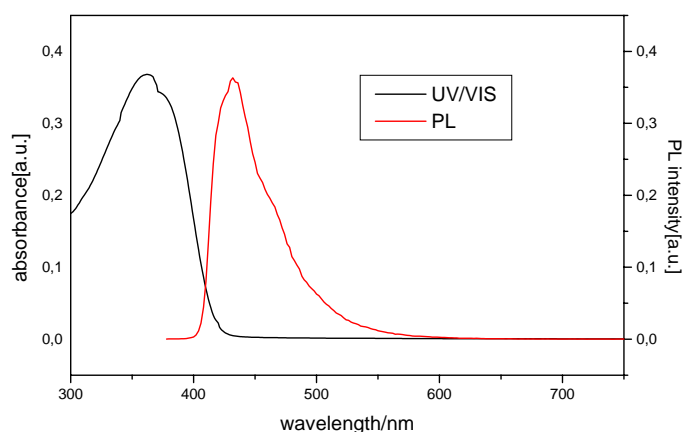
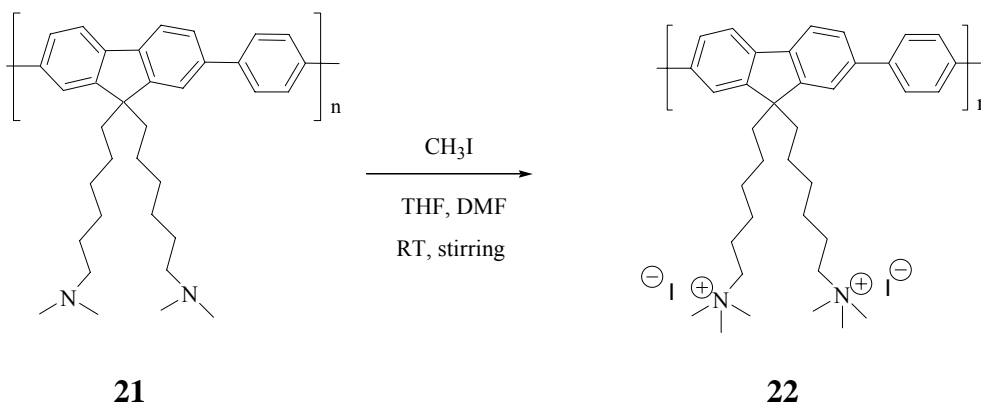


Fig. 20: UV/VIS & fluorescence spectra of **21** in chloroform at room temperature

Quarternization of poly{9,9-bis[6-(N,N-trimethylammonium)hexyl]fluorene-*co*-1,4-phenylene} **22** by methyl iodide in mixture of DMF and THF (Scheme **18**), gave poly{9,9-bis[6-(N,N-trimethylammonium)hexyl]fluorene-*co*-1,4-phenylene} **22** as a water-soluble cationic polyelectrolyte in 77 % yield after purification by dialysis (details in section **4.5**). The degree of quarternization was around 80 %. With this degree of quarternization the resulting polymer shows a solubility opposite to the neutral precursor, **22** is soluble in water but insoluble in CHCl₃, THF and toluene. Degree of quarternization could be determined by ¹H-NMR spectroscopy. After quarternization, the peaks in the aromatic region remain almost unchanged whereas the peaks corresponding to the α-methylene groups are splitted into two group of signals..



Scheme 28: Synthesis of poly{9,9-bis[6-(N,N-trimethylammonium)hexyl]fluorene-*co*-1,4-phenylene} **22**

3.6.2 Absorption and photoluminescence properties of **22**

UV/VIS and photoluminescence spectra of poly{9,9-bis[6-(N,N-trimethylammonium)hexyl]fluorene-*co*-1,4-phenylene} **22** were measured in water. An absorption band peaking at $\lambda_{\text{max}}=374$ nm was observed. Absorption at this wavelength suggests that the terminal ammonium functionality has no effect on the absorption of the polyfluorene backbone. The spectrum is red shifted by 6 and 12 nm resp, compared to the copolymers **17** and **18**. Optical excitation at $\lambda = 374$ nm gives an emission peaking at $\lambda_{\text{max}} = 423/ 450$ nm (Fig. **21**). There is also a slight red shift of 2 nm observed in the emission spectra of **22** with respect to **17** and **18**.

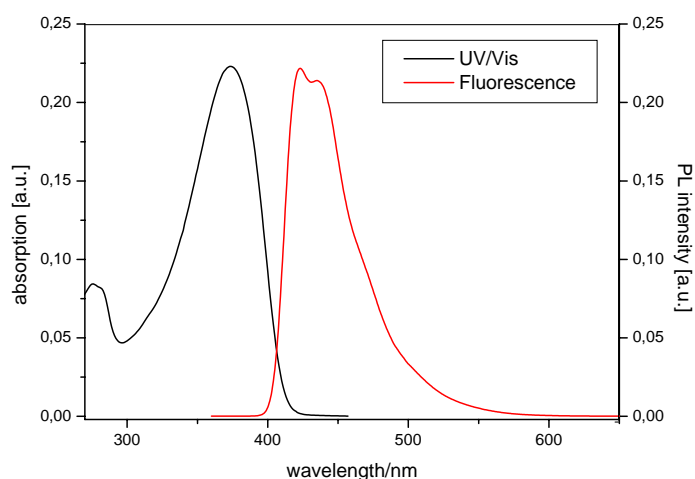


Fig. 21: UV/VIS & fluorescence spectra of **22** in water at room temperature

3.6.3 Optical properties of the water-soluble, cationic fluorene-type copolymer **22** in the presence of a nonionic surfactant ($C_{12}E_5$)

Earlier we have studied the deaggregation and fluorescence enhancement of anionic CPE/surfactant system, a poly{1,4-phenylene-[9,9-bis(4-phenoxy butyl-sulfonate)]fluorene-2,7-diyl}**17**- $C_{12}E_5$ mixture.^[126] The results suggest that **17** is located inside cylindrical $C_{12}E_5$ micelles when critical micell concentration (cmc) of $C_{12}E_5$ in water is achieved. The surfactant breaks up polymer aggregates resulting in a deaggregation and consequent fluorescence enhancement.

Now it was interesting to study the related cationic CPE/surfactant system. The nonionic surfactant used in this case was also *n*-dodecyl pentaoxyethylene glycol ether (C₁₂E₅).

Mixing poly{9,9-bis[6-(N,N-trimethylammonium)hexyl]fluorene-*co*-1,4-phenylene} **22** with the surfactant *n*-dodecyl pentaoxyethylene glycol ether (C₁₂E₅) seems to visually improve water solubility (clearing of the solution). The effect is maximal when ca. ten moles of C₁₂E₅ were used for each co-polymer repeat unit. Again it is assumed that monomolecular, cylindrical micelles which contain single CPE chains covered by surfactant molecules are formed. The anionic counter-part of poly[9,9-bis(4-sulfonylbutoxyphenyl)fluorene-*co*-1,4-phenylene] **17**, the cationic CPE **22**. C₁₂E₅ seems to behave in good analogy to **17**.

According to *Kato et al.* ^[110] pure C₁₂E₅ shows a biphasic behaviour in water above 30°C and forms a solution below 30°C, when the volume fraction of the surfactant is between 0.01 and 0.1. For our studies the temperature was therefore set to 25°C. The surfactant alone forms an isotropic solution at this temperature for the studied concentrations.

Lichterfeld et al. ^[109] described a ternary phase diagram for the tetradecane-C₁₂E₅ system in water and reported that C₁₂E₅ forms an isotropic liquid with water when the system contains 15 wt-% hydrocarbon and a two-phase system appears when >16 wt-% of tetradecane is added. Importantly, self-organized *e.g.* hexagonal or lamellar mesophases do not appear until a considerable amount of surfactant is added (>10 %) whether tetradecane is present or not.^[109, 110] Because the cmc of C₁₂E₅ is $5\pm 2\times 10^{-5}$ M ^[113] which is lower than the studied concentrations, the studied solutions are expected to contain (cylindrical) micelles.

C₁₂E₅ is non-ionic amphiphile and do not contain sites such as hydrogen bonding or donor acceptor sites which could form strong physical bonds with **22**. Therefore, it is unlikely that such system would form supramolecular structures via complexation ^[111, 92] but any inclusion is likely because of polar-non-polar effects. ^[112] Therefore, as described by *Burrows et al.* for the anionic copolymer **17**, any changes in PL spectra upon dissolution are likely due to

break-up of CPE aggregates, not due to complexation effects, affecting the electronic structure of the backbone.

3.6.4 Photoluminescence spectra of poly{9,9-bis[6-(N,N-trimethylammonium)hexyl]fluorene-co-1,4-phenylene} **22**/C₁₂E₅ mixtures in solution and the solid state

The molar ratio of C₁₂E₅/poly{9,9-bis[6-(N,N-trimethylammonium)hexyl]fluorene-co-1,4-phenylene}**22** was 10/1 for each repeat unit of **22** for the experiments done. Fig. **22** shows PL spectra of **22**-C₁₂E₅ films made from water. PL peaks are located at 412/433 nm for spin-coated and 425/442 nm for drop-cast film.

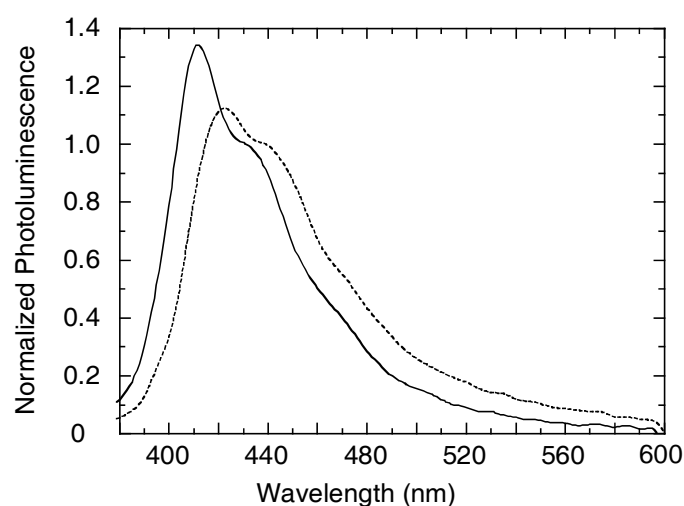


Fig. 22: PL spectra of **22**-C₁₂E₅ films. Spin-coated (solid line) and drop-cast films (dotted line) on quartz

Compared to the mixtures in water, drop-cast films are redshifted by around 10 nm. Because drop-cast films reveal some macrophase separation, they may contain non-isolated, aggregated polymer particles. In contrast to the drop-cast **22**-C₁₂E₅ film, a spin-coated **22**-C₁₂E₅ film behaves differently, and is almost similar to the solution spectrum (Fig. **23**) peaking at 413/434 nm. We assume that the spin-coated films do not form well-developed solid-state aggregates but form rather a disordered layer containing isolated surfactant-wrapped macromolecules.

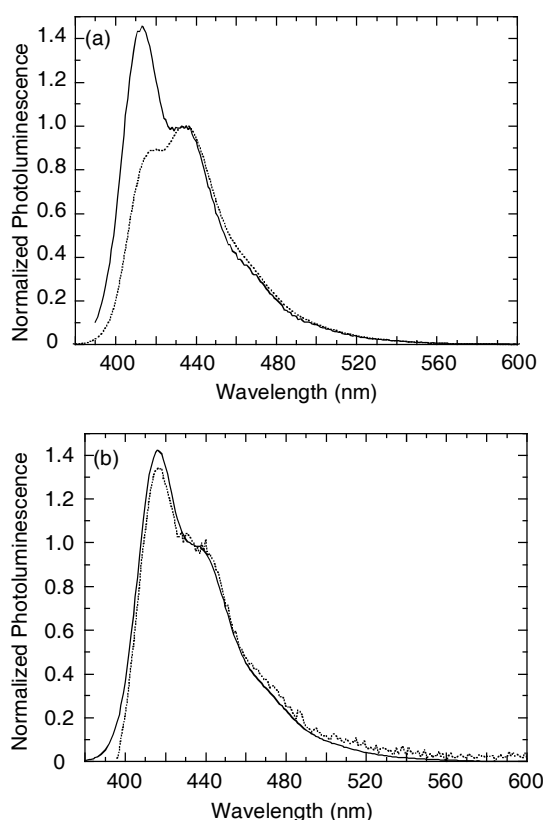


Fig. 23: PL spectra of **22**- $C_{12}E_5$ in water. (a) Solid line represents clear 0.1 mg/ml and dotted line cloudy 2 mg/ml solution. (b) PL spectra after filtration ($0.45 \mu\text{m}$). Solid line represents filtrated 1 mg/ml and filtrated 0.1 mg/ml solution.

Fig. 23 shows also that a cloudy, partially aggregated aqueous solution of **22**- $C_{12}E_5$ does not show considerable red-shifted PL contributions, this behaviour is only observed for drop-cast films (Fig. 22). Also a filtration of the mixtures (Fig. 23 b) does not lead to significant PL changes.

3.6.5 Small-Angle Neutron Scattering (SANS)

SANS is conventionally used to study hairy-rod-like molecules like proteins^[118] or polymers^[119, 120]. There are some SANS studies of rodlike π -conjugated polymers, (see *e.g.* Ballauf *et al.*^[121]), and also a few of water-soluble π -conjugated polymers,^[93, 122] but those of poly(2,7-fluorene)s and related copolymers seem scarce.

As it is found that the solubility of the {1,4-phenylene-[9,9-bis(4-phenoxy-butylsulfonate)]fluorene-2,7-diyl} copolymer is influenced in aqueous solution by addition of the surfactant n-dodecyl pentaoxyethylene glycol ether (C₁₂E₅),^[126] the same effect has been observed using the corresponding cationic polyelectrolyte **22**. The micelle formation was tentatively tested using small-angle neutron scattering (SANS).^[123]

In practice, the scattering studies are divided into two categories. There are studies of the short range order accomplished via the determination of the radial distribution function (RDF), and studies of larger density fluctuations, ("real" order). Amorphous materials, such as liquids, glasses, or glassy polymers barely reveal sharp diffraction maxima, while stronger scattering effects are observed in multicomponent materials, such as polymer blends, or single-component materials with well-defined molecular segments, such as block copolymers.

Like small-angle X-ray scattering, (SAXS), SANS is small-angle scattering (SAS) method. They are used to study relatively large, periodic structures of noncrystalline materials. The size of these objects is of the order of 10 Å or larger and information is obtained using either X-rays or neutrons at low detection angles, typically scattering angle 2θ less than 2°. This is the regime we applied for the solutions of the studied copolymers.

While X-ray studies only give a high intensity for high excitation energies neutrons provide advantages based on the scattering event resulting from the nuclei instead of the core electrons. The lower kinetic energy of the neutrons (~10 meV) compared with the energy of hard X-ray photons (~10 keV), is an additional advantage. Since the frequency is in the order of atomic movements, neutrons can provide information on atomic and molecular motions.

The tentative small-angle neutron scattering (SANS) measurements were performed with the small-angle scattering diffractometer Yellow Submarine operating on the cold neutron beamline at the Budapest Research Reactor (Hungary). The raw data were azimuthally averaged and grouped to about 30 points equidistant in the magnitude of the scattering vector (q). A broad scattering vector (q) range of 0.02-0.45 Å⁻¹ was covered using two sample-detector distances; acquisition times of several hours were used for each

sample at each detector position. The measurements were done at a temperature of 25 °C. For the measurements quartz cells (Hellma/Germany) with a sample thickness of 1 or 5 mm were employed, controlled by a thermostat (Julabo/ Germany). The scattered neutrons were detected by a two-dimensional position sensitive detector with pixel size 1x1 cm².

For SANS measurements the **22**-C₁₂E₅ system was prepared by dissolving both components in water and stirring overnight. The molar ratio of C₁₂E₅ to **22** was either 2 or 10. The concentration of the solution was allowed to vary from 0.1 to 2 mg/ml when calculated either with respect to **22** or the total system and marked by “polym” or “tot”, respectively. This convention was selected, because the surfactant may be regarded either as part of the complex or as co-solvent.

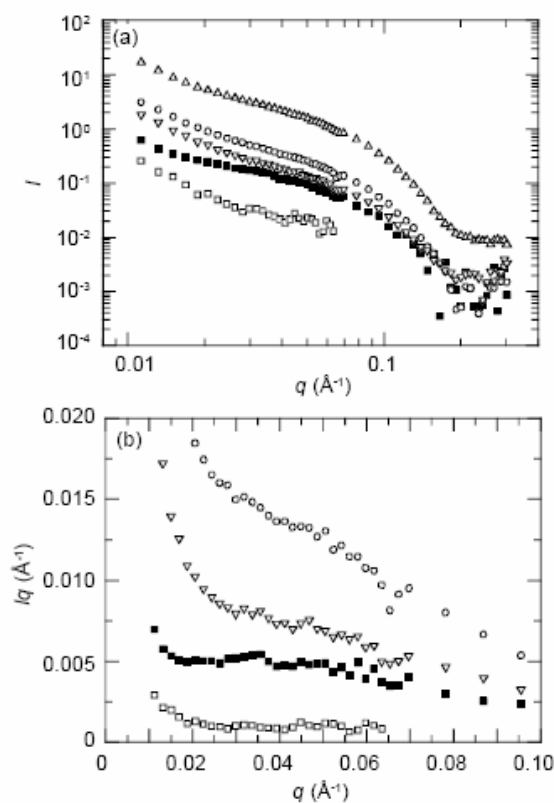


Fig. 24: (a) Porod plot of SANS data of **22**-C₁₂E₅ in D₂O normalized to the concentration. **22**-(C₁₂E₅)₂: 1 mg/ml (tot) (solid squares), **22**-(C₁₂E₅)₂: 0.1 mg/ml (tot) (open squares), **22**-(C₁₂E₅)₂: 0.1 mg/ml (polym) (open down triangles), **22**-(C₁₂E₅)₂: 1 mg/ml (open spheres), and 1 mg/ml (polym) (open up triangles). (b) Cassasa-Holtzer plot of the same data.

The results of our tentative study of **22**-C₁₂E₅ complexes are closely related to the surfactant-oil system studied by *Menge et al.* [6] using SANS. These authors studied 7 mg/ml aqueous solutions of C₁₂E₅ and added decane so that the decane fraction varied from 0.02 to 0.1. They found that the system contained cylindrical micelles whose cross sectional radius of gyration varied from 1.9 to 2.5 nm with increasing decane concentration, and showed a crossover from rodlike to coil behavior at ca. $q=0.02 \text{ \AA}^{-1}$.

Because there was an interest in testing whether surfactant free **22** approaches the behaviour of non-ionic polyfluorenes, [49] we decreased the surfactant vs. polymer concentration. We have not been able to use pure **22** in the concentration region discussed, but when the surfactant to polymer ratio is decreased from 10 to 2, a decay with the order of -1 is observed (Fig. 24 a), which indicates formation of cylindric micelles instead of a more fuzzy structure with a decay of the order -1.6 for the higher surfactant/polymer ratio of 10. Similarly, the Cassasa-Holtzer plot (Fig. 24 b) shows a plateau-like behaviour for a surfactant/polymer ratio of 10, while for a surfactant/polymer ratio of 2, the Iq curve is not increasing monotonically.

3.7 Synthesis of cationic, water-soluble fluorene-type copolymer **23** with a 2,5-thienylene spacer.

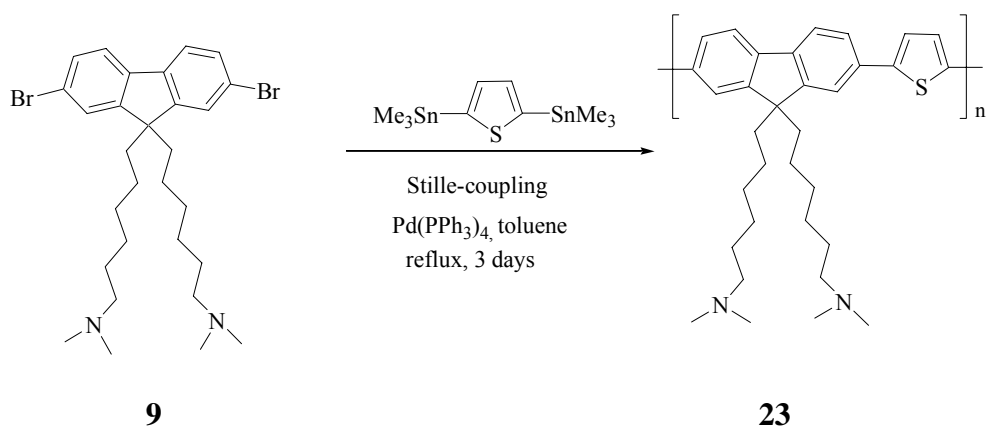
Cationic, water-soluble fluorene-type copolymer with thienylene building block have been also synthesized and compared with the corresponding anionic counterparts.

Poly{9,9-bis[6-(N,N-dimethylamino)hexyl]fluorene-co-2,5-thienylene} **23** as non-ionic precursor was synthesized by a Stille cross-coupling reaction of 2,7-dibromo-9,9-bis[6-(N,N-dimethylamino)hexyl]fluorene **9** and 2,5-bis-(trimethylstannyl)thiophene **11** using a palladium(0) catalyst and toluene as solvent. Extraction and precipitation yielded 41 % of poly{9,9-bis[6-(N,N-dimethylamino)hexyl] fluorene-co-2,5-thienylene} **23** (Scheme 29).

The ¹H-NMR spectrum shows 4 signals, one broad signal at 7.3-7.8 ppm for the aromatic protons and 3 other signals at 1.8-2.3 ppm, 1.0-1.4 ppm, and 0.7-0.9 ppm for the alkyl protons.

The GPC analysis of poly{9,9-bis[6-(*N,N*-dimethylamino)hexyl]fluorene-*co*-2,5-thienylene} **23** showed an average molecular weight (\overline{M}_n) of only 1,400 gmol^{-1} measured in THF, reflecting a low degree of polymerisation of only ca. 3.

However, the problems with the GPC measurements of the polar polymers have been already discussed.



Scheme 29: Synthesis of poly{9,9-bis[6-(*N,N*-dimethylamino)hexyl] fluorene-*co*-2, 5-thienylene} **23**

3.7.1 Absorption and photoluminescence properties of **23**

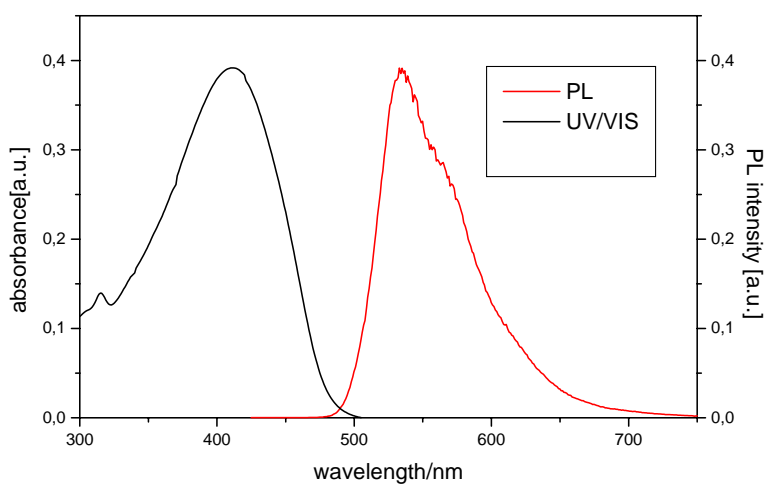
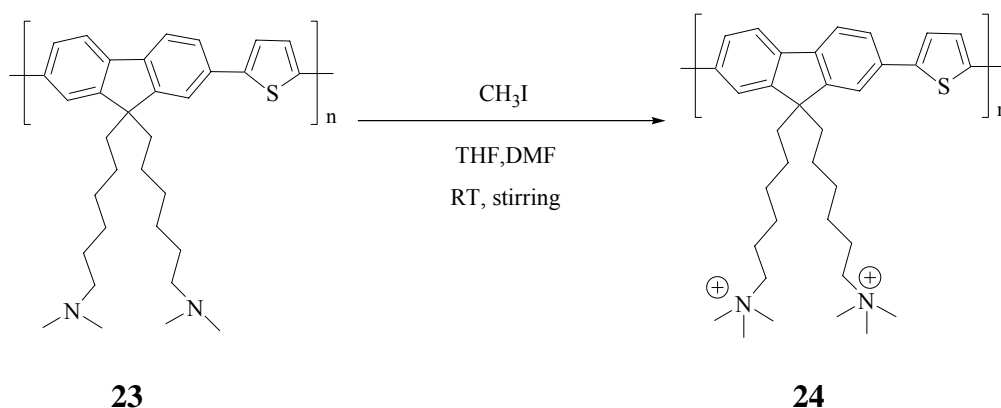


Fig. 25: UV/VIS & fluorescence spectra of **23** in chloroform at room temperature

UV/VIS and fluorescence spectra of poly{9,9-bis[6-(N,N-dimethyl-amino)hexyl]fluorene-*co*-2,5-thienylene} **23** shows an absorption maximum peaking at $\lambda_{\text{max}} = 412$ nm and an emission maximum at $\lambda_{\text{max}} = 500$ nm. Spectra were recorded in chloroform solution (Fig. 25).

Quarternization of poly{9,9-bis[6-(N,N-dimethylamino)hexyl]fluorene-*co*-2,5-thienylene} **23** was done with methyl iodide in mixture of DMF and THF. Poly{9,9-bis[6-(N,N-trimethylammonium)hexyl]fluorene-*co*-2,5-thienylene} **24** was obtained as a water-soluble polyelectrolyte in 58 % yield (Scheme 30).



Scheme 30: Synthesis of poly{9,9-bis[6-(N,N-trimethylammonium)hexyl]fluorene-*co*-2,5-thienylene} **24**

3.7.2 Absorption and photoluminescence properties of 24

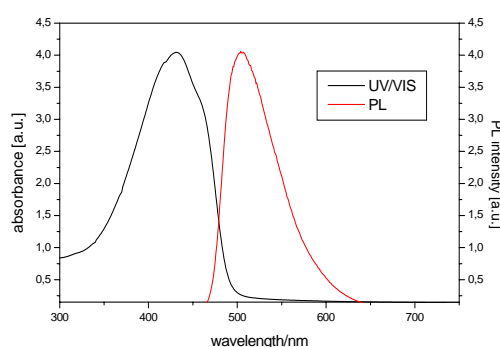


Fig. 26: UV/VIS & fluorescence spectra of **24** in water at room temperature

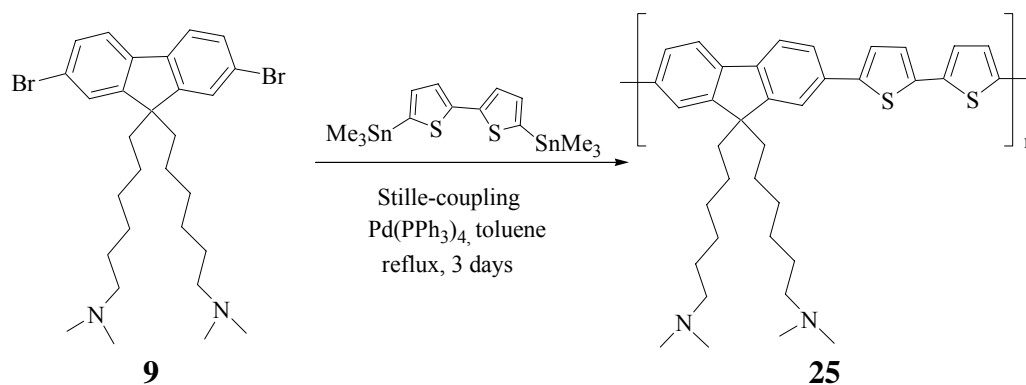
UV/VIS and fluorescence spectra of Poly{9,9-bis[6-(N,N-trimethylammonium)hexyl]fluorene-*co*-2,5-thienylene} **24** showed an absorption band peaking at $\lambda_{\text{max}} = 431$ nm and a shoulder at around 455 nm. There is a red shift

of 53 and 59 nm resp, as compared to the copolymers **17** and **18** respectively. Optical excitation at $\lambda_{\text{max}} = 431$ nm gives a yellow fluorescence in the range of 475-600 nm with a maximum at $\lambda_{\text{max}} = 503$ nm (Fig. **26**). There is a slight red-shift observed in absorption and emission spectra going from **23**→ **24**. (absorption:19 nm, emission:3 nm). The more pronounced red-shift of the absorption reflects a higher ordered (more extended) backbone structure. There is also a red shift observed in the emission spectra of **24** as compared to **17** and **18** respectively (78 nm each).

3.8 Synthesis of a cationic, water-soluble fluorene-type copolymer **25** with a bithiophene spacer.

A cationic water-soluble fluorene-type copolymer with a bithiophene spacer was also synthesized. Changes in the absorption and photoluminescence properties when increasing the size of oligothiophylene building blocks have been followed.

Poly{9,9-bis[6-(N,N-dimethylamino)hexyl]fluorene-co-2,2'-bithiophene} **25** as a non-ionic precursor was synthesized by a Stille-type cross-coupling reaction of 2,7-dibromo-9,9-bis[6-(N,N-dimethylamino)hexyl]fluorene **9** and 5,5'-bis(trimethylstannyl)-2,2'-bithiophene **13** using a palladium(0) catalyst and toluene as a solvent. The work-up and precipitation of **25** into methanol gave of poly{9,9-bis[6-(N,N-dimethyl-amino)hexyl]fluorene-co-2,2'-bithiophene} **25** as a yellow soild (Scheme **31**) in 43 % yield.



Scheme 31: Synthesis of poly{9,9-bis[6-(N,N-dimethylamino)hexyl]fluorene-co-2,2'-bithiophene} **25**

The $^1\text{H-NMR}$ spectrum of poly{9,9-bis[6-(N,N-dimethylamino)hexyl]fluorene-*co*-2,2'-bithiophene} **25** shows 4 signals, one broad signal at 7.4-7.8 ppm is for the aromatic protons and other 3 signals at 2.1-2.3 ppm, 1.2-1.6 ppm, 0.8-1.0 ppm for the alkyl protons.

GPC analysis in toluene gave a low number average molecular weight (\overline{M}_n) of only $1,300 \text{ gmol}^{-1}$, corresponding to oligomeric products. However, the solubility of **25** in toluene is limited.

3.8.1 Absorption and photoluminescence properties of **25**

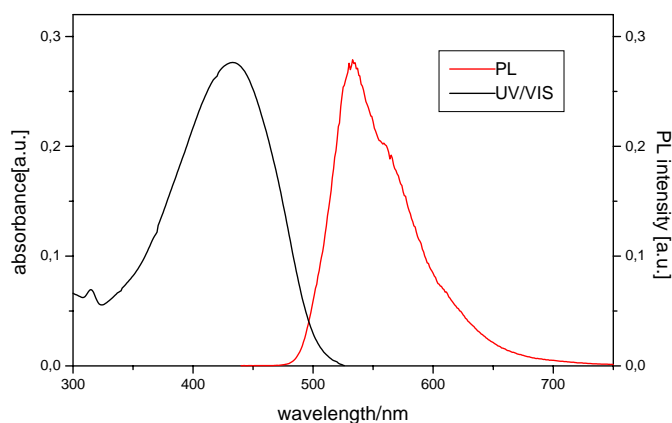
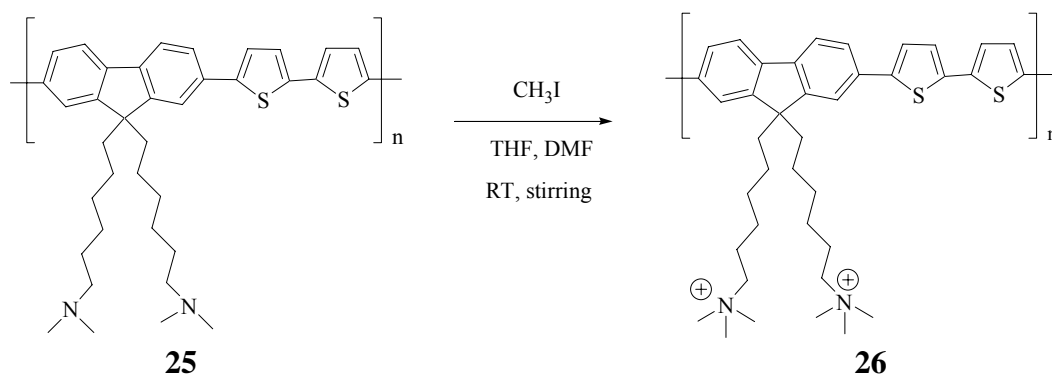


Fig. 27: UV/VIS & fluorescence spectra of **25** in chloroform at room temperature

UV/VIS and fluorescence spectra of poly{9,9-bis[6-(N,N-dimethylamino)hexyl]fluorene-*co*-2,2'-bithiophene} **25** showed an absorption band peaking at $\lambda_{\text{max}} = 430 \text{ nm}$. This spectrum is red shifted as compared to the thienylene copolymer **23** as result of the incorporation of an additional thiophene group. Excitation at $\lambda = 430 \text{ nm}$ gave an emission peaking at $\lambda_{\text{max}} = 530 \text{ nm}$ (Fig. **27**).

Poly{9,9-bis[6-(N,N-dimethylamino)hexyl]fluorene-*co*-2,2'-bithiophene} **25** was converted to poly{9,9-bis[6-(N,N-trimethylammonium)hexyl]fluorene-*co*-2, 5-thienylene} **26** by quaternization with methyl iodide in mixture of DMF and THF in 68 % yield (Scheme **32**).



Scheme 32: Synthesis of poly{9,9-bis[6-(*N,N*-trimethylammonium)hexyl]-fluorene-*co*-2,2'-bithiophene} **26**

3.8.2 Absorption and photoluminescence properties of **26**

UV/VIS and fluorescence spectra of poly{9,9-bis[6-(*N,N*-trimethylammonium)hexyl]fluorene-*co*-2,2'-bithiophene} **26** showed an absorption band peaking at $\lambda_{\max} = 435$ nm and a shoulder at around 455 nm. Optical excitation at $\lambda_{\max} = 435$ gives a emission at a maxima of $\lambda_{\max} = 486$ nm (Fig. **28**). There is a slight red-shift (5 nm) observed in the absorption spectrum going from **25** \rightarrow **26**. However, the PL displays a distinct blue shift from $\lambda_{\max} = 530$ nm (**25**) to $\lambda_{\max} = 486$ nm (**26**). The origin of this effect is unclear and needs some further investigation.

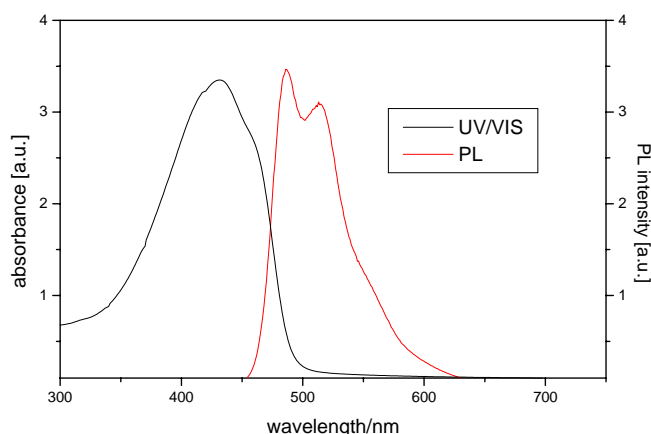


Fig. 28: UV/VIS & fluorescence spectra of **26** in water at room temperature

3.9 Synthesis of a polyfluorene with liquid-crystalline side chains

Side-chain liquid crystalline polymers are relatively new class of polymeric materials. These polymers consist of some type of liquid crystalline molecule (mesogen) attached to the polymer backbone through a spacer chain that is typically a few carbon atoms long. The possible uses for these materials take advantage of their physical properties. Among the potential uses are non-linear optical devices, optical data storage, etc.

Side chain liquid crystalline polymers can undergo several phase changes between the crystalline solid and the isotropic liquid state. These “between” phases are known as mesophases. The molecular arrangements in these mesophases vary with the type of the mesophase. The mesophases are more ordered than the liquid state, but they flow, unlike the crystalline state.

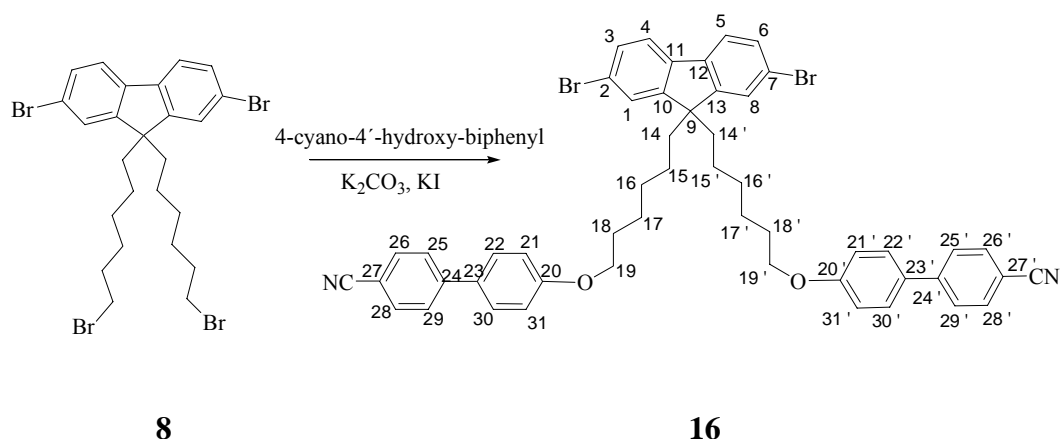
Side chain liquid crystals can be applied to orientation experiments. The orientation of nematic liquid crystals close to solid surfaces is of high interest for both fundamental physics and application in liquid crystal displays (LCDs). All LCDs contain polymeric alignment layers on their inside surfaces inducing a well defined ground state of the cell.^[127] The current technology mostly relies on mechanical rubbing of polyimide surfaces,^[128] where the rubbing direction defines the in-plane anisotropy.

Studies on the orientation of LC monolayers are most useful under conditions of “strong anchoring” that is, under conditions where the surface-LC interaction is stronger than the interaction between the first LC layer and the LC bulk. Experimental support for strong anchoring was found for the cyanobiphenyl family.^[129]

It was, therefore interesting to study the side-chain, liquid crystalline polymers with cyanobiphenyl mesogens and a polyfluorene backbone. Poly[9,9-bis(4-cyanobiphenyl-4'-oxyhexyl)-fluorene] **28** was synthesized as a novel rigid-rod, side-chain liquid-crystalline polymer with a fluorescent main-chain.

The monomer 2,7-dibromo-9,9-bis(4-cyanobiphenyl-4'-oxyhexyl)fluorene **16** was synthesized from 2,7-dibromo-9,9-bis-(6-bromohexyl)fluorene **8**, 4-cyano-4'-hydroxy-biphenyl, anhyd. K₂CO₃ and a trace of KI. Recrystallisation from

toluene gave 2,7-dibromo-9,9-bis(4-cyanobiphenyl-4'-oxyhexyl)fluorene **16** in around 70 % yield (Scheme 25).



Scheme 33: Synthesis of 2,7-dibromo-9,9-bis(4-cyanobiphenyl-4'-oxyhexyl)-fluorene **16**

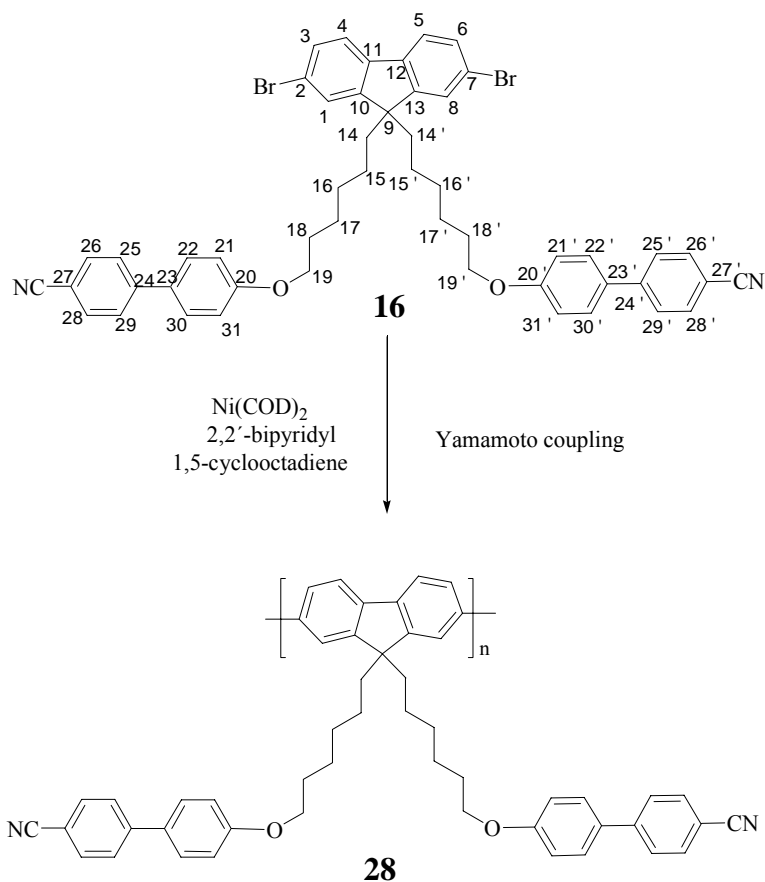
The $^1\text{H-NMR}$ spectrum of **16** showed 10 groups of signals, 5 at 7.70, 7.55, 7.30, 7.18, and 6.95 ppm are for aromatic protons and 5 at 3.9, 1.95, 1.65, 1.21, and 1.18 ppm for alkyl protons.

The $^{13}\text{C-NMR}$ spectrum displays 20 signals, 13 signals (δ : 110.1, 115.1, 119.0, 121.5, 126.1, 127.0, 128.2, 130.3, 132.5, 139.1, 145.2, 152.3, 159.7 ppm) of non-equivalent aromatic carbons, and 7 signals (δ : 21.4, 23.6, 25.6, 29.5, 40.1, 55.6, 67.9 ppm) for alkyl carbons. The M^+ peak was observed at 878. IR-spectrum showed signals at 2920, 2840, 2220, 1600, 1500, 1250, 1180, 1020, 820 cm^{-1} . The bands at 2920 and 2840 cm^{-1} are for alkyl C-H stretch, the signal at 2220 cm^{-1} for the aryl -CN function. The signals at 1600, 1250 and 820 cm^{-1} are characteristic for the aromatic C=C bending, C-O stretching, and aromatic C-H bending, respectively.

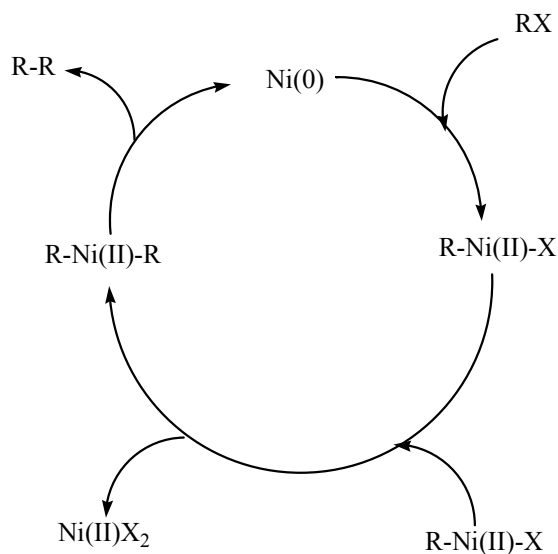
Poly[9,9-bis(4-cyanobiphenyl-4'-oxyhexyl)fluorene] **28** was synthesized by a Yamamoto-type coupling reaction of 2,7-dibromo-9,9-bis(4-cyano-biphenyl-4'-oxyhexyl)fluorene **16** with $\text{Ni}(\text{COD})_2$, bipyridyl, and 1,5 cyclooctadiene at 80° C for 5 days (Scheme 34).

$^1\text{H-NMR}$ spectroscopy of poly[9,9-bis(4-cyanobiphenyl-4'-oxyhexyl)fluorene] **28** shows 3 broad signals, one signal for aromatic protons at 6.7-7.9 ppm and two signals at 3.6-3.9 ppm and 0.8-2.3 ppm for the alkyl protons.

The GPC analysis displayed a number average molecular weight (\overline{M}_n) of 9,700 g mol^{-1} , corresponding to a degree of polymerization of ca.13.

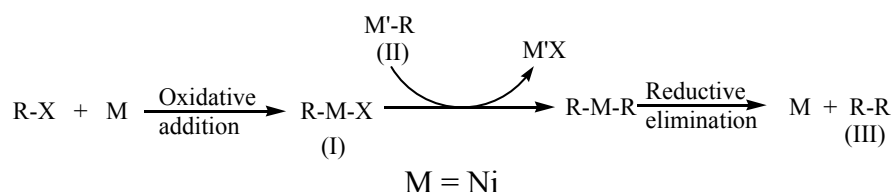


Scheme 34: Synthesis of poly[9,9-bis(4-cyanobiphenyl-4'-oxyhexyl)-fluorene] **28**



Scheme 35: Mechanism of the Yamamoto-type coupling reaction

The *Yamamoto-type aryl-aryl-coupling* uses stoichiometric amounts of $\text{Ni}(\text{COD})_2$ [95] (Scheme 35). A general catalytic cycle proceeds through the following cycle mediated by the organonickel species.



In the reaction cycle oxidative addition of halides to the transition metal complex, e.g. $\text{Ni}(0)$, occurs followed by transmetalation, and subsequent reductive elimination to give the coupling product. However, this mechanism is not fully accepted.

3.9.1 Absorption and photoluminescence properties of **28**

UV/VIS and fluorescence spectroscopy of poly[9,9-bis(4-cyanobiphenyl-4'-oxyhexyl)fluorene] **28** shows a long wavelength absorption band peaking at $\lambda_{\text{max}} = 370$ nm and an emission maximum at $\lambda_{\text{max}} = 430$ nm. The absorption band peaking at $\lambda_{\text{max}} = 297$ nm corresponds to the 4-cyanobiphenyl side chain, the band at $\lambda_{\text{max}} = 370$ nm is the polyfluorene absorption band (Fig. 29).

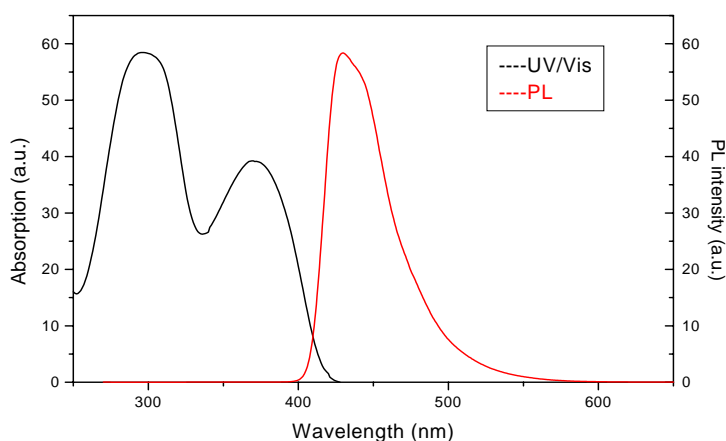


Fig. 29: UV/Vis and fluorescence spectra of **28** measured in chloroform.

The thermal properties of **28** have been analysed by DSC. Fig. 30 gives the DSC curve for poly[9,9-bis(4-cyanobiphenyl-4'-oxyhexyl)fluorene] **28** upon

heating. A glass transition of the amorphous phase is observed at ca. 98°C. A transition of the crystalline phase into a liquid-crystalline mesophase was observed at ca. 121°C, the transition into the isotropic melt at 147°C.

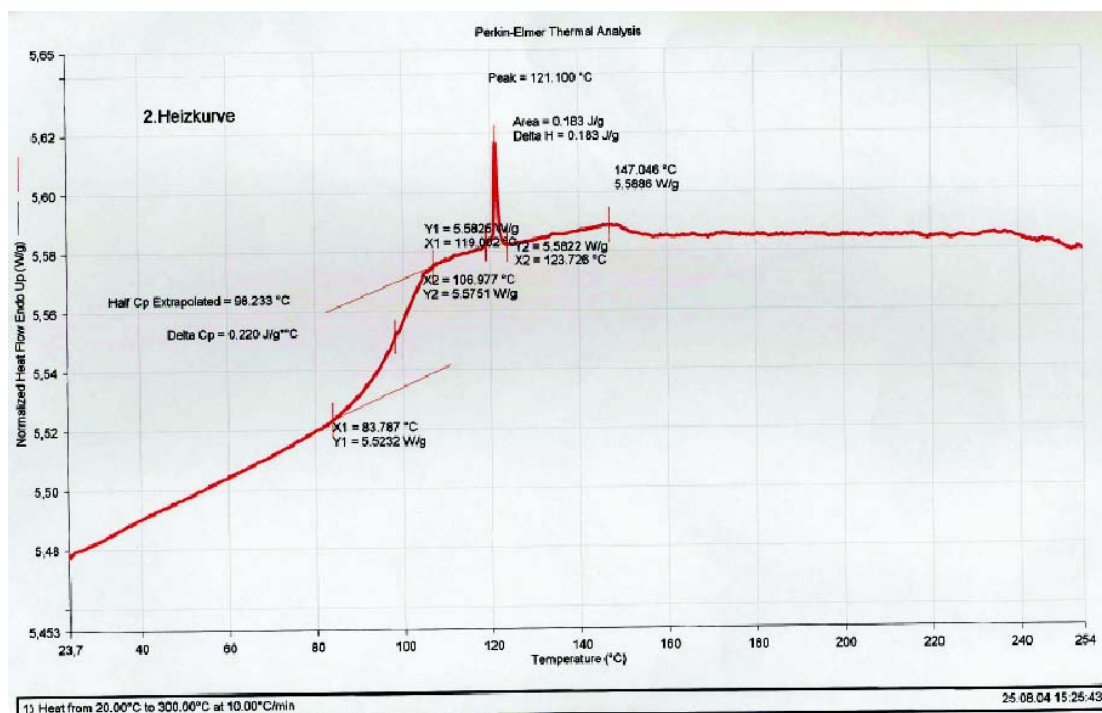


Fig. 30: DSC for compound **28** on heating.

Polarizing microscopy was used to investigate the liquid crystalline phases of the polymer **28**. Upon heating compound **28** shows the occurrence of a liquid crystalline mesophase at temperatures of >120°C. At temperatures >150°C the liquid crystalline phase is converted into the isotropic melt. On cooling no clear transitions have been observed, it seems that a frozen, glassy LC phase is formed (hindered recrystallisation). The texture of the LC mesophase is not a typical Schlieren texture of nematic phases (Fig. **31**). Further investigation of the textures will be done.

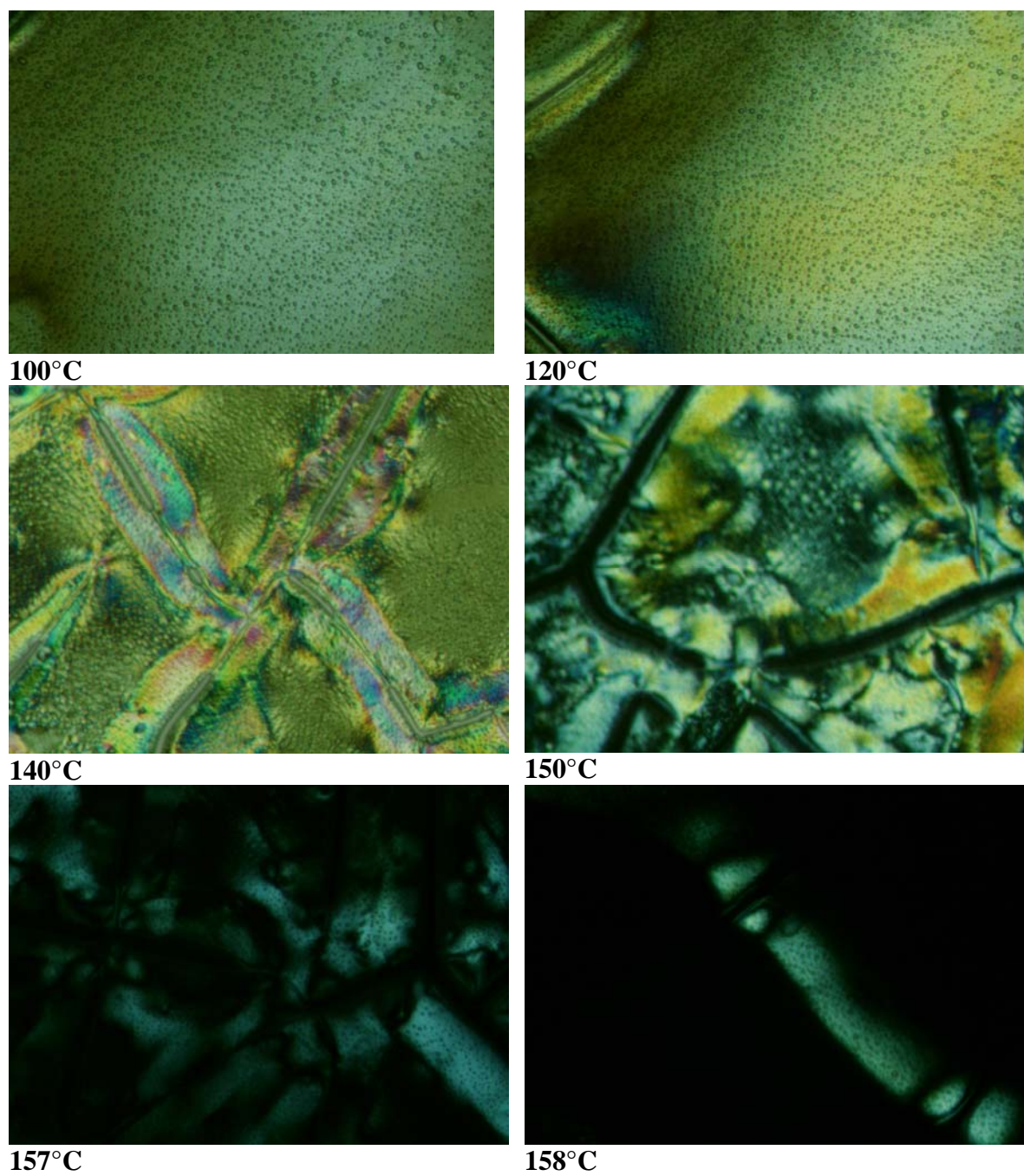


Fig. 31: *Polarising microscopy images of polymer 28 during heating*

4 Experimental

4.1 Instrumental details

Fluorescence spectrometer

Fluorescence spectra were measured at room temperature in chloroform, DMSO, toluene, THF or water on Fluoromax 3, Cary Eclipse, or Varian Spectrophotometer.

Gel permeation chromatography (GPC)

Gel permeation chromatography measurements were carried out using

1) Spectra 100, Column MZ sdv-Gel, RI detection-Shodex (RI-71) and UV-detector (UV 2000), toluene, and THF as a solvents using Polystyrene calibration (PSS).

2) Jasco AS950, Column MZ lineal mixed bed, UV detector (UV-2070), RI-detection-Jasco (RI-930), Viscotec T60, toluene and THF as a solvents using Polystyrene calibration (PSS).

For water soluble polymers:-1) Waters GPC, UV detector (SOMA S3702), RI-waters 7512, Calibration was with polystyrene in DMF. 2) Spectra 100, RI-(Shodex RI-71) and UV-detector (UV 2000), LiBr/NMP as eluents.

IR-spectroscopy

Infrared spectroscopy measurements were performed on a Nicolet, Model Impact 400 spectrophotometer. Samples were prepared as KBr pellets and measured in the 400 to 4000 cm^{-1} region.

Mass spectroscopy

Mass spectra were obtained on VG Instrument ZAB 2-SE-FPD & Bruker reflex II by using FD ionization.

NMR-spectroscopy

^1H -NMR and ^{13}C -NMR spectra are recorded in CDCl_3 , $\text{C}_2\text{D}_2\text{Cl}_4$, D_2O , d_6 -DMSO and d_6 -acetone on a Bruker ARX 400 and Bruker AMX 300 with use of the solvent proton or carbon signal as internal standard.

Polarizing light microscopy

Polarizing Light microscopy was carried out using Nikon Eclipse E 600. Images were taken on a digital camera directly connected to the microscope.

UV/Vis absorption spectroscopy

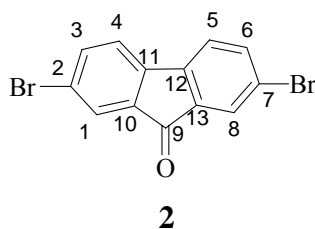
UV/Vis spectra were recorded at room temperature on a Jasco V-550 and Uvikon 931 spectrometers.

Chemicals and reagents

Commercially available chemicals were purchased from Sigma Aldrich and Acros, and were used as received. Reagents for Suzuki-type cross-coupling method, $[\text{PdCl}_2(\text{dppf})]$ and $\text{Pd}(\text{PPh}_3)_4$, were used as received from Strem. Purification for water soluble polymers was done using dialysis membrane with membrane cut-off of $\overline{M}_n = 3,500 \text{ gmol}^{-1}$ which was purchased from Sigma-Aldrich.

4.2 Monomers

4.2.1 2,7-Dibromofluorene-9-one **2**



2,7-Dibromofluorene **1** (10 g, 30.86 mmol) and sodium dichromate (15.72 g, 60 mmol) were dissolved in 120 ml of acetic acid under argon atmosphere and heated to reflux for 6 hours. It was then allowed to cool at room temperature. Water was added to the reaction mixture, the mixture was stirred again for another 10-15 min. The solid was filtered through the Buechner funnel. The residue was washed several times with water to get a yellow solid. It was recrystallised from 200 ml of ethanol. The yellow crystals formed were filtered off through a funnel to get 8.96 g of 2,7-Dibromofluorene-9-one **2** (86 %).

¹H NMR-spectrum (400 MHz, CDCl₃):

$\delta(^1\text{H})$ [ppm]: 7.93 (d, 2H, H1, H8), 7.68 (d, 2H, H3, H6, $J=8.1$ Hz), 7.4 (d, 2H, H4, H5, $J=8.1$ Hz)

¹³C NMR-spectrum (100 MHz, CDCl₃)

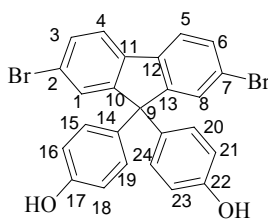
$\delta(^{13}\text{C})$ [ppm]: 185.5 (C=O), 138.9, 137.2, 136.0, 133.9, 129.3, 121.7

FD-MS (m/z): 338 (M⁺)

Elemental Analysis: (C₁₃H₆Br₂O)

Calculated (%): C: 46.20; H: 1.79; Br: 47.28

Found (%): C: 46.43; H: 1.93; Br: 47.11

4.2.2 2,7-Dibromo-9,9-bis(4-hydroxyphenyl)fluorene **3****3**

2,7-Dibromofluorene-9-one **2** (5 g, 14.8 mmol), phenol (10.44 ml, 118.4 mmol) and methanesulfonic acid (1 ml, 1 mmol) were refluxed at 100°C for 4 h under argon. Solvents were evaporated. 100 ml of ethanol was added to it and again refluxed overnight. Product falls out in ethanol. Filtered, washed with cold ethanol and dried. 2,7-Dibromo-9,9-bis(4-hydroxyphenyl)fluorene **3** was obtained as white solid (4.54 g, 60.37 %)

¹H NMR-spectrum (400 MHz, DMSO):

$\delta(^1\text{H})$ [ppm]: 7.82 (d, 4H, H1, H8), 7.62 (d, 2H, H3, H6, $J=8.1$ Hz), 7.50 (d, 2H, H4, H5, $J=8.1$ Hz), 6.85 (d, 4H, H15, H19, H20, H24, $J=8.7$ Hz), 6.65 (d, 4H, H16, H18, H21, H23, $J=8.7$ Hz)

¹³C NMR-spectrum (100 MHz, DMSO)

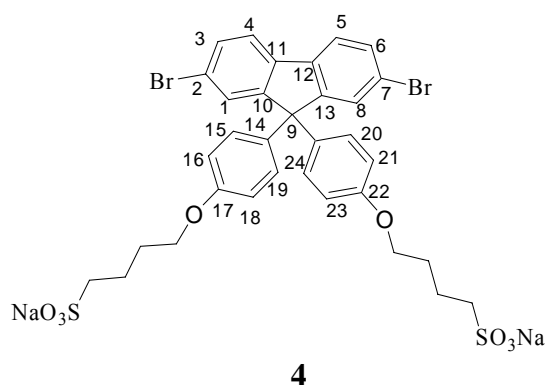
$\delta(^{13}\text{C})$ [ppm]: 63.94, 115.2, 118.7, 122.8, 128.5, 129.2, 130.5, 134.3, 137.4, 153.8, 156.3.

FD-MS (m/z): 508 (M^+)

Elemental Analysis: ($\text{C}_{25}\text{H}_{16}\text{Br}_2\text{O}_2$)

Calculated (%): C: 59.08; H: 3.17; Br: 31.45

Found (%): C: 58.97; H: 3.24; Br: 31.59

4.2.3 2,7-Dibromo-9,9-bis(4-sulfonylbutoxyphenyl)fluorene **4**

2,7-Dibromo-9,9-bis(4-hydroxyphenyl)fluorene **3** (2.5 g, 4.91 mmol) was dissolved in a solution of NaOH (0.7615 g, 19 mmol) in 70ml of water under argon. A solution of 1,4-butane sultone (1.054 g, 7.7 mmol) in 40ml of dioxane was added to the former solution at once. The resulting mixture was stirred at room temperature overnight. Then it was heated at 80-100°C for 30 minutes and cooled in a water/ice bath. Suspension obtained was vacuum filtered and the solid was washed with cold water followed by acetone. 2,7-Dibromo-9,9-bis(4-sulfonylbutoxyphenyl)fluorene **4** was obtained as a white solid (3.1 g, 76.44 %)

¹H NMR-spectrum (400 MHz, DMSO):

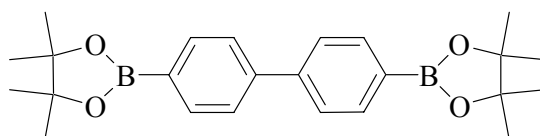
$\delta(^1\text{H})$ [ppm] : 7.82 (d, 4H, H1, H8), 7.62 (d, 2H, H3, H6, $J=8.1$ Hz), 7.50 (d, 2H, H4, H5, $J=8.1$ Hz), 6.85 (d, 4H, H15, H19, H21, H25, $J=8.7$ Hz), 6.65 (d, 4H, H16, H18, H22, H24, $J=8.7$ Hz), 3.9 (t, 4H, α -CH₂), 3.3 (t, 4H, δ -CH₂), 2.3 (m, 4H, γ -CH₂), 1.7 (m, 4H, β -CH₂)

¹³C NMR-spectrum (100 MHz, DMSO)

$\delta(^{13}\text{C})$ [ppm]: 21.7, 27.9, 51.3, 63.90, 67.2, 114.9, 118.7, 122.8, 128.5, 129.2, 130.5, 134.3, 137.4, 153.8, 157.7

IR: 3070, 2942, 2872, 1607, 1569, 1508, 1452, 1178, 1048, 807, 604cm⁻¹.

FD-MS (m/z): 824 (M⁺)

4.2.4 4,4'-Biphenyl-bis(4,4,5,5-tetramethyl-1,3,2-dioxaborolane) **6****6**

40 ml of n-butyllithium (100 mmol, 2.5 M) and 40 ml of dry THF were cooled to -78°C under an atmosphere of dry argon. Subsequently 4,4'-dibromobiphenyl **5** (12.8 g, 41 mmol) dissolved in dry 40 ml of THF was added dropwise over 30 min, followed by stirring for 3 h at -78°C . The resulting 4,4'-dilithiobiphenyl was treated with trimethyl borate (32 ml) and stirred for 1 h at -78°C . The reaction mixture was warmed to room temperature and stirred for 30 min before pouring onto crushed ice containing 40 ml of conc. HCl. After extraction into diethylether the organic layer was dried over anhydrous Na_2SO_4 , and the solvent was removed in vacuum to afford a white solid (7.9 g, 32.67 mmol). 5.34 g (45.21 mmol) of pinacol was added to it. Reaction mixture was refluxed in 100 ml dry toluene using a Dean-Stark trap for two days. Solvent was evaporated and the crude white powder obtained was purified by column chromatography using hexane:ethylacetate (90:10) as eluent. The solvent was evaporated giving the product as white powder. 4,4'-Biphenyl-bis(4,4,5,5-tetramethyl-1,3,2-dioxaborolane) **6** was obtained as a white solid in 2.65 g, 20 % yield.

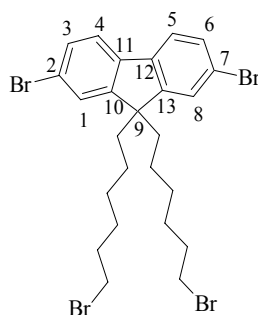
 ^1H NMR-spectrum (400 MHz, CDCl_3):

$\delta(^1\text{H})$ [ppm]: 7.9 (d, 4H, $J=8$ Hz), 7.6 (d, 4H, $J=8$ Hz), 1.26 (s, 24H, -CH₃)

 ^{13}C NMR-spectrum (100 MHz, CDCl_3)

$\delta(^{13}\text{C})$ [ppm]: 24.8, 83.8, 126.4, 128.7, 135.3, 143.6

FD-MS (m/z): 406 (M^+)

4.2.5 2,7-Dibromo-9,9-bis-(6-bromohexyl)fluorene **8****8**

A 250 ml flask was filled with 2,7-dibromofluorene **7** (5 g, 15.4 mmol), benzyl triethylammonium chloride (0.19 g, 3.33 mmol), and 20 ml of DMSO. The tube was flushed with argon and sealed with a rubber stopper. Freshly prepared aqueous NaOH solution (20 ml 1:1 weight/weight) was added at once with a syringe. The mixture turned orange and became viscous rapidly. 1,6-Dibromohexane (24 ml, 32.4 mmol) was added within 2 minutes. The reaction was carried out for 2 h at ambient temperature. *tert*-Butylmethylether (500 ml) and water (200 ml) were added, and mixture was stirred for additional 15 minutes. The phases were separated; the aqueous phase was extracted once again with *tert*-butylmethylether. The combined organic phases were washed with each 100 ml of 2N aqueous HCl, saturated NaCl solution, and deionized water. The organic phase was dried over MgSO₄, and the solvent was evaporated. The crude product was purified by column chromatography using hexane as eluent. The solvent was evaporated giving the product as a viscous oil. To remove the excess of 1,6-dibromohexane the product was distilled to give 2,7-Dibromo-9,9-bis(6-bromohexyl)fluorene **8** (6.5 g, 64.8 %) as a colorless liquid.

¹H NMR-spectrum (400 MHz, CDCl₃):

$\delta(^1\text{H})$ [ppm]: 7.35 (d, 2H), 7.3 (d, 2H), 7.2 (s, 2H), 3.34 (t, 4H), 1.85 (t, 4H), 1.65 (m, 4H), 1.15 (m, 8H), 0.55 (m, 4H)

¹³C NMR-spectrum (100 MHz, CDCl₃)

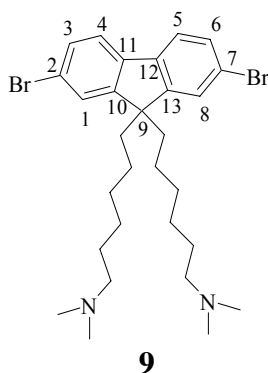
$\delta(^{13}\text{C})$ [ppm]: 23.6, 27.9, 29.08, 32.7, 34.1, 40.1, 55.6, 121.4, 121.7, 126.2, 130.2, 139.2, 152.3

FD-MS (m/z): 650 (M^+)

Elemental Analysis: ($C_{25}H_{30}Br_4$)

Calculated (%): C: 46.19; H: 4.65; Br: 49.16

Found (%): C: 46.36; H: 4.47; Br: 48.89

4.2.6 2,7-Dibromo-9,9-bis-[6-(N,N-dimethylamino)hexyl]fluorene **9**

To 2,7-Dibromo-9,9-bis(6-bromohexyl)fluorene **8** (1.54 g, 2.63 mmol) in 30 ml of THF, dimethylamine (52.5 ml, 2M in THF, 105 mmol) is added at -78°C. The mixture was allowed to warm up to room temperature and stirred for 3 days at this temperature. The mixture was concentrated, and 50 ml of aqueous sodium hydroxide solution (5 % w/w) were added. The mixture was extracted with 300 ml of Et₂O. The organic layer was dried over MgSO₄ and concentrated. The residue was purified by silica gel column chromatography (methanol/ethylacetate/triethylamine 10:88:2) to give **9** as a yellow oil (0.690 g, 50.36 %).

¹H NMR-spectrum (400 MHz, CDCl₃):

$\delta(^1\text{H})$ [ppm]: 7.55 (d, 2H), 7.5 (d, 2H), 7.42 (s, 2H), 2.1-2.2 (m, 16H), 1.3 (m, 4H), 1.1 (m, 8H), 0.6 (m, 4H)

¹³C NMR-spectrum (100 MHz, CDCl₃)

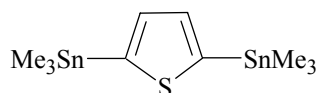
$\delta(^{13}\text{C})$ [ppm]: 23.6, 27.0, 27.53, 29.7, 40.1, 45.4, 55.6, 59.7, 121.1, 121.4, 126.1, 130.2, 139.0, 152.4

FD-MS (m/z): 584 (M⁺)

Elemental Analysis: (C₂₉H₄₂N₂Br₂)

Calculated (%): C: 69.72; H: 8.86; N: 5.61

Found (%): C: 68.18; H: 8.24; N: 5.42

4.2.7 2,5-Bis(trimethylstannyl)thiophene **11****11**

To a stirred cooled solution (-50°C) of thiophene **10** (1.009 g, 12 mmol) and N,N,N',N'-tetramethylethylenediamine (3.98 ml, 26.8 mmol) in anhydrous hexane-THF (10:20 ml) was added nBuLi (2.5 M in hexane) (17.56 ml, 28.1 mmol) dropwise with a syringe. The mixture was heated to reflux for 45 min and then cooled to -78°C. Trimethyltinchloride (28.1 ml, 112.4 mmol) was added to the resulting mixture, and the mixture was stirred for 2 h at room temperature. The solution was then poured into aqueous NH₄Cl (2M). The aqueous layer was extracted with 500 ml of Et₂O. The combined organic layers were washed with water, dried over MgSO₄, and the solvent was evaporated. The resulting solid was recrystallised from ethanol. 2,5-Bis(trimethylstannyl) thiophene **11** was obtained as a white solid (3.48 g, 70.5 %)

¹H NMR-spectrum (400 MHz, C₂D₂Cl₄):

$\delta(^1\text{H})$ [ppm]: 7.37 (s, 2H), 0.37 (s, 18H)

¹³C NMR-spectrum (100 MHz, C₂D₂Cl₄)

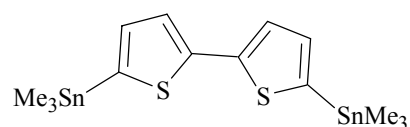
$\delta(^{13}\text{C})$ [ppm]: 143.4, 136.2, 7.68

FD-MS (m/z): 409 (M⁺)

Elemental Analysis: (C₁₀H₂₀SSn₂)

Calculated (%): C: 29.32; H: 4.92; S: 7.83; Sn: 57.93

Found (%): C: 29.30; H: 5.27; S: 7.59

4.2.8 5,5'-Bis(trimethylstannyl)-2,2'-bithiophene **13****13**

To a stirred cooled solution (-50°C) of bithiophene **12** (1.99g, 12mmol) and N,N,N',N'-tetramethylethylenediamine (3.98 ml, 26.8 mmol) in anhydrous hexane-THF (10:20 ml) was added nBuLi (2.5 M in hexane) (17.56 ml, 28.1 mmol) dropwise via a syringe. The mixture was heated to reflux for 45 min and then cooled to -78°C. Trimethyltinchloride (28.1 ml, 112.4 mmol) was added dropwise via a syringe, and the mixture was stirred for 2 h at room temperature. Workup and purification was similar to the above. 5,5'-Bis(trimethylstannyl)-2,2'-bithiophene **13** was obtained as a bright brown solid (4.25 g, 72 %).

¹H NMR-spectrum (400 MHz, C₂D₂Cl₄):

$\delta(^1\text{H})$ [ppm]: 7.20 (d, 2H, J=3 Hz), 7.02 (d, 2H, J=3.3 Hz), 0.31 (s, 18H)

¹³C NMR-spectrum (100 MHz, C₂D₂Cl₄)

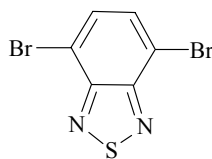
$\delta(^{13}\text{C})$ [ppm]: 143.1, 137.6, 136.3, 125.1, 7.73

FD-MS (m/z): 491.8 (M⁺)

Elemental Analysis: (C₁₄H₂₂S₂Sn₂)

Calculated (%): C: 34.19; H: 4.51; S: 13.04; Sn: 48.27

Found (%): C: 34.26; H: 4.14; S: 12.70

4.2.9 4,7-Dibromo-benzo[1,2,5]thiadiazole **15****15**

A mixture of 1,2,5-benzothiadiazole **14** (5g, 36.81 mmol) in 35 ml of aqueous hydrobromic acid (48%) was heated to reflux with stirring, while bromine (5.67 ml, 103.20 mmol) was added slowly within 10-15 min. Towards the end of the addition, the mixture became a suspension. To facilitate stirring, 20 ml of aq HBr was added and the mixture was heated to reflux for 2 h after completion of the bromine addition. Mixture was cooled, filtered, washed with water. Recrystallisation from methanol gave 4,7-Dibromo-benzo[1,2,5]thiadiazole **15** as white crystals in 58.5 % (6.28 g) yield.

¹H NMR-spectrum (400 MHz, C₂D₂Cl₄):

$\delta(^1\text{H})$ [ppm]: 7.78 (s, 2H)

¹³C NMR-spectrum (100 MHz, C₂D₂Cl₄)

$\delta(^{13}\text{C})$ [ppm]: 152.9, 132.24, 113.83

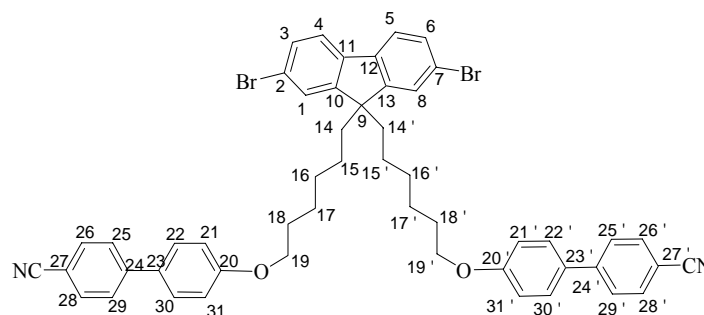
FD-MS (m/z): 293 (M⁺)

Elemental Analysis: (C₆H₂Br₂N₂S)

Calculated (%): C: 24.51; H: 0.69; Br: 54.36; N: 9.53; S: 10.91

Found (%): C: 24.11; H: 0.48; Br: 54.17; N: 9.14; S: 10.65

4.2.10 2,7-Dibromo-9,9-bis(4-cyanobiphenyl-4'-oxyhexyl)fluorene 16

**16**

2,7-Dibromo-9,9-bis(6-bromohexyl)fluorene 8 (2 g, 3.076 mmol), 4-cyano-hydroxy-biphenyl (1.3212 g, 6.76 mmol), anhydrous potassium carbonate (1.2756 g, 9.228 mmol) and a trace of potassium iodide were taken in a two neck flask. 40 ml of DMF was added to it and heated to 90-100° C for 2 hours. Complete conversion was observed by TLC. Then large excess of demineralised water was added. Product was precipitated out and filtered and dried on the high vacuum pump. The product was recrystallised from toluene. 2,7-Dibromo-9,9-bis(4-cyanobiphenyl-4'-oxyhexyl)fluorene 16 was obtained as a white solid (1.39 g, 70 %).

¹H NMR-spectrum (400 MHz, CDCl₃):

$\delta(^1\text{H})$ [ppm]: 7.70 (dd, 4H), 7.55 (m, 6H), 7.30 (dd, 4H), 7.18 (dd, 4H) 6.95 (d, 4H), 3.9 (t, 4H), 1.95 (m, 4H), 1.65 (m, 4H), 1.21 (m, 4H), 1.18 (m, 8H).

¹³C NMR-spectrum (100 MHz, CDCl₃)

$\delta(^{13}\text{C})$ [ppm]: 21.4, 23.6, 25.6, 29.5, 40.1, 55.6, 67.9, 110.1, 115.1, 119.0, 121.5, 126.1, 127.0, 128.2, 130.3, 132.5, 139.1, 145.2, 152.3, 159.7

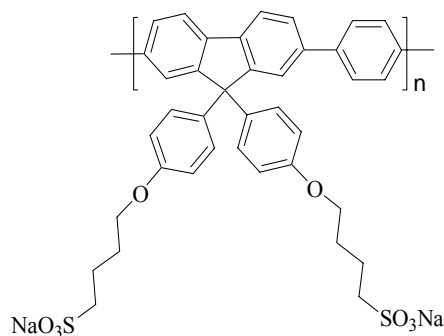
IR: 2920, 2840, 2220, 1600, 1500, 1250, 1180, 1020, 820 cm⁻¹.

FD-MS (m/z): 878 (M⁺)

4.3 Polymers

4.3.1 Poly[9,9-bis(4-sulfonylbutoxyphenyl)fluorene-co-1,4-phenylene] **17**

(Suzuki-type coupling)



17

A mixture of 2,7-dibromo-9,9-bis(4-sulfonylbutoxyphenyl)fluorene **4** (0.824 g, 1 mmol), 1,4-phenylenediboronic acid (0.166 g, 1 mmol), Pd(PPh₃)₄ (50 mg) and Na₂CO₃ (1 g, 9.4 mmol) in 5 ml of distilled water, 50 ml of toluene and 5ml of butanol was reacted for 3 days at 135°C (reflux). 100 ml of chloroform was added and the mixture was extracted with 300 ml of water. The aqueous layer was washed with chloroform and concentrated to dryness. The residue was redissolved in water and purified by dialysis with water using a dialysis membrane with a cutoff at $\overline{M}_n = 3,500 \text{ gmol}^{-1}$ to yield 0.50 g (54 %) of poly[9,9-bis(4-sulfonylbutoxy phenyl)fluorene-co-1,4-phenylene] **17**.

¹H NMR-spectrum (400 MHz, D₂O):

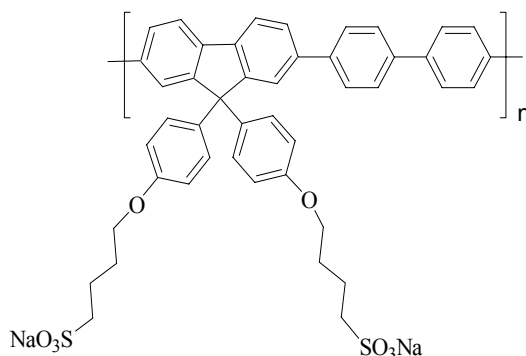
$\delta(^1\text{H})$ [ppm]: 6.8-7.9 (ar-H), 3.4-4.0 (α , δ -CH₂), 1.2-2.0 (β , γ -CH₂)

GPC (NMP/LiBr): $\overline{M}_n = 6,500 \text{ gmol}^{-1}$

UV/Vis (water): $\lambda_{\text{max, abs}} = 368 \text{ nm}$

Photoluminescence (water): $\lambda_{\text{max, PL}} = 425, 455 \text{ nm}$

4.3.2 Poly[9,9-bis(4-sulfonylbutoxyphenyl)fluorene-co-4,4'-biphenyl] **18** (Suzuki-type coupling)



18

A mixture of 2,7-dibromo-9,9-bis(4-sulfonylbutoxyphenyl)fluorene **4** (0.618 g, 0.75 mmol), 4,4'-biphenyl bis[4,4,5,5-tetramethyl-1,3,2-dioxaborolane] **6** (0.305 g, 0.75 mmol), Pd(PPh₃)₄ (35 mg) and Na₂CO₃ (0.75 g, 7.05 mmol) in 4 ml of distilled water, 35 ml of toluene and 4 ml of butanol was reacted for 3 days under reflux at 135°C. 100 ml of chloroform was added and the mixture was extracted with 300 ml of water. The aqueous layer was washed with chloroform and concentrated to dryness. The residue was redissolved in water and purified by dialysis with water using a dialysis membrane. Poly[9,9-bis(4-sulfonylbutoxyphenyl) fluorene-co-4,4'-biphenyl] **18** was obtained in 49 % yield (450 mg).

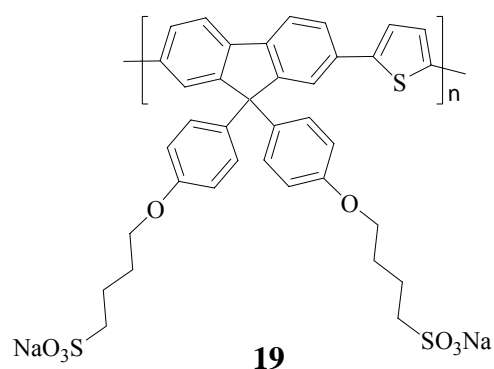
¹H NMR-spectrum (400 MHz, D₂O):

$\delta(^1\text{H})$ [ppm]: 5.5-7.9 (ar-H, broad), 2.5-3.5 (α , δ -CH₂), 1.1-2.2 (β , γ -CH₂)

GPC (NMP/LiBr): $\overline{M}_n = 8,400 \text{ gmol}^{-1}$

UV/Vis (water): $\lambda_{\text{max, abs}} = 362 \text{ nm}$

Photoluminescence (water): $\lambda_{\text{max, PL}} = 425, 455 \text{ nm}$

4.3.3 Poly[9,9-bis(4-sulfonylbutoxyphenyl)fluorene-co-2,5-thienylene] **19**

A solution of the 2,5-bis(trimethylstannyl)thiophene **11** (0.4097 g, 1 mmol), 2,7-dibromo-9,9-bis(4-sulfonylbutoxyphenyl)fluorene **4** (0.8245 g, 1 mmol) and Pd(PPh₃)₄ (40 mg) was refluxed in degassed, anhydrous toluene (25 ml) for 4 days under argon. After cooling to room temperature, toluene (50 ml) was added. The aqueous layer was removed carefully and evaporated to give a crume yellow solid. The residue was purified by dialysis with water using the dialysis membrane to yield 350 mg (42 %) of poly[9,9-bis(4-sulfonylbutoxyphenyl)fluorene-co-2,5-thienylene] **19**.

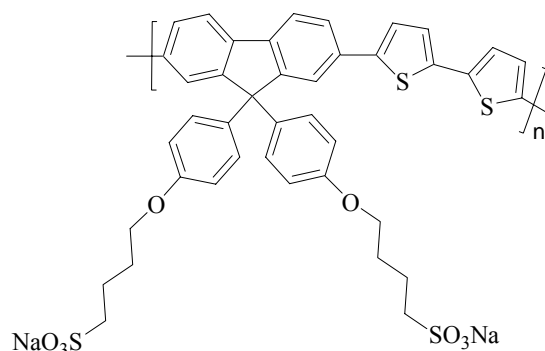
¹H NMR-spectrum (400 MHz, DMSO):

$\delta(^1\text{H})$ [ppm]: 6.0-7.6 (ar-H), 3.1-3.7 (α, δ -CH₂), 0.9-2.0 (β, γ -CH₂)

GPC (DMF): $\overline{M}_n = 3,500 \text{ gmol}^{-1}$

UV/Vis (water): $\lambda_{\text{max, abs}} = 418 \text{ nm}$

Photoluminescence (water): 505 nm

4.3.4 Poly[9,9-bis(4-sulfonylbutoxyphenyl)fluorene-co-2,2'-bithiophene] **20****20**

A solution of the 5,5'-bis(trimethylstannyl)-2,2'-bithiophene **13** (0.492 g, 1 mmol), 2,7-dibromo-9,9-bis(4-sulfonylbutoxyphenyl)fluorene **4** (0.8245 g, 1 mmol) and Pd(PPh₃)₄ (40 mg) was refluxed in degassed, anhydrous toluene (25 ml) for 4 days under argon. Workup and purification was similar to the above **19**, poly[9,9-bis(4-sulfonylbutoxyphenyl)fluorene-co-2,2'-bithiophene] **20** was obtained in 64 % yield (500 mg).

¹H NMR-spectrum (400 MHz, DMSO):

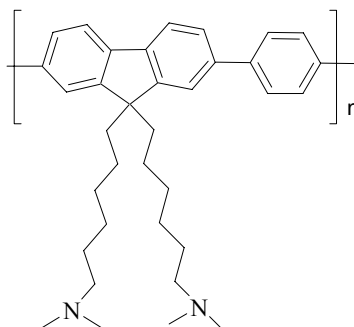
δ(¹H) [ppm]: 6.55-7.9 (ar-H), 3.1-4.45 (α, δ -CH₂), 0.9-2.0 (β, γ -CH₂)

GPC (DMF): $\overline{M}_n = 3,300 \text{ gmol}^{-1}$

UV/Vis (water): $\lambda_{\text{max abs}} = 405 \text{ nm}$

Photoluminescence (water): $\lambda_{\text{max, PL}} = 502, 530 \text{ nm}$

4.3.5 Poly{9,9-bis[6-(N,N-dimethylamino)hexyl]fluorene-co-1,4-phenylene} **21** (Suzuki-type coupling)

**21**

A mixture of 2,7-dibromo-9,9-bis[6-(N,N-dimethylamino)hexyl]fluorene **9** (0.5784 g, 1 mmol), 1,4-phenylenediboric acid (0.166 g, 1 mmol), PdCl₂ (dppf) (15 mg) and K₂CO₃ (0.56 g, 4 mmol) in 20 ml of THF and 20 ml of water was degassed and stirred for 3 days at 80°C. The resulting product was extracted with 500 ml of chloroform. The organic layer was washed with water and brine, dried over MgSO₄, and concentrated. Poly{9,9-bis[6-(N,N-dimethylamino)hexyl]fluorene-co-1,4-phenylene} **21** was isolated by precipitation into methanol as a yellowish solid (250 mg, 50.4 %).

¹H NMR-spectrum (400 MHz, CDCl₃):

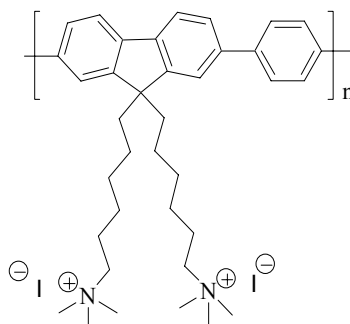
δ(¹H) [ppm]: 7.6-7.8 (m, 10 H), 2.0-2.3 (20 H), 1.2-1.3 (4 H), 1.1 (8 H), 0.7-0.8 (4 H).

GPC (THF): $\overline{M}_n = 3,500 \text{ gmol}^{-1}$

UV/Vis (CHCl₃): $\lambda_{\text{max, abs}} = 360 \text{ nm}$

Photoluminescence (CHCl₃): $\lambda_{\text{max, PL}} = 431 \text{ nm}$

4.3.6 Poly{9,9-bis[6-(N,N-trimethylammonium)hexyl]fluorene-co-1,4-phenylene} **22**

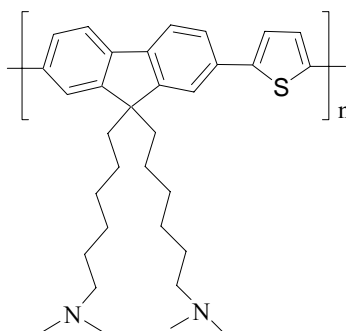
**22**

Methyl iodide (3.2 g, 22.5 mmol) was added to poly{9,9-bis[6-(N,N-dimethylamino)hexyl]fluorene-co-1,4-phenylene} **21** (100 mg) in 10 ml of THF and 10 ml of DMF at room temperature. After 1 min stirring, the formation of a precipitate was observed, which was redissolved by addition of 10 ml of water. After 24 h, 100 ml of Et₂O was added, and the mixture extracted with additional 300 ml of water. The aqueous layer was concentrated to dryness. The residue was purified by dialysis with water using a dialysis membrane to yield 120 mg of **22** (77 %).

UV/Vis (water): $\lambda_{\text{max, abs}} = 374 \text{ nm}$

Photoluminescence (water): $\lambda_{\text{max, PL}} = 423, 450 \text{ nm}$

4.3.7 Poly{9,9-bis[6-(N,N-dimethylamino)hexyl]fluorene-co-2,5-thienylene} **23**

**23**

A mixture of 2,7-Dibromo-9,9-bis[6-(N,N-dimethylamino)hexyl]fluorene **9** (0.5784 g, 1 mmol), 2,5-bis(trimethylstannyl)thiophene **11** (0.409 g, 1 mmol), Pd(PPh₃)₄ (40 mg) in 40 ml of toluene was degassed and stirred for 3 days at 80°C. The resulting product was extracted with 500 ml of chloroform. The organic layer was washed with water and brine, dried over MgSO₄, and concentrated. Poly{9,9-bis[6-(N,N-dimethylamino)hexyl]fluorene-co-2,5-thienylene} **23** was isolated by precipitation into methanol as a yellowish solid (400 mg, 41 %).

¹H NMR-spectrum (400 MHz, CDCl₃):

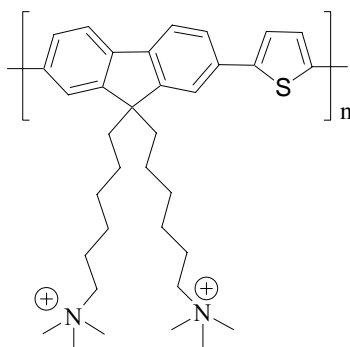
δ(¹H) [ppm]: 7.3-7.8 (m, 8 H), 1.8-2.3 (20 H), 1.0-1.4 (4 H), 0.7-0.9 (18 H).

GPC (toluene): $\overline{M}_n = 1,400 \text{ gmol}^{-1}$

UV/Vis (CHCl₃): $\lambda_{\text{max, abs}} = 412 \text{ nm}$

Photoluminescence (CHCl₃): $\lambda_{\text{max, PL}} = 532 \text{ nm}$

4.3.8 Poly{9,9-bis[6-(N,N-trimethylammonium)hexyl]fluorene-co-2,5-thienylene} **24**

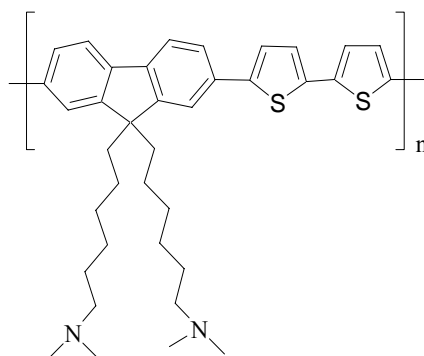
**24**

Methyl iodide (3.2 g, 22.5 mmol) was added to poly{9,9-bis[6-(N,N-dimethylamino)hexyl]fluorene-co-2,5-thienylene} **23** (100 mg) in 10 ml of THF and 10 ml of DMF at room temperature. After 1 min stirring, the formation of a precipitate was observed, which was redissolved by addition of 10 ml of water. After 24 h, 100 ml of Et₂O was added, and the mixture extracted with additional 300 ml of water. The aqueous layer was concentrated to dryness. Poly{9,9-bis[6-(N,N-trimethylammonium)hexyl]fluorene-co-2,5-thienylene} **24** was isolated in 58 %, 67 mg yield.

UV/Vis (water): $\lambda_{\text{max, abs}} = 431 \text{ nm}$

Photoluminescence (water): $\lambda_{\text{max, PL}} = 503 \text{ nm}$

4.3.9 Poly{9,9-bis[6-(N,N-dimethylamino)hexyl]fluorene-co-2,2'-bithiophene} **25**

**25**

A mixture of 2,7-dibromo-9,9-bis[6-(N,N-dimethylamino)hexyl]fluorene **9** (0.5784 g, 1 mmol), 5,5'-bis(trimethylstannyl)-2,2'-bithiophene **13** (0.492 g, 1 mmol), Pd(PPh₃)₄ (40 mg) in 40 ml of toluene was degassed and stirred for 3 days at 130°C. The resulting product was extracted with 500ml of chloroform. The organic layer was washed with water and brine, dried over MgSO₄, and concentrated. Poly{9,9-bis[6-(N,N-dimethyl amino)hexyl] fluorene-co-2,2' bithiophene} **25** was isolated by precipitation into methanol as a yellowish solid (435 mg, 43 %).

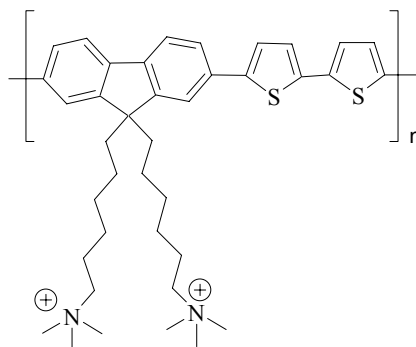
¹H NMR-spectrum (400 MHz, CDCl₃):

$\delta(^1\text{H})$ [ppm]: 7.4-7.8 (m, 10 H), 2.1-2.3 (20 H), 1.2-1.6 (4 H), 0.8-1.0 (18 H),

GPC (toluene): $\overline{M}_n = 1,300 \text{ gmol}^{-1}$

UV/Vis (CHCl₃): $\lambda_{\text{max, abs}} = 430 \text{ nm}$

Photoluminescence (CHCl₃): $\lambda_{\text{max, PL}} = 532 \text{ nm}$

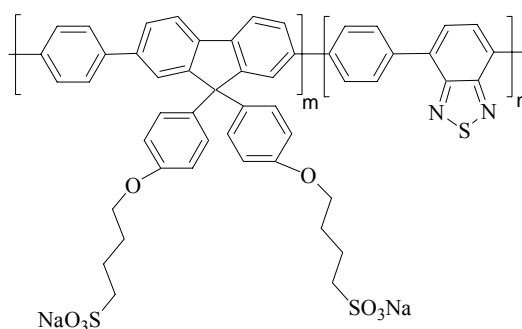
4.3.10 Poly{9,9-bis[6-(N,N-trimethylammonium)hexyl]fluorene-co-2,5-thienylene} 26**26**

Methyl iodide (3.2 g, 22.5 mmol) was added to Poly{9,9-bis[6-(N,N-dimethyl amino) hexyl] fluorene-co-2,2' bithiophene} **25** (100 mg) in 10 ml of THF and 10 ml of DMF at room temperature. After 1 min stirring, the formation of a precipitate was observed, which was redissolved by addition of 10 ml of water. Stirred at room temperature for 24 h, 100 ml of Et₂O was added to it. Work up and purification was similar to Poly{9,9-bis[6-(N,N-trimethylammonium) hexyl]fluorene-co-2,5-thienylene} **17**. Poly{9,9-bis[6-(N,N-trimethylammonium)hexyl]fluorene-co-2, 2''bithiophene} **26** was isolated in 68 % yield (75 mg).

UV/Vis (water): $\lambda_{\text{max, abs}} = 435 \text{ nm}$

Photoluminescence (water): $\lambda_{\text{max, PL}} = 486 \text{ nm}$

4.3.11 Poly[9,9-bis(4-sulfonylbutoxyphenyl)fluorene-1,4-phenylene]-co-
 ([1,2,5]benzo-thiadiazole-4,7-diyl-1,4-phenylene) **27**



27

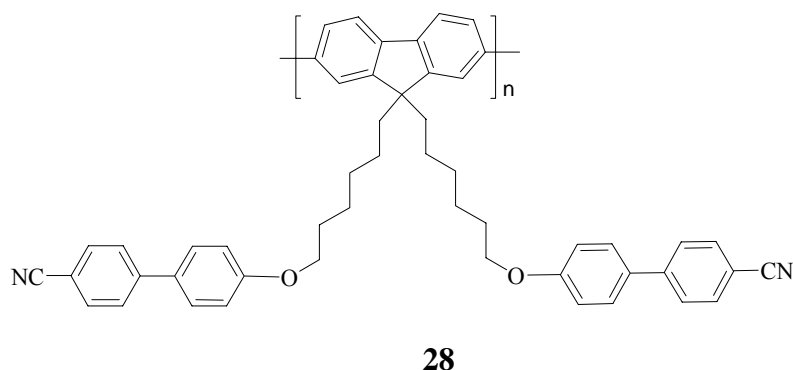
A mixture of 2,7-dibromo-9,9-bis(4-sulfonylbutoxyphenyl)fluorene **4** (different mole ratios), 1,4-phenylenediboronic acid (0.166 g, 1 mmol), 4,7-dibromo-benzo [1,2,5] thiadiazole **15** (different mole ratios), Pd(PPh₃)₄ (50 mg) and Na₂CO₃ (1 g, 9.4 mmol) in 5 ml of distilled water, 50 ml of toluene and 5ml of butanol was reacted for 3 days at 135°C (reflux). 100 ml of chloroform was added and the mixture was extracted with 300 ml of water. The aqueous layer was washed with chloroform and concentrated to dryness. The residue was redissolved in water and purified by dialysis with water.

Monomer 3	Monomer 9	UV / Vis (water, λ _{max})	Photoluminescence (water, λ _{max} , PL)
0.4122 g (0.50 mmol)	0.1470 g (0.50 mmol)	382 nm, 420-480 nm (shoulder)	538 nm
0.6183 g (0.75 mmol)	0.0735 g (0.25 mmol)	388 nm 420-480 nm (shoulder)	537 nm
0.7420 g (0.90 mmol)	0.0294 g (0.10 mmol)	385 nm 420-480 nm (shoulder)	531 nm

¹H NMR-spectrum (400 MHz, D₂O):

δ(¹H) [ppm]: 6.4-8.6 (ar-H), 3.8-4.3 (α, -CH₂), 3.0-3.7 (α, -CH₂), 1.4-2.7 (β,γ -CH₂)

4.3.12 Poly[9,9-bis(4-cyano-biphenyl-4'-oxyhexyl)fluorene] 28

**Yamamoto-type coupling reaction** ^[95]

Two Schlenk tubes sealed with rubber stoppers were taken. They were evacuated and dried thoroughly with a heat gun. One schlenk tube was flushed with argon and filled with the monomer under a light stream of argon. It was sealed with a rubber stopper and 45 ml of dry toluene was added using a syringe. The monomer was completely dissolved using an ultrasonic bath. The first schlenk tube was transferred into a glove box and flushed with argon. The tube was filled with Ni(COD)₂ and 2,2'-bipyridyl and sealed again with a new rubber stopper. Once outside the glovebox, 15 ml of dry DMF and 15 ml of dry toluene were added to the schlenk tube using a syringe. The solution turned deep blue after a while. The tube was put in an ultrasonic bath for one minute and wrapped completely with aluminium foil to exclude light. The tube was transferred into an oil bath (80° C) and vigorously stirred. 1,5-Cyclooctadiene (COD) was added with a syringe, and the tube was kept at that temperature for 35-40 minutes. Next, the monomer was transferred from the second schlenk tube into the reaction mixture using a syringe. The reaction was carried out at 80° C for 7 days.

The reaction was stopped by adding 10 ml of a 4M solution of HCl in dioxane. After addition HCl the mixture was stirred for 15 minutes. The tube was then filled with chloroform, stirred for another 15 minutes at 80 °C and finally shaken well. The complete mixture was transferred into a extraction funnel and 100 ml of 2N HCl and 200 ml of chloroform were added. The phases were separated; the organic phase was treated once again with 2N HCl. The organic phase was then treated with saturated aqueous Na₂-EDTA solution

and washed with saturated aqueous NaHCO₃ solution and treated once again with the aqueous Na₂-EDTA solution. The organic phase was passed through a short column with a filter plate of high porosity and a small layer of celite 545, a considerable amount of silica gel and a thin layer of sand. Afterwards, the solvent was evaporated until the solution becomes viscous. Then, the polymer was precipitated into mixture of methanol:acetone:2N HCl (400:20:20) ml. The polymer was collected by filtration and dried under vacuum to obtain poly[9,9-bis(4-cyano-biphenyl-4'-oxyhexyl) fluorene] **28**, (250 mg).

Compound	Amount	Mol. wt.	mmol	Equivalent
2,7 dibromo-9,9-bis(4-cyano-biphenyl-4'-oxyhexyl)fluorene	0.8787	878.73	1.0	1.0
Ni (COD) ₂	0.6325	275.08	2.3	2.3
2,2' Bipyridyl	0.3588	156.18	2.3	2.3
COD	0.1783	108.18	1.45	1.45

Solvents : 15 ml of toluene for monomer and 15 ml of DMF + 50 ml of toluene to dissolve Ni (COD)₂ / 2,2' - Bipyridyl

¹H NMR-spectrum (400 MHz, CDCl₃):

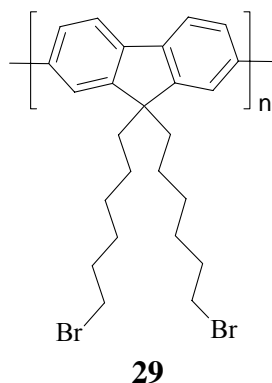
δ(¹H) [ppm]: 6.7-7.9 (ar-H), 3.6-3.9 (terminal CH₂), 0.8-2.3 (alkyl protons)

IR: 2920, 2840, 2220, 1600, 1500, 1250, 1180, 1020, 820 cm⁻¹.

GPC (THF): $\overline{M}_n = 9,700 \text{ gmol}^{-1}$

UV/Vis (CHCl₃): $\lambda_{\text{max, abs}} = 297, 370 \text{ nm}$

Photoluminescence (CHCl₃): $\lambda_{\text{max, PL}} = 430 \text{ nm}$

4.3.13 Poly[9,9-bis(6-bromohexyl)fluorene] **29**

Yamamoto coupling of 2,7-dibromo-9,9-bis(6-bromohexyl)fluorene **8** (2 g, 3 mmol) using Ni(COD)₂ (1.946 g, 8 mmol), 1,5 cyclooctadiene (0.456 ml, 4.2 mmol) and 2,2' bipyridyl (1.105 g, 8 mmol) gives the desired polymer. Purification was done by extracting it with acetone in a soxhlet extractor for 4 days. The product was dissolved in 150 ml of chloroform and washed with aqueous Na₂-EDTA solution. The organic solution was dried over MgSO₄ and evaporated until the solution becomes viscous. The polymer was precipitated into methanol and acetone (2:1). Poly[9,9-bis(6-bromohexyl)fluorene] **29** (1.2 g, 60 %) was finally collected and dried under high vacuum.

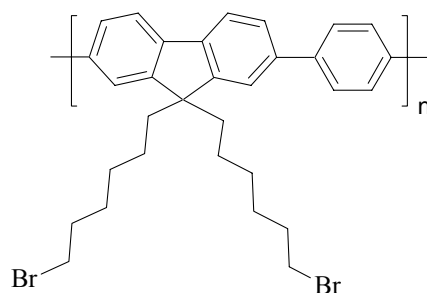
¹H NMR-spectrum (400 MHz, CDCl₃):

δ(¹H) [ppm]: 7.2-7.4 (ar-H), 3.0-3.4 (terminal CH₂), 0.5-2.2 (alkyl protons)

GPC (toluene): $\overline{M}_n = 10,200 \text{ gmol}^{-1}$

UV/Vis (toluene): $\lambda_{\text{max abs}} = 348 \text{ nm}$

Photoluminescence (toluene): $\lambda_{\text{max, PL}} = 446 \text{ nm}$

4.3.14 Poly[9,9-bis(6-bromohexyl)fluorene-co-1,4-phenylene] **30****30**

A mixture of 2,7-dibromo-9,9-bis(6-bromohexyl)fluorene **8** (2.0 g, 3 mmol), 1,4-phenylenediboric acid (509 mg, 3 mmol), PdCl₂(dppf) (45mg) and K₂CO₃ (5.10 g, 36 mmol) in 36 ml of THF and 18 ml of water was degassed and stirred for 3 days at 80°C. The mixture was extracted with 500 ml of chloroform. The organic layer was washed with water and brine, dried over MgSO₄, and concentrated. Poly[9,9-bis(6-bromohexyl)fluorene-co-1,4-phenylene] was precipitated from methanol to yield 1.16 g (78 %) of **30**.

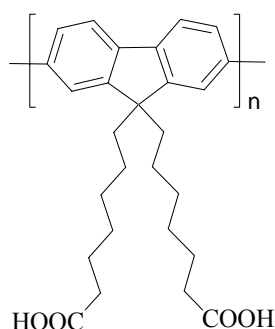
¹H NMR-spectrum (400 MHz, CDCl₃):

δ(¹H) [ppm]: 7.5-7.8 (m, ar-H), 3.0-3.4 (terminal CH₂), 0.8-2.1 (alkyl protons)

GPC (THF): $\overline{M}_n = 11,700 \text{ gmol}^{-1}$

UV/Vis (THF): $\lambda_{\text{max abs}} = 346 \text{ nm}$

Photoluminescence (THF): $\lambda_{\text{max, PL}} = 430 \text{ nm}$

4.3.15 Poly[9,9-bis(6-carboxyhexyl)fluorene] **31****31**

To a three-necked 100 ml round bottom flask was added 2,4,4-trimethyloxazoline (2.452 ml, 19 mmol) and 30 ml of dry THF was added via syringe. The flask was cooled to -70°C , and the solution was stirred for 10 minutes. 1.6 M n-BuLi (2.12 ml) was added dropwise with a syringe to the solution. The solution was stirred for 2 h. Poly 9,9-bis(6-bromohexyl)fluorene **29** (100 mg) was dissolved in 10 ml of THF. The polymer solution was transferred to oxazoline lithium salt solution with a syringe, and the addition was completed in 30 s. The cooling bath was removed, and the mixture was stirred for 1 h and quenched in hexane. The solid polymer was washed with hexane by using soxhlet extractor. Thus 150 mg of polymer was obtained. To this 60 ml of 3N HCl was added and refluxed for 12 h. The solid was filtered, rinsed with water and dried to recover Poly[9,9-bis-(6-carboxyhexyl)fluorene] **31** in 60-70 % yield.

IR: 3433, 2927, 2852, 2220, 1707, 1458, 1259, 813, 740 cm^{-1} .

UV/Vis (CHCl_3): $\lambda_{\text{max abs}} = 375 \text{ nm}$

Photoluminescence (CHCl_3): $\lambda_{\text{max, PL}} = 440 \text{ nm}$

- The GPC characterisation of Poly[9,9-bis-(6-carboxyhexyl)fluorene] **31** was not possible as there is a solubility problem.

4.4 Fabrication of PLEDs using **17** ^[125]

Procedure

- 1) Small pieces of glass which were coated with ITO and already had been etched were firstly wiped with acetone and to brake small ITO tips.
- 2) The glass was put into toluene followed by isopropanol and exposed to ultrasonic each for twenty minutes.
- 3) After that the plasma etching process was applied with the purpose of reducing the dust on the sample and achieving a better ITO layer and changing its work function. The plasma etching discharge took 10 minutes at a base pressure of $5 \cdot 10^{-1}$ mbar for each series.
- 4) After the plasma etching two steps of spin coating follows firstly PEDOT (from Bayer Incorporation Baytron P HO 154) was dropped on the carefully cleaned glass substrates via a 0,45 nylon filter and then spin coated at a spin rate of 1500 rpm for 12 sec. followed by 3000 rpm for 40 sec. Before drying up the films, the vacuum chamber was flooded by argon for a few minutes.
- 5) Then using an integrated heater the films were heated up to about 70°C for 60 minutes and afterwards to ca. 140°C for 15 hours. After that, **17** dissolved in water was spin coated on top of the PEDOT layer.
- 6) The film was dried in the same oven but now at 70°C under argon atmosphere for 2-3 hours and after that at 100°C for 20-24 hours under vacuum.
- 7) The first step under the argon atmosphere is to avoid damages of the polymer film caused by quick evaporating water out of the film. To except such damages AFM investigation were made. A Balzers MED010 vacuum coating unit was used at a minimum base pressure of approximately $1 \cdot 10^{-6}$ mbar in the worst case for depositing the aluminum top electrodes.
- 8) All devices were contacted on air and than measured in an argon atmosphere.

4.5 Purification of water-soluble polymers

For neutral polymers (water-insoluble) catalysts and impurities present can be removed by washing it with water or acids. But in case of water-soluble polymers, excess catalysts, impurities and low molecular weight compounds have to be removed by special purification techniques.

Water-soluble polymers can be purified by dialysis, ultrafiltration or size exclusion. The size exclusion effect becomes overshadowed by a host of other effects, most of which stem from molecular interactions. A serious difficulty in ultrafiltration derives from the fact that the pores are somewhat distorted by pressure and become more or less plugged as filtration proceeds, thus altering the effective pore size. Dialysis is free from this disadvantage because only diffusional activity would tend to cause a particle to enter a pore. If the particle should be too large to pass through, the diffusional activity of the solvent in the reverse direction should be effective in dislodging it.

Dialysis: Dialysis involves separation of lower molecular weight compounds from macromolecular solutions. It is a simple technique to separate/purify different sized molecules. Macromolecules are dialyzed by placing them in size-selective permeable tubing and subsequently equilibrating the sample with large volumes of distilled water. Efficient dialysis relies upon appropriate selection of dialysis tubing and effective ‘washing’ that results from large volumes of distilled water.

Dialysis tubing is made of either regenerated cellulose (RC) or cellulose ester (CE). Cellulose has long been used for dialysis as it is uncharged. The selectivity of cellulose membranes is not altered greatly by many chemicals or reasonable pH and temperature ranges. Processed cellulose contains crystalline regions. Depending upon how the cellulose is processed the number of crystalline areas varies and the regions in between can act as size-selective pores.

The method of dialysis makes use of **semi-permeable membranes**. In the simplest example, this membrane is manufactured in the form of a tube. The pore size of the membrane allows smaller molecules to pass through the membrane, larger molecules cannot (i.e. they are retained, Fig. 32). The dialysis membranes are characterized by the molecular mass of the smallest

molecule which will be retarded. This is commonly referred to as the **cutoff** of the membrane.

Procedure for dialysis:

Dialysis proceeds by placing the polymer solution in a dialysis tube (i.e. the dialysis "bag") and putting it into a beaker filled with water. The low molecular mass solutes pass through the membrane into the beaker filled with water. The water was changed several times and checked with the help of UV, until no low molecular weight compounds pass through the membrane (see Fig. 32).

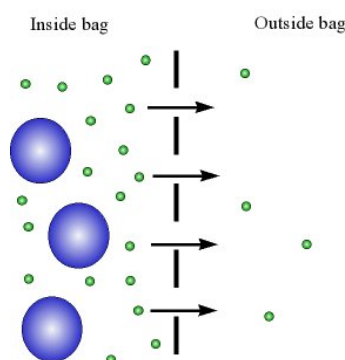


Fig. 32: *Dialysis using a semi-permeable membrane*

- 1) A membrane of appropriate molecular weight cutoff (MWCO) is selected. The dry bag was cut to the proper length.
- 2) The tube was immersed in distilled water.
- 3) One end of the tube was closed with the corresponding clip.
- 4) The sample was filled in with the help of a funnel. When the sample addition was complete, the funnel was removed and the tube was squeezed with the fingers to eliminate the air space. Now the other end was also closed with a clip. The bag was checked for the absence of leakages.
- 5) The filled dialysis bag was placed in a beaker with a stir bar containing at least ten times distilled water compared to the sample volume at room temperature.
- 6) The progress of the dialysis was followed by monitoring the fluorescence of the aqueous phase in the beaker. The water was repeatedly replaced with an equal volume of fresh water. Replacing the water was continued until no more low molecular weight molecules pass through.



Fig. 33: *Dialysis membranes handling*

7) The dialysis bag was removed from the beaker and rinsed with water. The dialysed sample was transferred carefully in a round bottom flask, evaporated to dryness and carefully dried to get the desired water-soluble anionic/cationic copolymer.

5 Summary

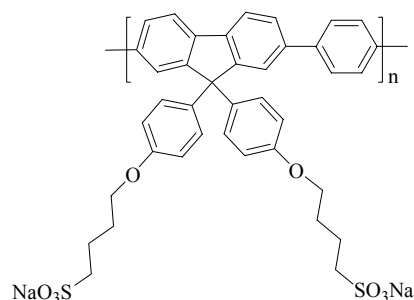
The aim of the present work ***“Ionic, Water-Soluble Polyfluorene-Type Copolymers”*** was

- a) to synthesize water soluble semiconducting polymers,*
- b) to investigate the effect of surfactant on the aqueous polymer solutions,*
- c) to check applications in optical, electronic & optoelectronic devices.*

Water-soluble conjugated polymers are of particular interest as fluorescent components in sensors both for chemical and biological analysis as well as for OLEDs which are built in a layer-by-layer self assembly approach. Solubility in water is essential for an interaction with biological substrates and this can be achieved by introducing neutral or charged hydrophilic functionalities to the terminal position of the polyfluorene backbone.

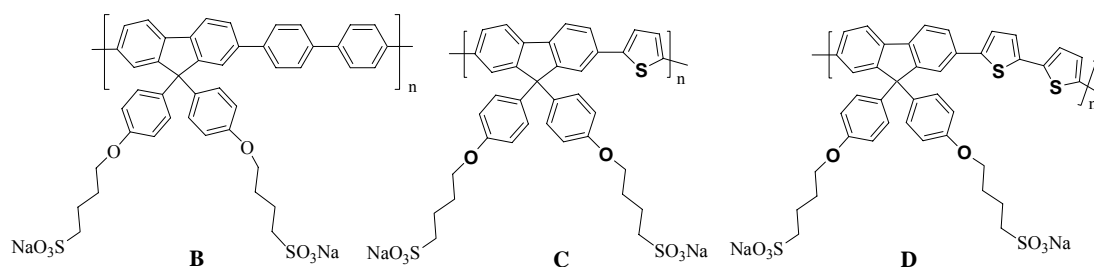
In case of anionic polyelectrolytes, the water solubility was achieved by functionalizing the side chain by attaching sulfonate group. In case of cationic polyelectrolytes, water solubility was achieved by functionalizing the side chain by attaching ammonium groups.

Anionic, water-soluble fluorene-type copolymers were synthesized in three steps. The first step, 2,7-dibromofluorene-9-one was reacted with phenol/methane sulfonic acid to give 2,7-dibromo-9,9-bis(4-hydroxyphenyl)fluorene. The second step was the etherification of 2,7-dibromo-9,9-bis(4-hydroxyphenyl)fluorene with 1,4-butane sultone to 2,7-dibromo-9,9-bis(4-sulfonylbutoxyphenyl)fluorene in dioxane/NaOH. The key step was a *Suzuki-* or *Stille-* type cross coupling of this monomer (2,7-dibromo-9,9-bis(4-sulfonylbutoxyphenyl)fluorene) with a suited comonomer (1,4-phenylene diboronic acid, 4,4'-biphenylene diboronic acid, 2,5-bis(trimethylstannyl)thiophene, 5,5'-bis(trimethylstannyl)-2,2'-bithiophene).

**A**

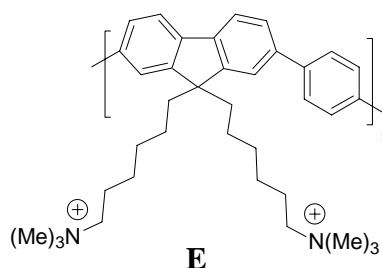
Structure of the anionic copolymer poly[9,9-bis(4-sulfonylbutoxyphenyl)fluorene-co-1,4-phenylene] A

Solutions of the anionic copolymer poly[9,9-bis(4-sulfonylbutoxyphenyl)fluorene-co-1,4-phenylene] in water were turbid (low PL efficiency of ca. 23 %). Addition of surfactants leads to a clear solution (PL efficiency increases to ~100%). The surfactant used in our study was C₁₂E₃ (Triethyleneglycol monododecyl ether) as a non-ionic surfactant, the experiments have been done in collaboration with Burrows et. al. The dramatic increase of the fluorescence quantum yield of the copolymer A on incorporation into surfactant (C₁₂E₃) micelles can be important for sensor applications. Further efforts are being made to check the applicability of this copolymer in polymer LEDs with active layers which have been processed from aqueous solution. Other anionic, water-soluble copolymers **B-D** with biphenyl, thienylene and bithiophene spacer groups were synthesized by *Suzuki*- or *Stille*-type cross-coupling reactions.



Structures of other anionic water-soluble copolymers B) poly[9,9-bis(4-sulfonylbutoxyphenyl)fluorene-co-4,4'-biphenyl], C) poly [9,9-bis(4-sulfonylbutoxyphenyl) fluorene-co-2,5-thienylene], D) poly[9,9-bis- (4-sulfonylbutoxyphenyl)fluorene-co-2,2'-bithiophene]

Corresponding cationic, water-soluble copolymers were synthesized using the procedure developed by *Bazan et. al.*,^[58] who used related oligomers and polymers for DNA sensing. The synthesis involves four steps with a *Suzuki*-type cross-coupling reaction in the key step towards a non-ionic precursor polymer.



*Structure of the cationic, water-soluble copolymer poly{9,9-bis[6-(N,N-trimethylammonium)hexyl]fluorene-co-1,4-phenylene} **E***

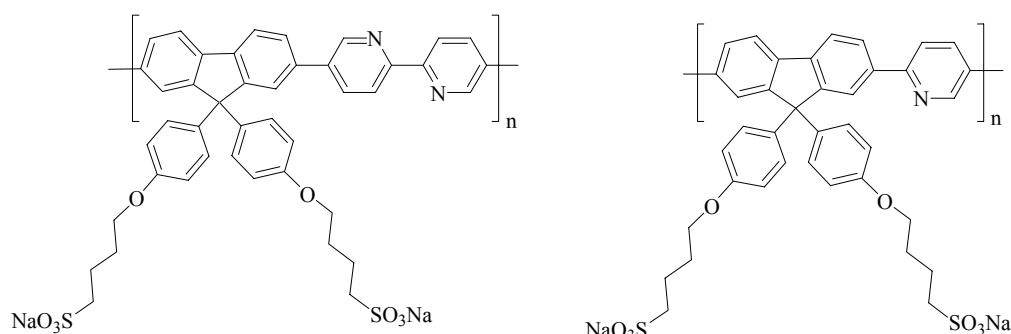
Studies of a polyelectrolyte-surfactant system, poly{9,9-bis[6-(N,N-trimethylammonium)hexyl]fluorene-co-1,4-phenylene} **E**/C₁₂E₅ have been done by *Monkman et. al.*^[123] Other cationic, water-soluble copolymers with thienylene and bithiophene spacer units have been also synthesized.

The purification of the water-soluble polyelectrolytes was done by dialysis with water using a dialysis membrane with a cutoff of 3,500 g mol⁻¹.

6 Future research

Water-soluble conjugated polymers are of great interest in various application fields as fluorescent component in chemical and biological sensors or for OLEDs made by the layer-by-layer approach. Structurally related ionic polymers and co-polymers can be synthesized using different building blocks to modify the optical and optoelectronic properties of the polyelectrolytes.

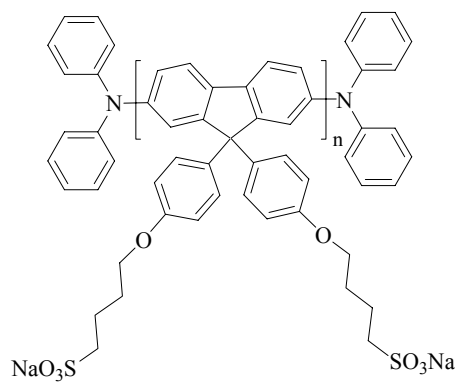
Novel copolymers with pyridine and bipyridine spacing will be available using Stille-type cross-coupling reactions and may be applicable in OLEDs and for a modification of optoelectronic properties.



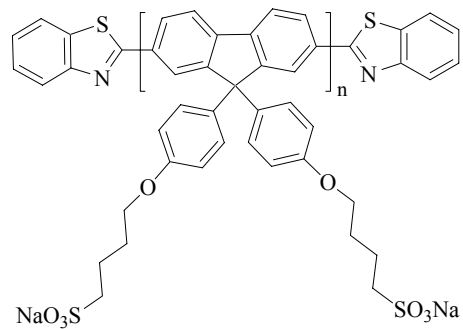
There is an increasing interest in effective two photon absorption (2PA) molecules with high 2PA cross sections because of possible applications in multiphoton fluorescence imaging, optical data storage, optical power limiting, 3D microfabrication and photodynamic therapy. Towards this goal, also water-soluble molecules are very attractive.

Symmetrical conjugated molecules with two electron donating (D) or two electron withdrawing (A) end groups should exhibit high non-linear absorption properties and large 2PA cross section values δ . Enhancement in δ was correlated to an intramolecular charge redistribution that occurs between the ends and center of the molecule.

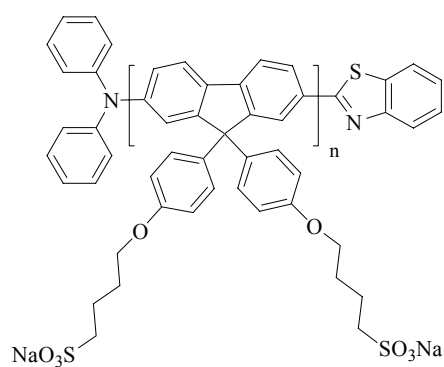
Additionally, a water-soluble fluorene derivative containing a benzothiazole acceptor group and diphenylamine donor group could be synthesized. Some of the target structures are depicted in the following scheme.



D-π-D



A-π-A



n: 1,2,3

D-π-A

7 References

- [1] C. K. Chiang, C. R. Fincher, Y. W. Park, A. J. Heeger, H. Shirakawa, E. J. Louis, S. C. Gau, A.G. McDiarmid, *Phys. Rev. Lett.* **1977**, *39*, 1098.
- [2] R. H. Friend, J. Borroughes, T. Shimoda, *Lasers and optics*, Physics world June, **1999**.
- [3] M. Knaapila, B. P. Lyons, K. Kisko, J. P. Foreman, U. Vainio, M. Mihaylova, O. H. Seeck, L. O. Palsson, R. Serimaa, M. Torkkeli, A. P. Monkman, *J. Phys. Chem. B.* **2003**, *107*, 12425.
- [4] M. Knaapila, K. Kisko, P. B. Lyons, R. Stepanyan, J. P. Foreman, O. H. Seeck, U. Vainio, L. O. Palsson, R. Serimaa, M. Torkkeli, A. P. Monkman, *J. Phys. Chem. B* **2004**, *30*, 10711.
- [5] A. W. Grice, D. D. C. Bradley, M. T. Bernius, M. Inbasekaran, W. W. Wu, E. P. Woo, *Appl. Phys. Lett.* **1998**, *73*, 629.
- [6] M. J. Winokur, Structural Studies of Conducting Polymers. *In Handbook of Conducting Polymers*; Skotheim, T. A., Elsenbaumer, R. L., Reynolds, J. R., Eds. Marcel Dekker, New York, **1998**, 707.
- [7] U. Scherf, E. J. W. List, *Adv. Mater.* **2002**, *14*, 477.
- [8] M. Grell, W. Knoll, D. Lupo, A. Meisel, T. Miteva, D. Neher, H.-G. Nothofer, U. Scherf, A. Yasuda, *Adv. Mater.* **1999**, *11*, 671.
- [9] M. Leclerc, *J. Polymer. Sci. Part A* **2001**, *39*, 2867.
- [10] H. Sirringhaus, T. Kawase, R. H. Friend, T. Shimoda, M. Inbasekaran, W. Wu, E. P. Woo, *Science* **2000**, *290*, 2123.
- [11] W. L. Yu, J. Pei, Y. Cao, W. Huang, A. J. Heeger, *Chem. Commun.* **1999**, 1837.
- [12] S. Kim, J. Jackiw, E. Robinson, K. S. Schanze, J. R. Reynolds, J. Baur, M. F. Rubner, D. Boils, *Macromolecules* **1998**, *31*, 964.
- [13] P. B. Balanda, M. B. Ramay, J. R. Reynolds, *Macromolecules* **1999**, *32*, 3970.

- [14] J. W. Baur, M. F. Rubner, J. R. Reynolds, S. Kim, *Langmuir* **1999**, *15*, 6460.
- [15] B. S. Harrison, M. B. Ramay, J. R. Reynolds, K. S. Schanze, *J. Am. Chem. Soc.* **2000**, *122*, 8561.
- [16] L. Chen, D. W. McBranch, H.-L. Wang, R. Helgeson, F. Wudl, D. G. Whitten, *Proc. Natl. Acad. Sci.* **1999**, *96*, 12287.
- [17] L. H. Chen, D. McBranch, R. Wang, D. Whitten, *Chem. Phys. Lett.* **2000**, *330*, 27.
- [18] L. Chen, S. Xu, D. McBranch, D. Whitten, *J. Am. Chem. Soc.* **2000**, *122*, 9302.
- [19] C. Tan, M. R. Pinto, K. S. Schanze, *Chem. Commun.* **2002**, 446.
- [20] H. Schnablegger, M. Antonietti, C. Göltner, J. Hartmann, H. Cölfen, P. Samori, J. P. Rabe, H. Häger, W. Heitz, *J. Colloid Interface Sci.* **1999**, *212*, 24.
- [21] A. F. Thünemann, D. Ruppelt, *Langmuir* **1999**, *15*, 6460.
- [22] S. Shi, F. Wudl, *J. Am. Chem. Soc.* **1990**, *23*, 2119.
- [23] A. O. Patil, Y. Ikenoue, F. Wudl, A. J. Heeger, *J. Am. Chem. Soc.* **1987**, *109*, 1858.
- [24] J. Lukkari, M. Salomaki, A. Viinikanoja, T. Aaritalo, J. Paukkunene, N. Kocharova, J. Kankare, *J. Am. Chem. Soc.* **2001**, *123*, 6083.
- [25] (a) M. Ferreira, M. F. Rubner, *Macromolecules* **1995**, *28*, 7101; (b) A. C. Fou, O. Onitsuka, M. Ferreira, M. F. Rubner, *J. Appl. Phys.*, **1996**, *79*, 7501; (c) J. W. Baur, S. Kim, P. B. Balanda, J. R. Reynolds, M. F. Rubner, *Adv. Mater.* **1998**, *10*, 1452.
- [26] (a) J. Bharathan and Y. Yang, *Appl. Phys. Lett.* **1998**, *72*, 2660; (b) S. C. Chang, J. Bharathan and Y. Yang, *Appl. Phys. Lett.* **1998**, *73*, 2561.
- [27] K. Fäid, M. Leclere, *Chem. Commun.*, **1996**, 2761, *J. Am. Chem. Soc.*, **1998**, *120*, 5274.
- [28] (a) A. D. Child, J. R. Reynolds, *Macromolecules* **1994**, *27*, 1975, (b) P. B. Balanda, M. B. Ramey, J. R. Reynolds, *Macromolecules* **1999**, *32*, 3970.
- [29] Q. L. Fan, S. Lu, Y. H. Lai, W. Huang, *Macromolecules* submitted.

- [30] R. D. McCullough, P. C. Ewbank, R. S. Loewe, *J. Am. Chem. Soc.* **1997**, *119*, 633.
- [31] T. I. Wallow, B. M. Novak, *J. Am. Chem. Soc.* **1991**, *113*, 7411.
- [32] P. Kovacic, M. B. Jones, *Chem. Rev.* **1987**, *87*, 357.
- [33] I. U. Rau, M. Rehahn, *Polymer* **1993**, *34*, 2889.
- [34] R. Rulkens, M. Schulze, G. Wegner, *Macromol. Rapid Commun.* **1994**, *15*, 669.
- [35] G. Brodowski, A. Horvath, M. Ballauf, M. Rehahn, *Macromolecules* **1996**, *29*, 6962.
- [36] M. Wittmann, M. Rehahn, *Chem. Commun.* **1998**, 623.
- [37] Z. Peng, B. Xu, J. Zhang, Y. Pan, *Chem. Commun.* **1999**, 1855.
- [38] A. Fujii, T. Sonoda, Jpn. Yoshino. *J. Appl. Phys.* **2000**, *39*, L249.
- [39] A. Fujii, T. Sonoda, T. Fujisawa, R. Ootake, K. Yoshino, *Synth. Met.* **2001**, *119*, 189.
- [40] Li, C. J. Slaven, W.T. IV John, V. T. Banerjee, S. *Chem. Commun.* **1997**, 1569.
- [41] W. T. IV. Slaven, C. -J. Li, Y. P. Chen, V. T. John S. H. Rachakonda, *J. Macro. Sci. Pure Appl. Chem.* **1999**, *A36*, 971
- [42] M. R. Pinto, J. R. Reynolds, K. S. Schanze, *Polym. Prepr. (Am. Chem. Soc. Div. Polym. Chem.)* **2002**, *43*, 139
- [43] B. Liu, W. L. Yu, Y. H. Lai, W. Huang, *Chem. Commun.* **2000**, 551.
- [44] J. W. Baur, S. Kim, P. B. Balanda, J. R. Reynolds, M. F. Rubner, *Adv. Mater.* **1998**, *10*, 1452
- [45] N. S. Sariciftci, D. Braun, C. Zhang, V. I. Srdanov, A. J. Heeger. G. Stucky, F. Wudl, *App. Phys. Lett.* **1993**, *62*, 585.
- [46] D. T. McQuade, A. E. Pullen, T. M. Swager, *Chem. Rev.* **2000**, *100*, 2537
- [47] A. P. Monkman, H. D. Burrows, L. J. Hartwell, L. E. Horsburgh, I. Hamblett, S. Navaratnam, *Phys. Rev. Lett.* **2001**, *86*, 1358.

- [48] S. Sinha, C. Rothe, R. Güntner, U. Scherf, A. P. Monkman, *Phys. Rev. Lett.* **2003**, *90*, 127402.
- [49] G. Fytas, H. G. Nothofer, U. Scherf, D. Vlassopoulos, G. Meier, *Macromolecules* **2002**, *35*, 481.
- [50] B. Tanto, S. Guha, C. M. Martin, U. Scherf, M. J. Winokur, *Macromolecules* **2004**, *submitted*.
- [51] M. Grell, D. D. C. Bradley, G. Ungar, J. Hill, K. S. Whitehead, *Macromolecules* **1999**, *32*, 5810.
- [52] G. Lieser, M. Oda, T. Miteva, A. Meisel, H. G. Nothofer, U. Scherf, D. Neher, *Macromolecules* **2000**, *33*, 4490.
- [53] G. Decher, Y. Luou, H. W. Schmitt, *Thin Solid Films* **1994**, *244*, 772
- [54] G. Decher, *Science*, **1997**, *277*, 1232.
- [55] R. H. Friend, *Pure Appl. Chem.* **2001**, *73*, 425.
- [56] J. H. Burroughes, D. D. C. Bradley, A. R. Brown, R. N. Marks, K. Mackay, R. H. Friend, P. L. Burn, A. B. Holmes. *Nature* **1990**, *347*, 539.
- [57] D. Wang, X. Gong, P. S. Heeger, F. Rininsland, G. C. Bazan, A. J. Heeger, *Proc. Natl. Acad. Sci. USA* **1999**, *96*, 12219.
- [58] M. Stork, B. S. Gaylord, A. J. Heeger, G. C. Bazan, *Adv. Mater.* **2002**, *14*, 361.
- [59] B. S. Gaylord, A. J. Heeger, G. C. Bazan, *Proc. Natl. Acad. Sci. USA* **2002**, *99*, 10954.
- [60] B. Liu, B. S. Gaylord, S. Wang, G. C. Bazan, *J. Am. Chem. Soc.* **2003**, *125*, 6705.
- [61] M. Leclerc, *Adv. Mater.* **1999**, *11*, 491
- [62] D. T. McQuade, A. E. Pullen, T. M. Swager, *Chem. Rev.* **2000**, *122*, 12389.
- [63] T. M. Swager, *Acc. Chem. Res.* **1998**, *31*, 20.
- [64] (a) J. E. Guillet, *Polymer Photophysics and Photochemistry*, Cambridge University Press, Cambridge **1985**, (b) S. E. Webber, *Chem. Rev.* **1990**, *90*,

- 1469, (c) Y.-J. Miao, W. G. Herkstroeter, B. J. Sun, A. G. Wong-Foy, G. C. Bazan, *J. Am. Chem. Soc.* **1995**, *117*, 11407.
- [65] Yang, J. S. Swager, T. M. *J. Am. Chem. Soc.* **1998**, *120*, 11864.
- [66] K. Faod, M. Leclerc, *Chem. Commun.* **1996**, 2761.
- [67] S. Q. Shi, F. Wudl, *Macromolecules* **1990**, *23*, 2119.
- [68] L. Chen, D. W. McBranch, H. L. Wang, R. Helgeson, F. Wudl, D. G. Whitten, *Proc. Natl. Acad. Sci.* **1999**, *96*, 12287.
- [69] Q. Pei, Y. Yang, *J. Am. Chem. Soc.* **1996**, *118*, 7416.
- [70] H. Kobayashi, S. Kanbe, S. Seki, H. Kiguchi, M. Kimura, I. Yudasaka, S. Miyashita, T. Shimoda, C. R. Towns, J. H. Burroughes, R. H. Friend, *Synth. Met.* **2000**, *111-112*, 125.
- [71] T. Kawase, T. Shimoda, C. Newsome, H. Sirringhaus, R. H. Friend, *Thin Solid Films* **2003**, *438-439*, 279.
- [72] J. J. Lavigne, D. L. Broughton, J. N. Wilson, B. Erdogan, U. H. F. Bunz, *Macromolecules* **2003**, *36*, 7409.
- [73] Q. Zhu, T. M. Swager, *J. Am. Chem. Soc.* **1995**, *117*, 7017.
- [74] B. S. Harrison, M. B. Ramay, J. R. Reynolds, K. S. Schanze, *J. Am. Chem. Soc.* **2000**, *122*, 8561.
- [75] L. Chen, D. W. McBranch, H.-L. Wang, R. Helgeson, F. Wudl, D. G. Whitten, *Proc. Natl. Acad. Sci. USA*, **2000**, *96*, 12287.
- [76] D. Neher, *Macromol. Rapid Commun.* **2001**, *22*, 1365.
- [77] A. V. Kabanov, P. Felgner, L. W. Seymour, Eds. *Self-assembling Complexes for Gene Delivery, From Laboratory to Clinical Trial*; John Wiley Chichester, **1998**.
- [78] T. K. Bronich, H. K. Nguyen, A. Eisenberg, A. V. Kabanov, *J. Am. Chem. Soc.* **2000**, *122*, 8339.
- [79] B. S. Gaylord, A. J. Heeger, G. C. Bazan, *J. Am. Chem. Soc.* **2003**, *125*, 896.
- [80] S. Wang, B. S. Gaylord, G. C. Bazan, *Adv. Funct. Mater.* **2003**, *13*, No. 6.

- [81] J. W. Hong, H. Benmansour, G. C. Bazan, *Chem. Eur. J.* **2003**, *9*, 3186.
- [82] S. Becker, C. Ego, A. C. Grimsdale, E. J. W. List, D. Marsitzky, A. Pogantsch, S. Setayesh, G. Leising, K. Müllen, *Synth. Met.* **2002**, *125*, 73.
- [83] (a) D. Wang, X. Gong, P. S. Heeger, F. Rininsland, G. C. Bazan, A. J. Heeger, *Proc. Natl. Acad. Sci. U.S.A.* **2002**, *99*, 49, (b) H. A. Ho, M. Boissinot, M. G. Bergeron, G. Corbeil, K. Dore, D. Boudreau, M. Leclerc, *Angew. Chem. Int. Ed.* **2002**, *41*, 1548.
- [84] (a) M. Egholm, O. Buchardt, L. Christensen, C. Behrens, S. M. Freier, D. A. Driver, R. H. Berg, S. K. Kim, B. Norden, P. E. Nielsen, *Nature* **1993**, *365*, 556, (b) P. E. Nielsen, *Curr. Opin. Biotechnol.* **1999**, *10*, 71, (c) Demidov, V. V. *Biochem. Pharmacol.* **1994**, *48*, 1310.
- [85] (a) B. Pullman, R. Lavery, A. Pullman, *Eur. J. Biochem.* **1982**, *124*, 229. (b) D. S. Minehan, D. A. Marx, S. K. Tripathy, *Macromolecules* **1994**, *27*, 777.
- [86] I. A. Levitsky, J. Kim, T. M. Swager, *Macromolecules* **2001**, *34*, 2315.
- [87] J. Kim, T. M. Swager, *Nature* **2001**, *411*, 1030.
- [88] G. Decher, Y. Luou, J. Schmitt, *J. Thin Solid Films* **1994**, *244*, 772.
- [89] F. -C. Chen, Y. Yang, M. E. Thompson, J. Kido, *Appl. Phys. Lett.* **2002**, *80*, 2308.
- [90] S. T. Dubas, J. B. Schlenoff, *Macromolecules* **1999**, *32*, 8153.
- [91] S. T. Dubas, J. B. Schlenoff, *Macromolecules* **2001**, *34*, 3736.
- [92] M. Knaapila, R. Stepanyan, L. E. Horsburgh, A. P. Monkman, R. Serimaa, O. Ikkala, A. Subbotin, M. Torkkeli, G. J. Brinke, *J. Phys. Chem. B.* **2003**, *107*, 14199.
- [93] D. Wang, J. Lal, D. Moses, G. C. Bazan, A. J. Heeger, *Chem. Phys. Lett.* **2001**, *348*, 411.
- [94] U. Menge, P. Lang, G. H. Findenegg, P. Strunz, *J. Phys. Chem. B.* **2003**, *107*, 1316.
- [95] H. -G. Nothofer, *Ph.D Thesis, Department of Mathematics and Science, University of Potsdam*, **2001**.

- [96] H. H. Hörhold, M. Helbig, D. Raabe, J. Opfermann, U. Scherf, R. Stockmann, *Z. Chem.* **1987**, 27, 126.
- [97] A. Kraft, A. C. Grimsdale, A. B. Holmes, *Angew. Chem., Int. Ed.* **1998**, 37, 402.
- [98] R. H. Friend, R. W. Gymer, A. B. Holmes, J. H. Burroughes, R. N. Marks, C. Taliani, D. D. C. Bradley, D. A. Dos Santos, J. L. Bredas, M. Lögdlund, W. R. Salaneck, *Nature*, **1999**, 397, 121.
- [99] M. T. Bernius, M. Inbasekaran, J. O'Brien, W. Wu, *Adv. Mater.* **2000**, 12, 1737.
- [100] U. Mitschke, P. J. Bäuerle, *J. Mater. Chem.* **2000**, 10, 1471.
- [101] J. Kido, K. Hongawa, K. Okuyama, K. Nagai, *Appl. Phys. Lett.* **1994**, 64, 815.
- [102] J. Kido, H. Shionoya, K. Nagai, *Appl. Phys. Lett.* **1995**, 67, 2281.
- [103] M. D. McGehee, T. Bergstedt, C. Zhang, A. P. Saab, M. B. O'Regan, G. C. Bazan, V. I. Srdanov, A. J. Heeger, *Adv. Mater.* **1999**, 11, 1349.
- [104] F. -C. Chen, Y. Yang, M. E. Thompson, J. Kido, *Appl. Phys. Lett.* **2002**, 80, 2308.
- [105] Y. Ohmori, M. Uchida, K. Muro, K. Yoshino, *Jpn. J. Appl. Phys. Part 2 - Lett.* 1991, 30, L1941.
- [106] (a) J. W. Eastman, S. J. Rehfeld, *J. Phys. Chem.* **1970**, 74, 1438. (b) F. P. Schwarz, S. D. Wasik, *Anal. Chem.* **1976**, 48, 524.
- [107] H. Suzuki, *Bull. Chem. Soc. Japan* **1959**, 32, 1357.
- [108] A. Charas, J. Morgado, J. M. G. Martinho, L. Alcácer, S. F. Lim, R. H. Friend, F. Cacialli, *Polymer* **2003**, 44, 1843.
- [109] F. Lichterfeld, T. Schmeling, R. J. Strey, *J. Phys. Chem.* **1986**, 90, 5762.
- [110] T. Kato, S.-i. Anzai, T. Seimiya, *J. Phys. Chem.* **1990**, 94, 7255.
- [111] A. Subbotin, R. Stepanyan, M. Knaapila, O. Ikkala, G. ten Brinke, *Eur. Phys. J. E.* **2003**, 12, 333.
- [112] T. Hellweg, *Current Opinion in Colloid & Interface Science* **2002**, 7, 50.

- [113] K. Holmberg, B. Jönsson, B. Kronberg, B. Lindman, *Surfactants and Polymers in Aqueous Solutions*, 2nd ed.; Wiley: Chichester, 2003.
- [114] J. K. Stille, *Angew. Chem. Int. Ed.* **1996**, *25*, 508
- [115] A. Iraqi, G. W. Barker, *J. Mater. Chem.* **1998**, *8*, 25.
- [116] N. Miyaura, T. Ishiyama, H. Sasaki, M. Ishiyama, M. Satoh, A. Suzuki, *J. Am. Chem. Soc.* **1989**, *111*, 314.
- [117] S. Guillerez, G. Bidan, *Synth. Met.* **1998**, *93*, 123.
- [118] S. U. Egelhaaf, E. van Swieten, T. Bosma, E. de Boef, A. van Dijk, G. T. Robillard, *Biopolymers* **2003**, *69*, 311.
- [119] E. T. Hanson, R. Borsali, R. Pecora, *Macromolecules* **2001**, *34*, 2208.
- [120] S. Lecommandoux, F. Chécot, R. Borsali, M. Schappacher, A. Deffieux, A. Brület, J. P. Cotton, *Macromolecules* **2002**, *35*, 8878.
- [121] P. Hickl, M. Ballauf, U. Scherf, K. Müllen, P. Lindner, *Macromolecules* **1997**, *30*, 273.
- [122] Y. D. Zaroslov, V. I. Gordeliy, A. I. Kuklin, A. H. Islamov, O. E. Philippova, A. R. Khokhlov, G. Wegner, *Macromolecules*, **2002**, *35*, 4466.
- [123] M. Knaapila, B. P. Lyons, T. P. Hase, L. Almasy, S. Pradhan, T. Ikonen, R. Serimaa, B. K. Tanner, U. Scherf, H. D. Burrows, A. P. Monkman, *In preparation*.
- [124] B. Liu, G. C. Bazan, *J. Am. Chem. Soc.* **2004**, *126*, 1942.
- [125] S. Sax, Emil J.W. List, S. Pradhan, Ullrich Scherf, *In preparation*.
- [126] H. D. Burrows, V. M. M. Lobo, J. Piny, M. L. Ramos, J. Seixas de Melo, A. J. M. Valente, M.J. Tapia, S. Pradhan, U. Scherf, *Macromolecules*, **2004**, *37*, 7425.
- [127] T. Uchida, H. Seki, *Liquid Crystals and Uses*, edited by Bahadur (World Scientific, Singapore, **1990**), 3
- [128] J. Cognard, *Alignment of liquid Crystals and their Mixtures* (Gordon and Breach, London, **1982**)
- [129] P. Guyot-Sionnest, H. Hsiung, Y. R. Shen, *Phys. Rev. Lett.* **1986**, *57*, 2963.

- [130] D. Beljonne, G. Pourtois, C. Silva, E. Hennebicq, L. M. Herz, R. H. Friend, G. D. Scholes, S. Setayesh, K. Mullen, J. L. Bredas, *Proc. Natl. Acad. Sci. U.S.A.* **2002**, *99*, 10982
- [131] T. Q. Nguyen, J. J. Wu, V. Doan, B. J. Schwartz, S. H. Tolbert, *Science*, **2000**, *288*, 652.
- [132] U. Asawapirom, R. Güntner, M. Forster, T. Farrell, U. Scherf, *Synthesis*, **2002**, *9*, 1136.
- [133] C. Tan, R. Pinto, K. S. Kirk, *Chem. Commun.* **2002**, 446.
- [134] A. D. Child, J. R. Reynolds, *Macromolecules*, **1994**, *27*, 1975.
- [135] H. Kreyenschmidt, G. Klärner, T. Fuhrer, J. Ashenurst, S. Karg, W. Chen, V.Y. Lee, J. C. Scott, R. D. Miller, *Macromolecules*, **1998**, *31*, 1099.
- [136] G. Klärner, M. H. Davey, W. D. Chen, J. C. Scott, R. D. Miller, *Adv. Mater.* **1998**, *10*, 993.

8 List of publications

1)“Fluorescence enhancement of the water soluble poly{1,4-phenylene-[bis(4-phenoxy-butylsulfonate)]fluorene-2,7-diyl} copolymer in n-dodecyl pentaerythritol ether micells” H. D. Burrows, V.M.M. Lobo, J. Pina, M.L. Ramos, J. Seixas de Melo, A.J.M. Valente, M.J. Tapia, **S. Pradhan**, U. Scherf

Macromolecules, **2004**, *37*, 7425.

2)“Dissolution and thin film formation of water soluble polyfluorene-surfactant system”, M. Knaapila, B. P. Lyons, T. P. Hase, L. Almasy, **S. Pradhan**, T. Ikonen, R. Serimaa, B. K. Tanner, U. Scherf, H. D. Burrows, A. P. Monkman

J.Phys.Chem.B to be submitted (2004)

3)“Interaction between the water soluble poly{1,4-phenylene-[9,9-bis(4-phenoxy-butylsulfonate)]fluorene-2,7-diyl} copolymer and ionic surfactants followed by spectroscopic and conductive measurements”, H. D. Burrows, V. M. M. Lobo, J. Pina, J. Seixas de Melo, A. J. M. Valente, M. J. Tapia, **S. Pradhan**, U. Scherf

J.Phys.Chem.B, to be submitted (2004)

4)“Interactions between surfactants and poly{1,4-phenylene-[9,9-bis(4-phenoxy-butylsulfonate)]fluorene-2,7-diyl} copolymer”, H. D. Burrows, V. M. M. Lobo, J. Pina, M. L. Ramos, J. Seixas de Melo, A. J. M. Valente, M. J. Tapia, **S. Pradhan**, U. Scherf, S. I. Hintschich, A. P. Monkman

Colloids and Surfaces A, submitted (ECIS 2004)

5)“Light emitting devices based on water soluble PPP type polymers” S. Sax, **S. Pradhan**, E. J.W. List, U. Scherf

In preparation

KOPO'03- From Synthesis to Electronics Heinrich-Fabri-Institut in Blaubeuren (Ulm) Germany, **November 2–5, 2003**, “Ionic water soluble polyfluorene type copolymer”

(Talk)

9 Curriculum Vitae

Swapna Pradhan

PERSONAL DETAILS

Date of birth : 20 March 1974

Place of Birth: Pune, India

Nationality: Indian

Marital Status: Married

UNIVERSITY EDUCATION

10/02-01/04

03/01-09/02

Ph. D. Studies, Prof. Dr. Ullrich Scherf
Bergische University Wuppertal

University of Potsdam

TOPIC:

“Ionic, water soluble polyfluorene-type-copolymers”

08/99-08/01

M. S. (Chemistry)

Lamar University, Beaumont, TX, USA

Research Assistant

08/2000-08/2001

Dept. of Chemistry, Lamar University Beaumont, TX,
USA

08/1999-05/2000

Teaching Assistant

Dept. of Chemistry, Lamar University Beaumont, TX,
USA

08/95-11/97

M. Sc. (Organic Chemistry)

University of Pune, India

06/91-04/94

B. Sc. (Chemistry)

University of Pune, India

SCHOOL EDUCATION

06/89-03/91

Science, Pune Board

Higher Secondary (School) Certificate (**H.S.C.**)

06/80-03/89

General, Pune Board

Secondary School Certificate (**S.S.C.**)

10 Acknowledgement

It is indeed an immense pleasure for me to acknowledge **Prof. Ullrich Scherf** for his guidance and encouragement provided. Working with him was a great experience.

I would like to thank **Michael Forster** for being such a wonderful person and providing a helping hand throughout. **Tony Farrell** for the interesting ideas and suggestions, which he provided.

I would like to express my thanks to my colleagues **Roland Güntner, Udom Asawapirom and Askin Bilge**, for being really good friends and for tolerating the spicy Indian food made by me.

Thanks to **Edward Preis, Sascha Prentzel and Daniel Krüger** for being very good technicians.

I would like to thank **Torsten Bünnagel** for all his help and always saying “*you are welcome*” with a broad smile.

My thanks also go to **Deqing Gao** for being such a nice friend. We had a lot of fun having lunch together.

Thanks to my colleagues **Benjamin Souharce, Frank Galbrecht, Benjamin Nehls**.

Anke Helfer and **Sylvia Adamczyk** for G.P.C measurements

My thanks are due to our nicest secretary ever **Bianca Enz**. Her presence is so valuable for us; we feel that we are missing someone very precious when she isn't around.

My heartfelt thanks go to **Angeliki Tasina**. With her pleasant and caring nature she has created a place deep inside my heart.

I would like to thank my **parents** and **brother** for their everlasting support and encouragement. I have immensely benefited from my father who is a chemist himself. I would also like to thank my Aunt, uncle and the entire family.

Finally, last but not least my heartfelt thanks go to my friend and now my lifepartner, **Jiten** for his understanding and always being beside me. Without his precious support and guidance this work wouldn't have been possible.

Thanks go to each and every friend. I have greatly benefited from their criticism and encouragement. Apologies to the person whom I might have forgot to mention.